CHEMICAL CLASSIFICATION OF SPHERULES RECOVERED FROM THE PACIFIC OCEAN SITE OF THE CNEOS 2014-01-08 (IM1) BOLIDE.

A. Loeb[1,2], S.B. Jacobsen[2,3], R. Tagle[2], T. Adamson[2], S. Bergstrom[2], J. Cherston[1,2], R. Cloete[1,2], S. Cohen[2,7], L. Domine[1,2], H. Fu[2,3], C. Hoskinson[2], E. Hyung[2,3], M. Kelly[2], E. Lard[2], F. Laukien[2,6], J. Lem[2,5], R. McCallum[2], R. Millsap[2], C. Parendo[2,3], C. Peddeti[2,4], J. Pugh[2], S. Samuha[2,7], D.D. Sasselov[1,2], M. Schlereth[2], J. Siler[2], A. Siraj[1,2], P.M. Smith[2], J. Taylor[2], R. Weed[2,4], A. Wright[2], J. Wynn[2].

[1]Dept. of Astronomy, Harvard Univ., Cambridge, 02138, MA (aloeb@cfa.harvard.edu).
[2]Interstellar Expedition of the Galileo Project, Cambridge, 02138, MA.
[3]Dept. of Earth and Planet. Sci., Harvard Univ., Cambridge, 02138, MA.
[4]Dept. of Nuclear Eng., Univ. of California Berkeley, Berkeley, 94720, CA.
[5]Dept. of Mining Eng., PNG Univ. of Technology, Lae, 411, Papua New Guinea.
[6]Dept. of Chemistry and Chemical Biology, Harvard Univ., Cambridge, 02138, MA.
[7]Dept. of Materials Eng., NRCN, P.O. Box 9001, Beer-Sheva, 84190, Israel.

Abstract: We have conducted an extensive towed-magnetic-sled survey during the period of June 14-28, 2023, over the seafloor about 85 km north of Manus Island, Papua New Guinea, centered around the calculated path of the bolide CNEOS 2014-01-08 (IM1). We found about 850 spherules of diameter 0.1-1.3 millimeters in our samples. The samples were analyzed by micro-XRF, Electron Probe Microanalyzer and ICP Mass spectrometry. Here we report major and trace element compositions of the samples and classify spherules based on that analysis. We identified 78% of the spherules as primitive, in that their compositions have not been affected by planetary differentiation. We divided these into four groups corresponding to previously described cosmic spherule types. The remaining 22% appear to all reflect planetary igneous differentiation and are all different from previously described spherules. We call them D-type spherules. A portion of the D-spherules show an excess of Be, La and U, by up to three orders of magnitude relative to the solar system standard of CI chondrites. Detailed mass spectroscopy of 12 of these "BeLaU"-type spherules, the population of which may constitute up to ~10% of our entire collected sample, suggests that they are derived from material formed by planetary igneous fractionation. Their chemical composition is unlike any known solar system material. We compare these compositions to known differentiated bodies in the solar system and find them similar to evolved planetary materials - with lunar KREEP the closest in terms of its trace element enrichment pattern, but unusual in terms of their elevated CI-normalized incompatible elements. The "BeLaU"-type spherules reflect a highly differentiated, extremely evolved composition of an unknown source.

Introduction

The retrieval of cosmic spherules from meteor sites has a long history, with related morphology and composition analyses linking them to various components of the solar system (Brownlee et al., 1979; Maurette et al., 1991; Taylor and Brownlee, 1991; Xue et al., 1994; Brownlee et al., 1997; Herzog et al., 1999; Taylor et al., 2000; Engrand et al., 2005; Genge et al., 2008; Vondrak et al., 2008; Wittke et al., 2013; Folco et al., 2015; Rudraswami et al., 2015; Genge et al., 2017). The spherules range in diameter from a minimum recoverable size of 0.25 to 1.7 mm. They have been classified as I, S and G-types.

Marvin and Einaudi (1967) and others (Folco and Cordier 2015; Blanchard et al. 1980; Brownlee et al. 1997) have listed possible extraterrestrial and terrestrial origins for magnetic spherules like those discussed in this paper. Extraterrestrial origins may be: (i) ablation of meteorites during flight in the atmosphere; (ii) disintegration of carbonaceous chondrites in flight through the atmosphere; (iii) vaporization of large meteorites during impact crater formation; and (iv) infall of particles containing iron or iron oxide, of either asteroid or comet origin (they may enter the atmosphere as spherules, resulting from collisions in space, or may become spherules in the atmosphere). The terrestrial origins proposed were: (i) volcanic; (ii) industrial combustion of coal, crude oil, or wood; (iii) smelting products; and (iv) others such as forest fires and lightning discharges.

On 8 January 2014 US government satellite sensors detected three atmospheric detonations in rapid succession about 84 km north of Manus Island, outside the territorial waters of Papua New Guinea (20 km). Analysis of the trajectory suggested an interstellar origin of the causative object CNEOS 2014-01-08: an arrival velocity relative to Earth more than ~45 km s^{-1}, and a vector tracked back to outside the plane of the ecliptic (Siraj and Loeb 2022a). In 2022 the US Space Command issued a formal letter to NASA certifying a 99.999% likelihood that the object was interstellar in origin. Along with this letter, the US Government released the fireball light curve as measured by satellites, which showed three flares separated by a tenth of a second from each other. The bolide broke apart at an unusually low altitude of ~17 km. The object was likely substantially stronger than any of the other 272 objects in the CNEOS catalog, including the ~5%-fraction of iron meteorites from the solar system (Siraj and Loeb 2022b). Calculations of the fireball light energy suggest that about 500 kg of material was ablated by the fireball and converted into ablation spherules with a small efficiency. The fireball path was localized also based on the delay in arrival time of the direct and reflected sound waves to a seismometer located on Manus Island (Siraj and Loeb 2023), but this inference has been debated (e.g., Brown and Borovicka 2023). In this paper, we characterize spherules retrieved in an expedition that surveyed the region identified by the US Government satellites as the meteor site without assuming their association with the IM1 bolide.

Sampling Expedition

The expedition was mounted from Port Moresby, Papua New Guinea (PNG), to search for remnants of the bolide, labeled hereafter IM1. It utilized a 40-meter catamaran workboat, the M/V Silver Star. A 200-kg sled (**Fig. 1**) was used with 300 neodymium magnets mounted on both of its sides and video cameras mounted on the tow-bridle. Approximately 0.06 km^2 were sampled in the target area (**Fig. 2**). The fine material collected on the neodymium magnets was extracted and brought in a wet slurry up to a laboratory set up on the bridge of the vessel for further examination. There, an initial wet-magnetic separation took place. Subsequently, both magnetic and non-magnetic separations were processed through sieves and dried. Spherules were handpicked with tweezers using a binocular zoom microscope. They ranged in size from 100 microns to 2 mm. We obtained a total of ~850 fragments consisting of spherules and shards by this method.

Spherule Samples and Location

The terminology and measurements will be explained in the upcoming subsections (see also Loeb et al. 2024a,b). Figure 2 shows the tracks of our expedition survey. Tracks 22 and 17 were located outside the Department of Defense error box for IM1's fireball, but the full extent of IM1's strewn field is unknown.

Figure 1: Magnetic sled design. Left: Isometric view of the magnetic sled design, Right: Side view of the sled when placed on the ocean floor. The 250-kg, 1 by 2 meter sled was covered with an array of 300 neodymium magnets on both sides and equipped with video cameras in the metal tow-halter ahead of it, which was anchored by a synthetic cable to a winch on the ship, the M/V Silver Star.
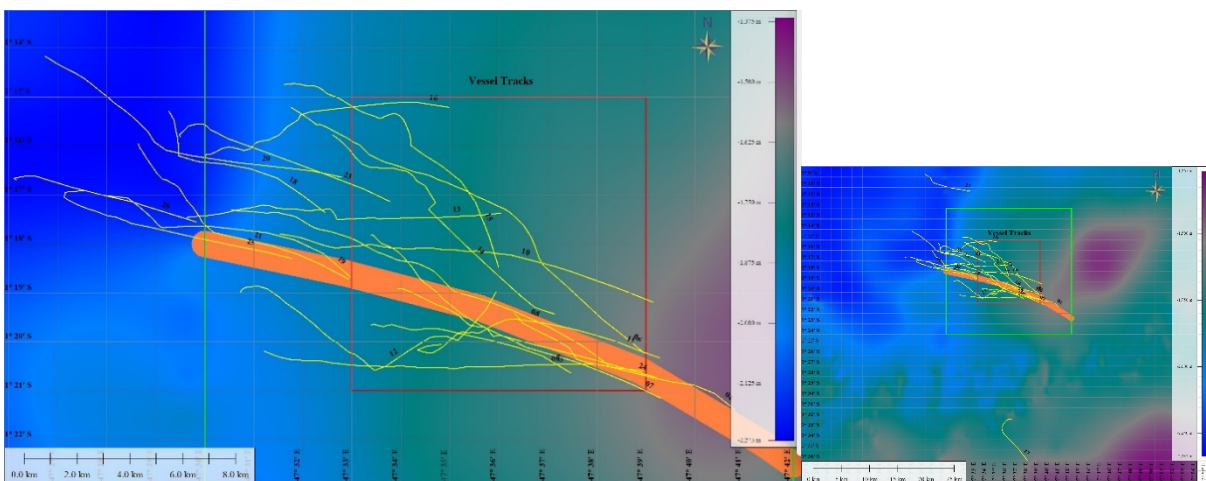

Figure 2: List of ship track numbers around the expected path of IM1 based on seismometer data (Siraj and Loeb, 2023) from Manus Island (orange strip). Left: Tracks within the Department of Defense error box (in red). Right: Full map including runs 22 and 17. Background colors indicate ocean depth (with scale on the right). Latitude and longitude are marked in degrees and decimal minutes. At one degree south latitude, one minute of latitude or longitude equals one nautical mile which is 1.852 km. The red box, measuring 11.112 km on a side, marks the uncertainty in the Department of Defense (DoD) localization of IM1's fireball, and the green box marks twice that size.

Analytical Methods

Most samples (~802) were first analyzed by microXRF with a Bruker Tornado M4 for their bulk major element composition, followed by imaging (SEM and EDS chemical mapping) and spot chemical analyses of ~80 samples with a JEOL Model JXA 8230 Electron Probe Microanalyzer (EPMA). Measurements of elemental abundances for about 60 major and trace elements were performed for 68 samples with an iCAP TQ triple quadrupole ICP-MS (ThermoFisher Scientific).

microXRF: The major and trace element compositions of separated spherule and shard samples was analyzed using the M4 TORNADO PLUS micro XRF instrument from Bruker, situated at the central application facility in Berlin, Germany. This instrument features a 30 W micro-focus X-ray tube and a rhodium anode, with X-rays focused through a polycapillary lens to achieve a spot size of 20 µm for the high-energy range above 20 keV. The measurements were conducted under specific conditions: 50 kV, 200 µA, and 2 mbar for a duration of 60 s. The pressure of 2 mbar was chosen to enhance the detection of light elements and minimize absorption caused by air between the sample and detector. Fluorescent signals were collected using two light element window silicon drift detectors, each with a 60 mm² active area, with

independently operating signal processing units, allowing a maximal throughput of 250 kcps each at a spectroscopic resolution lower than 145 eV for manganese Kα. The samples were analyzed using the single-spot approach, capitalizing on the benefits arising from the significant information depth of X-rays (e.g. Beckhoff, B. et al., 2006) and the beam divergence of the poly-capillary lenses (approximately 60 μm/mm). This combination ensured optimal coverage of the sample volume and yielded representative results. Sample quantification was attained through standard-less fundamental parameter quantification after instrument calibration, involving a mix of pure elements and the NIST 620 certified reference glass sample to describe lens transmission and element sensitivity. The quantification algorithm uses the forward calculation of the complete spectrum following the approach describe by Sherman (1955). To eliminate any potential for blank signals, spherules and shards were mounted on acrylic plates using double-sided tape. The results for major and trace elements were computed, presenting major elements as oxides and traces as individual elements. The primary advantage of micro XRF lies in the combination of speed, major and trace element sensitivity as well as its non-invasiveness, positioning it as a pre-screening tool for more time-consuming and invasive analytical procedures with uncertainties below tens of percent.

EPMA: We used the JEOL JXA-8230 electron microprobe at the Harvard Electron Microprobe Laboratory to obtain high-resolution backscatter (BSE) and secondary (SEI) electron images, elemental X-ray maps, and chemical analyses, using focused beam of ~1 mm in diameter. Most objects were mounted on sticky tape, while several spherules were mounted in epoxy and polished. All samples were carbon-coated. The chemical compositions of intact objects were measured by energy dispersive spectroscopy (EDS) using factory calibration curves. The polished areas of several spherules were analyzed by wavelength dispersive spectroscopy (WDS) using common natural minerals and synthetic glasses as calibration standards (e.g., Petaev and Jacobsen, 2009). The EDS analyses and imaging we performed at accelerating voltage of 20 kV and beam currents of 5-10 nA and ~0.1 nA at low- (< 1000×) and high-resolution (> 2000×), respectively. In the WDS analyses we used accelerating voltage of 15 kV, beam current of 20 nA, and counting times of 30 sec and 15 sec on peak and background, respectively.

TQ-ICP-MS (Triple Quad elemental analysis): Measurements of elemental abundances for major and trace elements were performed on the iCAP TQ quadrupole ICP-MS (ThermoFisher Scientific) in the Cosmochemistry Laboratory at Harvard University. USGS reference materials were thoroughly dissolved and diluted in a 2% HNO_3 solution spiked with 10 ppb indium diluted to a factor of 5000 to be used as standards. Spherules were prepared for mass spectrometry measurements by first individually digesting the samples in a mixture of concentrated HF-HNO_3-HCl at a 1:3:1 ratio at 120-140 °C overnight. The samples were subsequently dried down and then redissolved in a second acid mixture involving an aqua regia solution mixed with H_2O at a 3:2 ratio and heated to 120-140 °C overnight. This dissolution was dried down for the second time and redissolved in a high-purity 2% HNO_3 solution. A small aliquot (3%) was drawn from this solution and further diluted for elemental analysis. To account for and to correct instrumental drift, the 2% HNO_3 solution used for dilution was spiked with 2 ppb indium as an internal standard, prepared identically to the standard solutions. Measurements were performed in KED mode with He as a collision cell gas as recommended by the Reaction Finder function built in the iCAP TQ Qtegra software, with the exception of Cr, which was measured in TQ mode with O_2 as a mass-shifted molecule. The prepared spherule solutions were measured as an unknown against a four-point calibration line consisting of a blank and three USGS standards: BCR-2, BHVO-2, and AGV-2. Calibration curves for individual elements were checked for linear intensity to concentration correlations for accurate measurements. Routine measurements of AGV-2 as an unknown on the iCAP TQ suggest fractional errors to be within 6% using this method.

Results: Imaging and morphology of the spherules

Electron microprobe images of recovered spherules are shown in **Figs. 3, 4 and 5.** The spherules in **Fig. 3** are what we call primitive spherules, identified as such by their chemical composition (see next section). The dendritic textures of these spherules suggest rapid cooling. The spherules in **Fig. 4** and **5** are

all identified as differentiated spherules by their chemical compositions (see next section) and do not in general have as perfect a spherical shape as the primitive group, and some of them are clusters of coalesced spherules. The complete spherule dataset will be released in a future publication. The shapes of the BeLaU-type spherules in Fig. 4c and f have been seen before in spherules from airbursts (Tankersley et al. (2024); van Ginneken et al. (2021, 2024). In addition to electron microprobe images, low resolution photos were taken for 684 samples prior to micro-XRF analysis. Among these, ~64 were determined to be "shards" as opposed to "spherules," which were discerned based on sharp angles resembling broken surfaces or evidence of fragmentation.
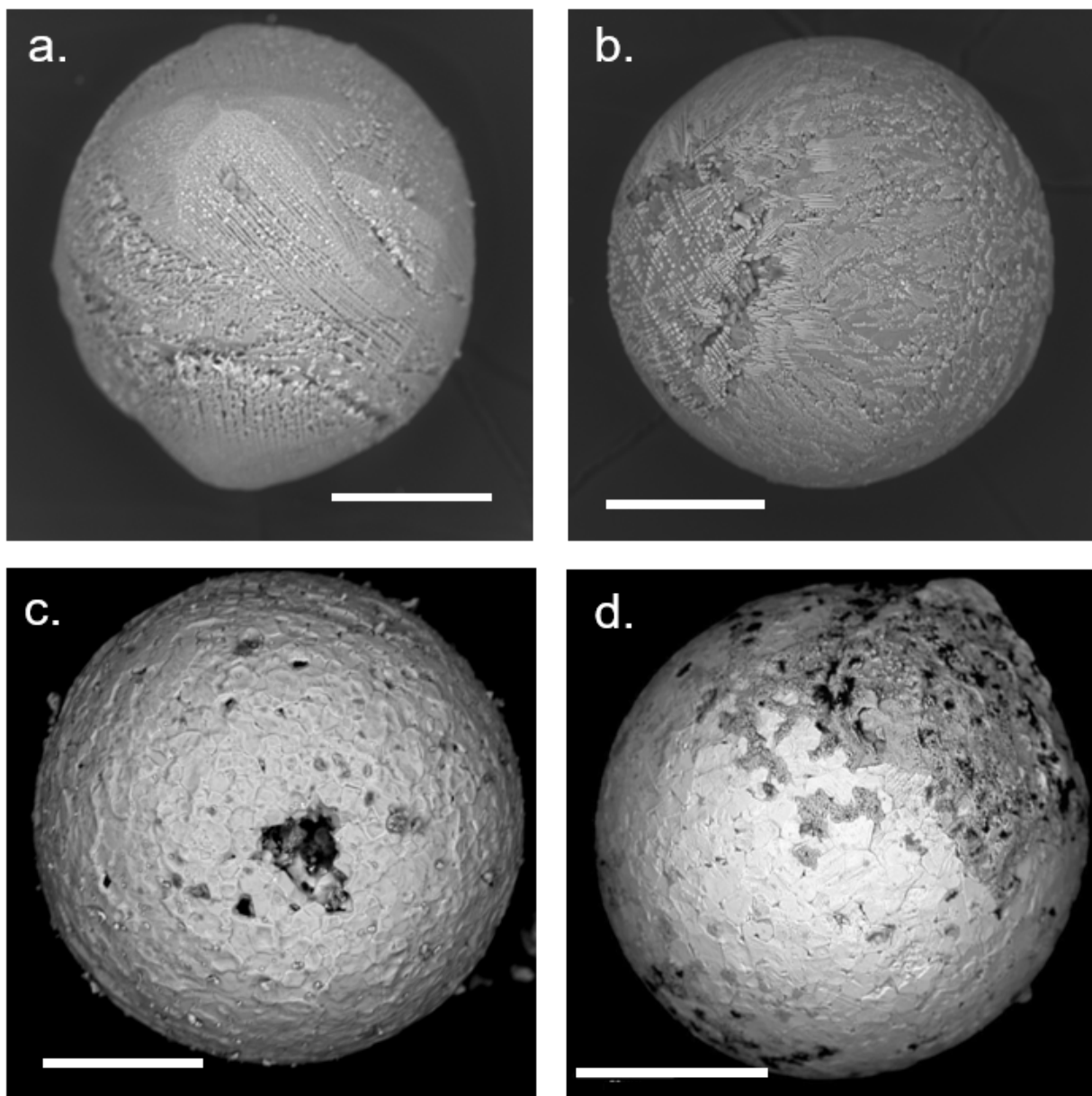
Figure 3. BSE images of primitive spherules from the a) S-type (IS20M-1) b) G-type (IS20M-21) c) I-type, high Ni (IS8M2-20) and d) I-type, low Ni (IS16A-SPH1) groups. The scale bar is 100 microns.
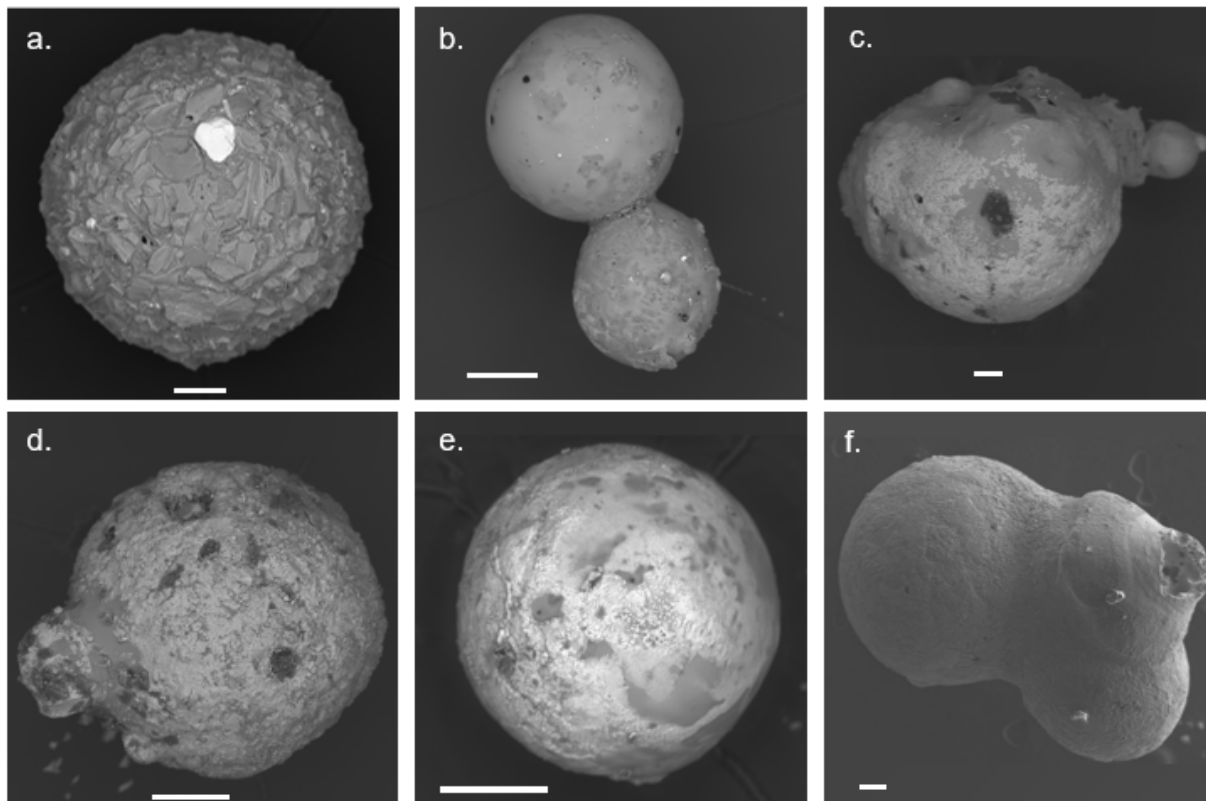
Figure 4. BSE images of differentiated spherules from each of the differentiated (D-type) spherule classifications: a) D-type low Sr, high Si (IS11M2-2) b) D-type high Sr, high Si (IS19M-14) c) D-type, high Si (17NMAG-5) d) D-type, low Sr, low Si (IS21-4) e) D-type high Sr, low Si (IS14M-2) and f) D-type, low Si (S21 or IS14-SPH1) groups. The images c) and f) are also classified as "BeLaU"-type spherules. The scale bar is 100 microns.
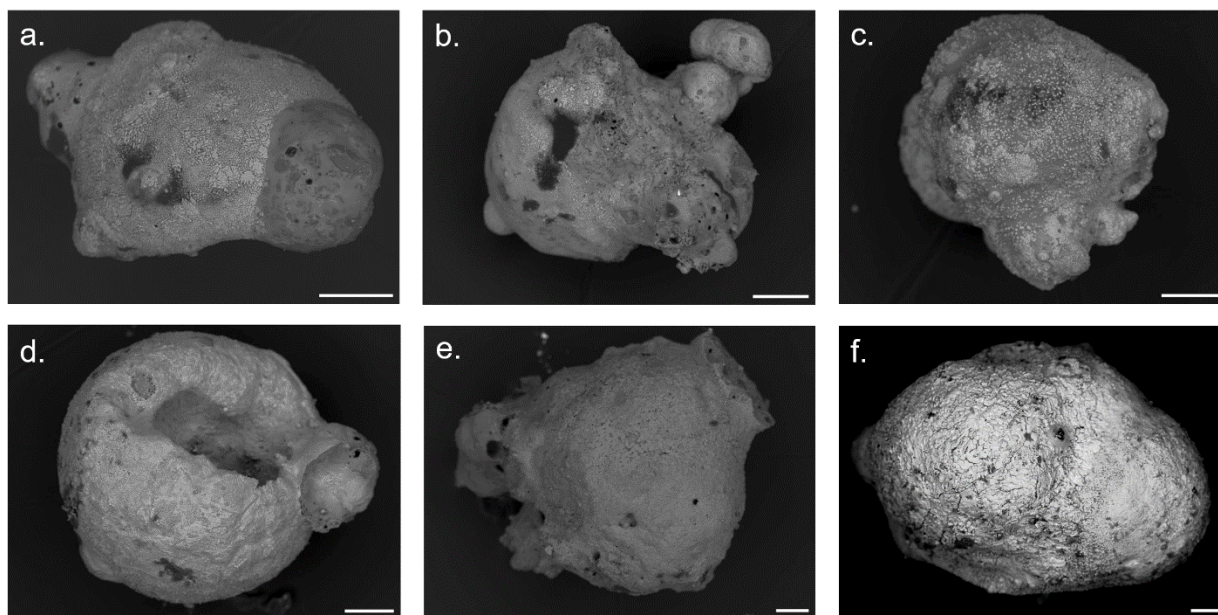
Figure 5. Additional BSE images of D-type spherules: a) 19NMAG-52 (D-type, high Sr, low Si), b) 19MAG-50 (D-type, high Sr, low Si), c) 19MAGx-4 (BeLaU, low Si), d) 17MAG-2 (BeLaU, low Si), e) 17MAG-29 (BeLaU, low Si), and f) 17MAG-6 (D-type, high Sr, low Si). The scale bar is 100 microns.

Classification of the spherules based on elemental compositions.

Cosmic spherules are sub-divided into three compositional types (Blanchard et al., 1980). These are the silicate-rich spherules or S-type, the Fe-rich spherules or I-type and glassy spherules or G-types. There is strong evidence that S-type cosmic spherules with chondritic-like composition are related to carbonaceous chondrites and ordinary chondrites (Blanchard et al., 1980). It has been suggested that I-type spherules are metal grains released from carbonaceous chondrites disaggregated in space (Herzog et al. 1999). The glassy or G-type spherules are thought to be mixtures of S and I. Relatively rare spherules have been called *differentiated* as they have similarities to achondrite meteorites and have been treated as a subgroup of S-type spherules. Differentiated spherules have major-element compositions with higher Si/Mg and Al/Si ratios, and higher refractory lithophile trace element contents relative to chondritic spherules (cf. Folco and Cordier 2015).

The major element, Sr and Ni compositions of 745 spherules from the IM1 site measured by micro-XRF are in **Table S1** (supplement). The data are plotted in a Mg/Si histogram (**Figure 6**) and show a minimum at Mg/Si = 1/3. Spherules with Mg/Si > 1/3 are similar to chondritic meteorites and cosmic S-type spherules, while those with Mg/Si <1/3 are similar to igneous rocks from Earth and other planetary bodies. The data are also plotted in a Mg-Si-Fe ternary diagram (**Figure 7**), since such a diagram has been shown to effectively distinguish the S-, I- and G-type groups (cf. Folco and Cordier 2015). We note that there are two distinct groups of spherule compositions in this plot. About 78 % of the spherules fall along the trend of S, G and I-type spherules. These are referred to as primitive spherules as they are thought to be related to primitive chondritic meteorites and represent materials that have not gone through planetary differentiation. The remaining 22% of the spherules have low Mg and plot close to the Si-Fe side of the diagram. The high-Si part of this group plots within the range of terrestrial igneous rocks that are shown for comparison. These spherules are thus called differentiated, meaning they are likely derived from crustal rocks of a differentiated planet. Since they are clearly different from the differentiated subgroup of S-type spherules we give them a new name *D-type spherules*. The Mg/Si = 1/3 is used to distinguish primitive and differentiated spherules. The D-type spherules were discovered in 17 of the 24 tracks explored during this expedition.
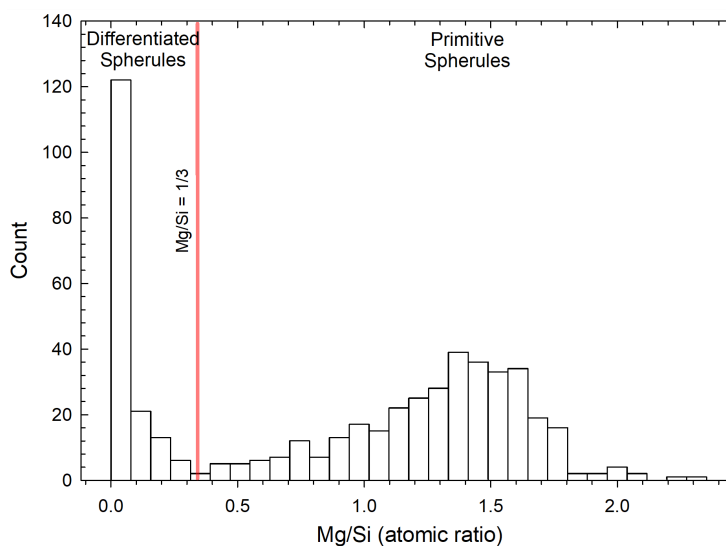
Figure 6. Histogram of the Mg/Si ratio measured with micro-XRF for 745 IM1 site spherules. This diagram shows a clear dividing line between primitive and differentiated spherules.

Figure 7. Atomic Mg-Si-Fe plot (atom %) of micro-XRF data for 745 IM1 site spherules and shards. The spherules are classified with the parameter values in **Table 1**. The spherule groups are compared to reference values of Earth materials (Bulk Earth, bulk silicate Earth [BSE], upper continental crust [UCC], shale, normal midocean ridge basalts [N-MORB], Hawaiian basalt [BHVO-1], Columbia River basalt [BCR-1], Guano Valley andesite [AGV-1]) and CI meteorites. Also shown is the range of chemical compositions of terrestrial igneous rocks.

For the primitive spherules we use $100Fe/(Fe+Si+Mg) > 90$ to distinguish I-types from S- and G-types. This group is supposed to be primarily made of iron compounds and is clearly distinct from the other primitive spherules in the $100Fe/(Fe+Si+Mg)$ histogram (**Figure 8a**). This I-group is further subdivided into high Ni (>4000 ppm) and low Ni (<4000 ppm) groups (**Figure 8b**), as high Ni spherules are most likely of cosmic origin and typically have Ni > 4000 ppm (Engrand et al. 2006). The S- and G-type dividing line is $100Si/(Fe+Si+Mg) = 50$ (**Figure 8a**), relatively consistent with previous literature (cf. Brownlee et al. 1997; Taylor et al. 2000; Folco and Cordier 2015). The primitive spherule groups are compared to reference values of Bulk Earth, bulk silicate Earth (BSE) (McDonough and Sun 1995), and CI meteorites (Anders and Grevesse 1989) that are and should be on the primitive trend (**Figure 7**).
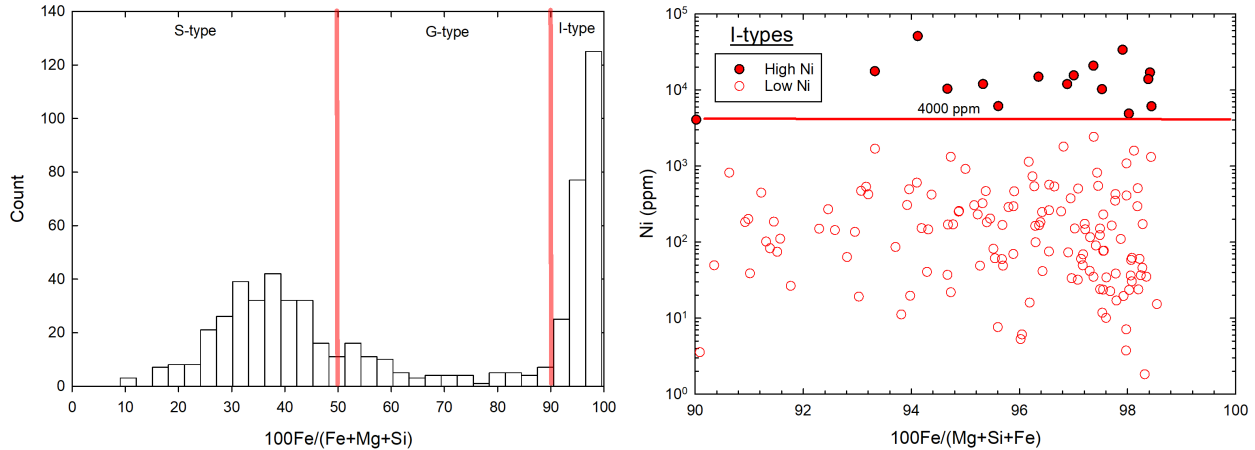
Figure 8. Left: Histogram of the 100Fe/(Fe+Si+Mg) measured with micro-XRF for 745 IM1 site spherules. This diagram shows the dividing lines selected between S-, G-, and I-types. Right: Plot of Ni(ppm) vs. 100Fe/(Fe+Si+Mg), showing the dividing line selected for high-Ni vs low-Ni spherules.

Owing to the incompatible nature of Sr, the Sr content of differentiated spherules is a good indication of the enrichment of refractory lithophile elements in the spherules and thus the extent of differentiation. The differentiated spherules in this study are thus divided into high Sr (>450 ppm) and low Sr groups (<450 ppm). They are further subdivided on the Si-content. For high Sr spherules we use $100Si/(Fe+Si+Mg) = 60$ as the dividing line and for low Sr spherules a value of $100Si/(Fe+Si+Mg) = 70$. These dividing lines are shown in **Figure 9**. The spherule groups are compared to reference values for samples of the Earth's crust in **Figure 7**. This includes average composition of normal midocean ridge basalts (N-MORB) (Gale et al. 2013), average upper continental crust (UCC) (Rudnick and Gao 2014) and shale (Ray and Paul 2021). Also plotted is the outline of the field of 37000 terrestrial igneous rocks as well as 3 USGS standards [Hawaiian basalt (BHVO-1), Columbia River basalt (BCR-1), Guano Valley andesite (AGV-1) (Jochum et al. 2007)].

We note that the high Si varieties of D-spherules plot close to or within the range of terrestrial igneous rocks, while the low Si groups do not. Thus, the D-type spherules and have been divided into four distinct groups. This results in eight distinct spherule groups that are all shown in **Figure 7**. The parameters used to subdivide the spherules are summarized in **Table 1**. The total number of spherules identified in each group are listed in **Table 2**.
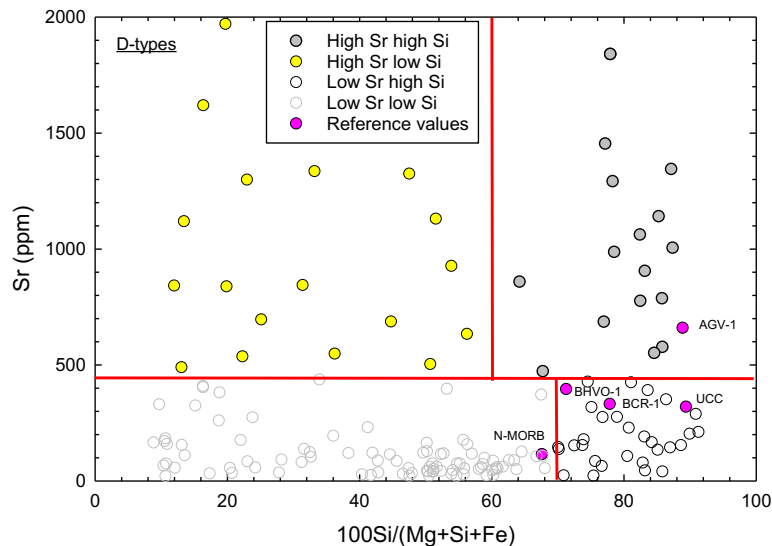
Figure 9. Micro-XRF data for 745 IM1 site spherules. Plot of Sr(ppm) vs. 100Si/(Fe+Si+Mg).

Table 1. Classification of the spherules with the Mg-Si-Fe diagram.

	Type	100Fe/ (Fe+Si+Mg)	Ni (ppm)	Mg/Si	Sr (ppm)	100Si/ (Fe+Si+Mg)
Primitive spherules	I-type, high Ni	>90	>4000			
	I-type, low Ni	>90	<4000			
	S-type	<50		>1/3		
	G-type	>50 and <90		>1/3		
Differentiat ed spherules	D-type, high Sr, high Si			<1/3	>450	>60
	D-type, high Sr, low Si			<1/3	>450	>60
	D-type, low Sr, high Si			<1/3	<450	>70
	D-type, low Sr, low Si			<1/3	<450	>70

Table 2. Comparison of the number of each spherule type identified by micro-XRF and by ICP-MS results.

	Type	Micro-XRF Number	Micro-XRF Percent	ICP-MS Number	ICP-MS Percent
Primitive spherules	I-type, high Ni	18	2.4	5	7.4
	I-type, low Ni	212	28.5	18	26.5
	S-type	275	36.9	19	27.9
	G-type	78	10.5	0	0
Differentiated spherules	D-type, high Sr, high Si	20	2.7	6	8.8
	D-type, high Sr, low Si	23	3.1	5	7.4
	D-type, low Sr, high Si	29	3.9	0	0
	D-type, low Sr, low Si	90	12.1	3	4.4
	D-type, BeLaU high Si			2	2.9
	D-type, BeLaU low Si			10	14.7
	Total	745	100	68	100

The major element and trace element compositions of 68 spherules from the IM1 site measured by ICP-MS are in **Table S2** (supplement). ICP-MS data for the spherules include many more elements than the micro-XRF data but does not include measurement of Si. Thus, we also plot the micro-XRF data in a Mg-Al-Fe diagram (**Figure 9a**) and compare it to the same diagram with ICP-MS measurements (**Figure 9b**). The micro-XRF results show the same groups in the Mg-Al-Fe plot as for the Mg-Si-Fe plot in **Figure 8.** Note that the primitive and differentiated trends are even better separated in **Figure 9a**, and the fields of the primitive spherule groups are also well defined by this diagram. We conclude that this new diagram is a good alternative to the Mg-Si-Fe diagram, when Si data are missing. The Sr concentrations of the D-type spherules measured by micro-XRF are plotted versus the Al/Fe ratio in **Figure 10a**. While there is some overlap, this diagram gives a relatively good separation of the high Si and low Si groups after separating the differentiated spherules into high (>450 ppm) and low (<450 ppm) Sr groups and is thus also useful for data with missing Si measurements. Classification of the spherules with the parameters in **Table 3** will thus yield a relatively equivalent classification of the spherules compared to that obtained with the Mg-Si-Fe diagram. The primitive spherules are identified by 100Al/(Fe+Al+Mg) <10 and the differentiated spherules by 100Al/(Fe+Al+Mg) >10. For the primitive spherules the I-types are identified by 100Fe/(Fe+Al+Mg) >90, the S-types by 100Fe/(Fe+Al+Mg) <65, and the G-types in between these two values.
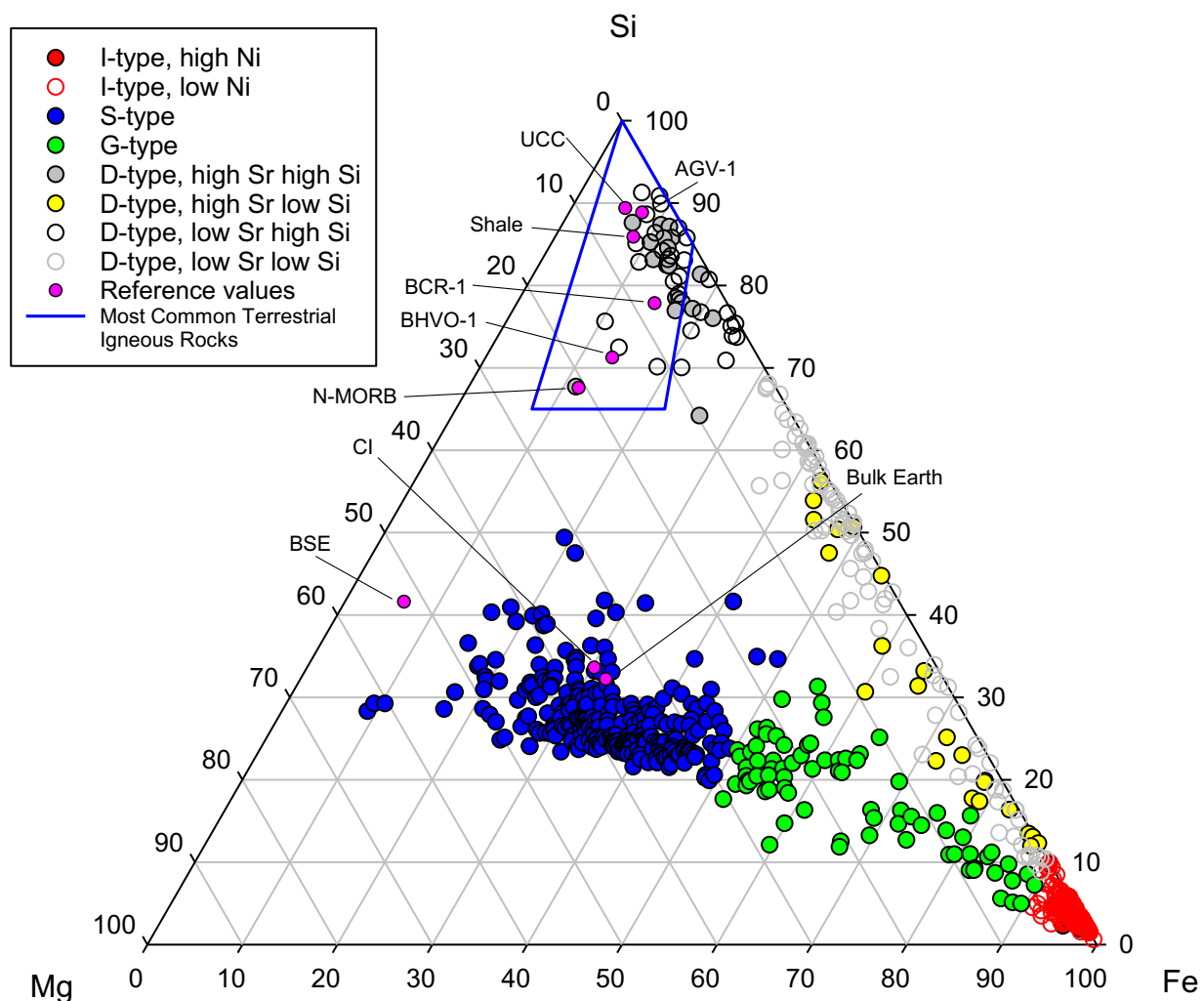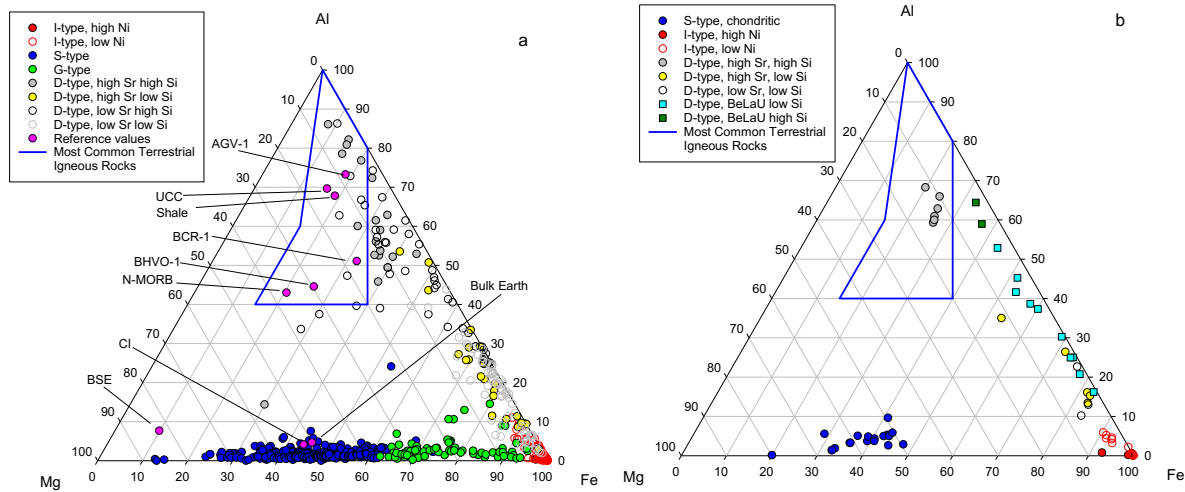
Figure 10. (Figure formatting, faint grey lines present as outlines) a) Atomic Mg-Al-Fe plot (atom %) of micro-XRF data for 745 IM1 site spherules. The spherules are classified with the parameter values in **Table 1** and are the same spherules shown in **Figure 7**. b) ICP-MS data for 68 spherules, classified with the parameters in **Table 3** as discussed in the text.

Table 3. Classification of the spherules with the Mg-Al-Fe diagram.

	Type	100Fe/(Fe+Al+Mg)	Ni (ppm)	100Al/(Fe+Al+Mg)	Sr (ppm)	Sr vs Al/Fe	BeLaU
Primitive spherules	I-type, high Ni	>90	>4000	<10			
	I-type, low Ni	>90	<4000	<10			
	S-type	<65		<10			
	G-type	>65 and <90		<10			
Differentiated spherules	D-type, high Sr, high Si			>10	>450	See Figure 3a	<80
	D-type, high Sr, low Si			>10	>450	See Figure 3a	<80
	D-type, low Sr, high Si			>10	<450	See Figure 3a	<80
	D-type, low Sr, low Si			>10	<450	See Figure 3a	<80
	D-type, BeLaU, high Si			>10			>80
	D-type, BeLaU, low Si			>10			>80
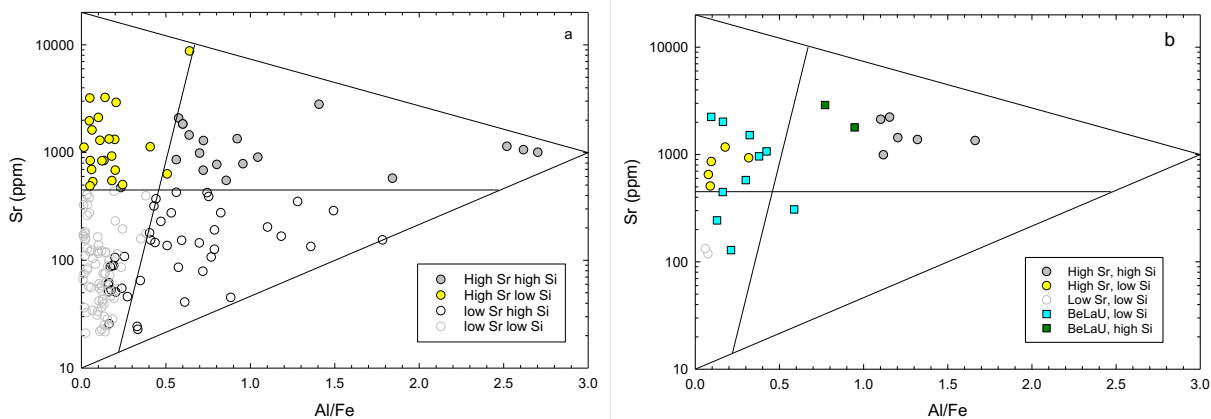
Figure 11. Sr (ppm) vs the Al/Fe weight ratio for D-type spherules from the IM1 site. a) Micro-XRF data, b) ICP-MS data.

For differentiated spherules we first use the fields of the four different D-types shown in **Figure 10a** to identify the same types for the ICP-MS data. In addition, we use **Figure 11** to identify spherules with particularly high contents of refractory lithophile elements, based on the enrichments of Be, La and U relative to Mg and Fe. First the concentrations of these elements are normalized to the same elements in CI chondrites. The CI-normalized values (Be_{CI}, La_{CI}, U_{CI}, Mg_{CI} and Fe_{CI}) are used to calculate the following plotting parameters for the ternary diagram in **Figure 12**:

$$BeLaU = \frac{Be_{CI} + La_{CI} + U_{CI}}{Be_{CI} + La_{CI} + U_{CI} + Mg_{CI} + Fe_{CI}}$$

$$M = \frac{1000(Mg_{CI})}{Be_{CI} + La_{CI} + U_{CI} + Mg_{CI} + Fe_{CI}}$$

$$F = \frac{100(Fe_{CI})}{Be_{CI} + La_{CI} + U_{CI} + Mg_{CI} + Fe_{CI}}$$

The BeLaU parameter was divided by 100, while the M-parameter was multiplied by 10 to make use of the entire area inside the ternary diagram. We define a BeLaU-type spherule as having BeLaU > 80, and we define high and low Si varieties based on the Al/Fe ratio, as in **Figure 11a**. This procedure identifies 10 of D-type spherules as low Si BeLaU-type spherules and 2 as high Si BeLaU-type spherules as shown in **Figure 12**. These spherules are also shown in **Figures 10b and 11b**.

BeLaU-type spherules can only be identified with ICP measurements. We found 12 BeLaU-type spherules out 26 D-type spherules identified with ICP measurements (**Table 2**). The BeLaU spherules were found in tracks 4, 13, 14, 17 and 19. With the micro-XRF measurements, we identified 162 D-type spherules out of a total of 745 spherules. This results in an estimate of 10 % of all spherules to be of BeLaU-type. Thus, out of the ~802 spherule identified as natural materials by our micro-XRF and ICPMS measurements we estimate that there should be up to 80 BeLaU-type spherules in our collection.
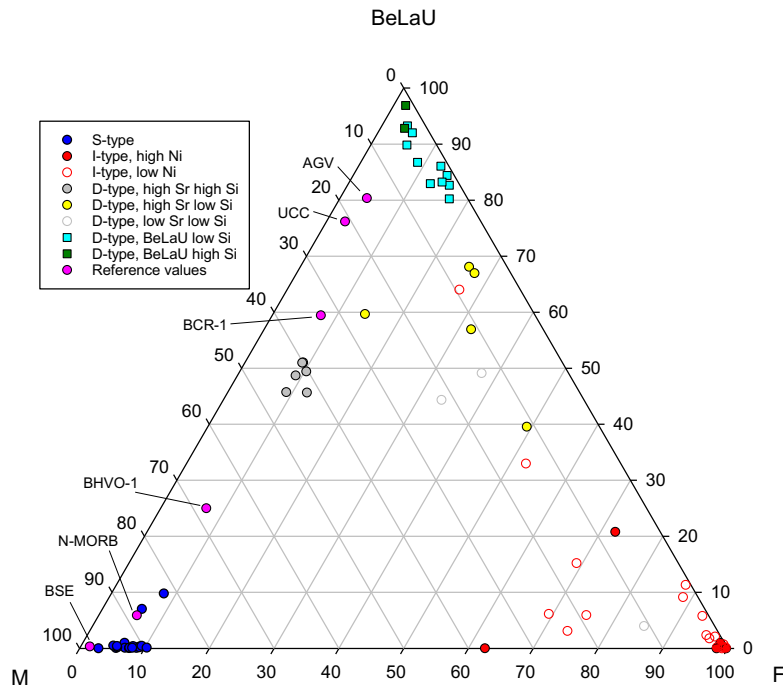
Figure 12. Ternary diagram for identifying the spherules that are most enriched in Be, La and U (BeLaU) relative to Mg (M) and Fe (F). The parameters are CI chondrite normalized (see text).

Origins of the spherule groups

In total we analyzed 850 magnetic particles by either micro-XRF (792) or ICP-MS (68) or both (11). We found that 48 have simple chemical compositions that likely make them derived from industrial products or terrestrial minerals. They were thus not included in this study and so we are left with 802 spherules for which we report data in this paper.

Origin of Primitive spherules: The primitive spherules are in general characterized by high Cr, Co, and Ni and highly variable Mn. Cr is moderately volatile, similar to Mn, thus in a Cr/Fe vs Mn/Fe plot (**Figure 13**) there is an overall positive correlation as expected for these ratios. We note that S-type spherules have both Cr/Fe and Mn/Fe similar carbonaceous chondrites (CCs) and non-carbonaceous chondrites (NCs), and there is no major effect from volatile loss of Cr and Mn for this type of spherules. The Ni-rich I-type spherules have very low Mn/Fe showing substantial volatile loss of Mn and also some for Cr. Most of the low Ni I-type spherules have normal chondritic Mn/Fe and slightly lower, so these do not have evidence for substantial volatile loss for Mn. This suggests that their low Cr content is due to some other partitioning process. The primitive nature of S- and I-type spherules are supported by their chondrite-like Cr/Fe and Mn/Fe, distinctly different from the planetary values (Earth, Moon, Vesta, Mars) shown in **Figure 13**. In a plot of Co/Fe vs Mn/Fe (**Figure 14a**) when comparing S-type spherules similar CCs and NCs, there is no major effect from volatile loss. When comparing with planetary bodies we see an overall negative correlation that is likely due to core formation in the planets. Ni-rich I-type spherules have very low Mn/Fe showing substantial volatile loss. Low Ni I-type again have normal chondritic Mn/Fe and slightly lower, so these do not have evidence for substantial volatile loss. The primitive nature of S- and I-type spherules are supported by their chondrite-like Co/Fe and Mn/Fe, distinctly different from planetary values. In a plot of Ni/Fe vs Mn/Fe (**Figure 14b**) we also see an overall negative correlation. Here the S-type spherules have lower Ni/Fe compared to CCs and NCs. Ni is more strongly partitioned into metal compared to Co, so some Ni rich metal must have been lost in producing the S-type Spherules. Thus, overall Mn, Cr, Co and Ni relative to Fe in S- and I-type spherules supports their origin from primitive chondritic meteorites but do show evidence of volatile loss as well as metal-silicate separation due the processing into spherules.
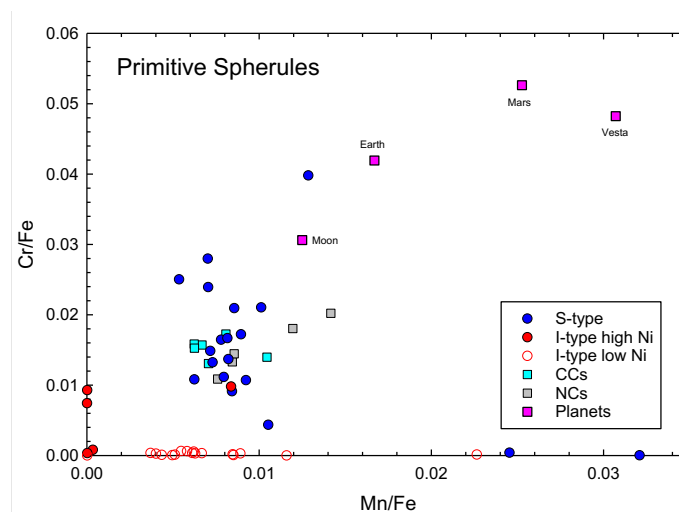
Figure 13. A plot of Cr/Fe vs Mn/Fe for primitive spherules compared to carbonaceous (CC) and non-carbonaceous (NC) chondrites, Earth, Mars, Vesta and the Moon. Sources: CCs and NCs from Alexander

2019ab. Mars: Yoshizaki and McDonough (2020), Vesta: Dreibus and Wänke (1980), Moon: Hauri et al. (2015).
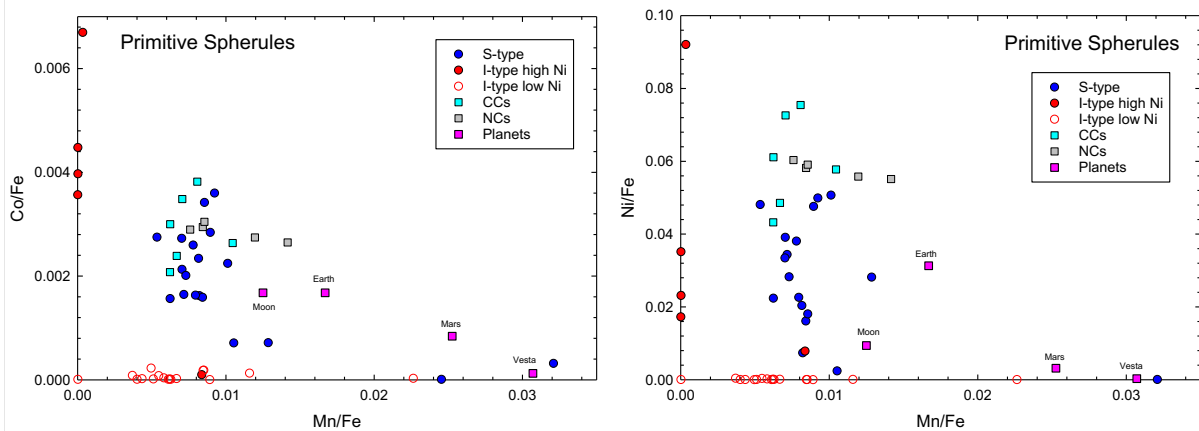
Figure 14. A plot of Co/Fe (a) and Ni/Fe (b) vs Mn/Fe for primitive spherules compared to carbonaceous (CC) and non-carbonaceous (NC) chondrites, Earth, Mars, Vesta and the Moon. Sources: CCs and NCs from Alexander 2019ab. Mars: Yoshizaki and McDonough (2020), Vesta: Dreibus and Wänke (1980), Moon: Hauri et al. (2015).

Origin of D-type spherules: The Mg-Al-Fe plot in **Figure 10** has also been used for classifying terrestrial komatiites, ultramafic lavas that are primarily found in the Archean (cf. Rickwood 1989). The only modification is that Fe is replaced with Fe+Ti. Such a plot is used in **Figure 15** to further understand the origin of D-type spherules. The importance of this diagram is that it shows komatiites as separate fields from tholeiitic basalts and calc-alkaline and tholeiitic magma series. The blue outline shows the field of common terrestrial rock while the red outline includes all terrestrial igneous rocks. The importance for interpreting the D-type spherules is that all except some of the Si-rich D-type spherules are outside the field of common terrestrial igneous rocks and most of them are outside the red outline where there are no terrestrial igneous rocks. In particular, the low-Si BeLaU spherules are all close to the expected meteor path, except for two outside this field. The BeLaU spherules are also clearly different from the lunar high-K KREEP composition, which is the magmatic composition on the Moon with the highest concentration of Be, La and U. Martian SNC meteorites reflect the Fe-rich composition of the martian mantle and are the only known solar system igneous rocks that plot in the triangle between the red line and the Fe+Ti apex of the diagram. However, there are no Martian igneous rock that get as close to the Al-(Fe+Ti) side of the diagram as the BeLaU-type spherules. The BeLaU-type spherules composition could probably be produced by extreme differentiation of an iron-rich Martian-like magma that produced the igneous rocks among the Martian SNC meteorite.

BeLaU spherules are observed to be depleted in volatile elements such as Zn, Mn, K, and Pb. In addition, potassium and Mn are both volatile during planet formation while U and Fe are more refractory, so planets end up with different K/U and Mn/Fe ratios. The data for the D-type spherules are shown in a K/U vs Mn/Fe diagram (**Figure 16**). The reason for using these elemental ratios is that they both have for a long time been used to distinguish materials from different bodies in the solar system (cf. Papike et al. 2017; Halliday and Porcelli 2001). This works because K and U are both highly enriched in melts, so their ratio does not change much during igneous processes. Therefore, unaltered igneous rocks typically directly reflect a ratio close to the planetary value. In contrast Fe and Mn are both roughly equally distributed between melts and solids, so their ratio also does not change during igneous processes. Since K and Mn are both volatile one would expect both to be lost from the spherules during their flight through the atmosphere. The D-type spherules are compared with primitive chondritic meteorite and planetary values in **Figure 16**. There are three distinct groups. The group A spherules are similar to the Earth values and could by this comparison represent some terrestrial volcanic material. We note that these are all Si-rich spherules which

also make them similar in composition to terrestrial igneous rocks. Group B is strongly depleted in K relative to the Earth. Group C is strongly depleted in both K and Mn relative to the Earth. Most of the BeLaU spherules are in the group C field and none are in the Earth-like group A field. This shows that all the BeLaU spherules have exceptionally high volatile element loss, suggestive of extraterrestrial origin.
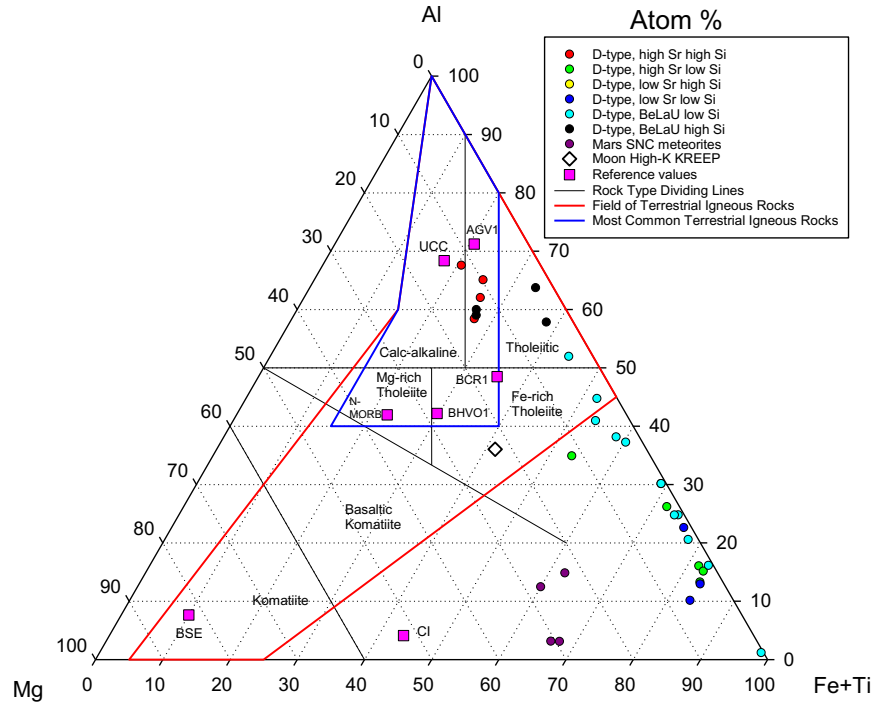
Figure 15. Atomic Mg-Al-Fe plot (atom %) Comparison of IM1 site spherules to differentiated materials from Earth (same references as for **Figure 7**), Moon (High-K KREEP; Warren (1989)) and Mars (SNC meteorites; Lodders (1998)).
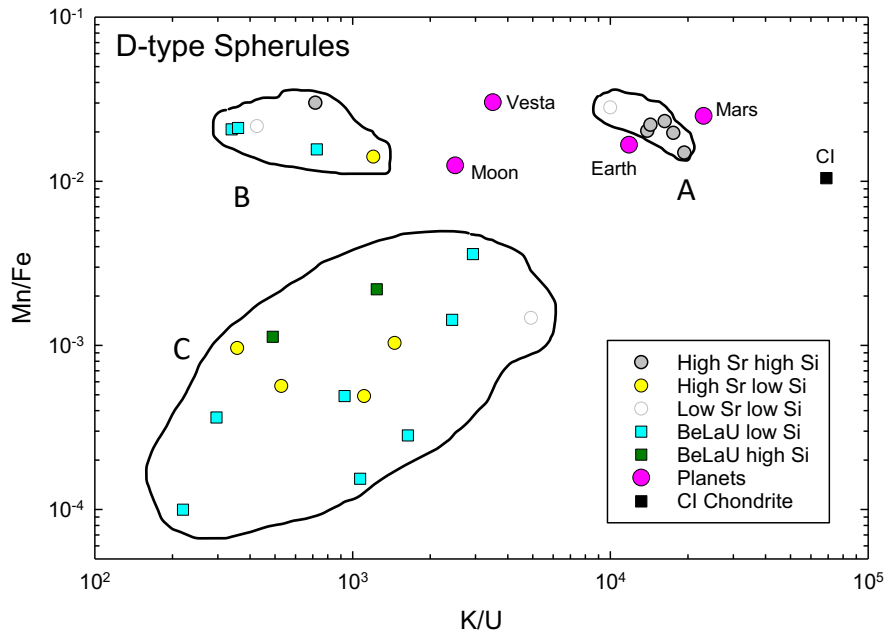
Figure 16. A plot of Mn/Fe vs K/U for D-type spherules compared to CI chondrites, Earth, Mars, Vesta and the Moon. Sources: Anders and Grevesse 1989; McDonough and Sun 1995 Mars: Yoshizaki and McDonough (2020), Vesta: Dreibus and Wänke (1980), Moon: Hauri et al. (2015).

Origin of the novel BeLaU-type spherules: The spherules with enrichment of beryllium (Be), lanthanum (La) and uranium (U), labeled "BeLaU", appear to have an exotic composition different from other Solar System materials. The results for the "BeLaU" spherule S21 are displayed in **Figures 17a and 17b**. We use this spherule to point out some of the unique feature of the "BeLaU" elemental composition. A plot of the elemental abundances of the spherule S21 (normalized to CI chondrites) as a function of atomic number for 56 elements is shown in **Figure 17a**. Across the diagram the peak abundances are for Be, La and U, hence the name "BeLaU." The abundance pattern of S21 implies derivation from a planetary crust, highly enriched in refractory lithophile elements (red dots). The volatile element abundances (green dots) are very low, suggesting either derivation from an extremely volatile-depleted planet or evaporative loss during passage through the Earth's atmosphere. The very low content of refractory siderophile elements with affinity to iron (Re) suggest a source planet with an Fe core. Since there are strong indications that the spherules are derived from a differentiated planet, the data are also plotted in **Figure 17b** as a function of an igneous compatibility sequence. Compatibility is a geochemical parameter measuring how readily a particular element substitutes for a major element in mantle source minerals during melting to produce magma. It also roughly represents the sequence of enrichments of elements in a crystallizing magma.

The abundances of elements as function of their compatibility for all **12** "BeLaU"-type spherules are shown in **Figure 18**. The "BeLaU" spherules' variations in the abundances of trace elements relative to CI chondrites are higher by 1-3 orders of magnitude compared to cosmic spherules from the solar system reviewed by Folco et al. (2015). The "BeLaU" element patterns are compared in **Figure 19** with the highly enriched sources of differentiated bodies in the solar system, including Earth's upper continental crust (Rudnick and Gao, 2014) and kimberlites (Giuliani et al., 2020), lunar magma ocean residual liquid (KREEP) (Warren, 1989), Shergottites from Mars (Lodders, 1998; Jambon et al., 2002) and eucrites from Vesta (Kitts and Lodders, 1998). **Figure 19** presents the comparison of refractory lithophiles that are not easily lost by evaporation or altered by fluids. Shergottites and eucrites are markedly distinct from the "BeLaU" samples due to the systematically lower incompatible element enrichments. The upper continental crust is also overall depleted in incompatible elements compared to "BeLaU." Additionally, "BeLaU" samples have prominent negative anomalies of Ti, Li, higher Lu/Al, and variable Be and Sr enrichments that do not match the smooth pattern of the upper continental crust. Kimberlite is also remarkably distinguished from the "BeLaU" pattern in their Ta and Nb positive anomalies and the strong heavy rare earth element depletion. Lastly, despite the resembling overall element enrichments, the lunar KREEP displays pronounced differences in light rare earth element enrichment and strong Sr, Eu, and Cr negative anomalies from "BeLaU" that distinguish the two groups.

Figure 20 compares the BeLaU elemental pattern with the average upper continental crust composition. This shows that BeLaU-type spherules are depleted by a factor of 2 to more than 10 for all volatile elements (Na, K, Mn, Zn, Rb, Cs, Tl, Pb and Bi), while refractory lithophile elements are enriched by a factor of 3-20 compared to the average continental crust. Also, the rare earth element pattern is substantially fractionated when compared to the average upper continental crust. We must conclude that the elemental pattern of the BeLaU spherules is very different from the upper continental crust composition. The volatile elements (such as K, Mn, Zn and Pb) were most likely lost by evaporation during the passage of a bolide like IM1 through the Earth's lower atmosphere.

We pointed out earlier the difference of the BeLaU signature from KREEP in major elements (**Figure 15**). In spite of some distinct differences from KREEP there are enough similarities in the elemental composition to consider a similar type of origin for both patterns. The lunar KREEP composition is widely believed to be the result of crystallization of an early lunar magma ocean (Snyder et al., 1992; Rapp and Draper, 2018; Charlier et al., 2018). We conclude that the "BeLaU" samples possibly reflect a highly differentiated and extremely evolved composition, but from an unknown source.
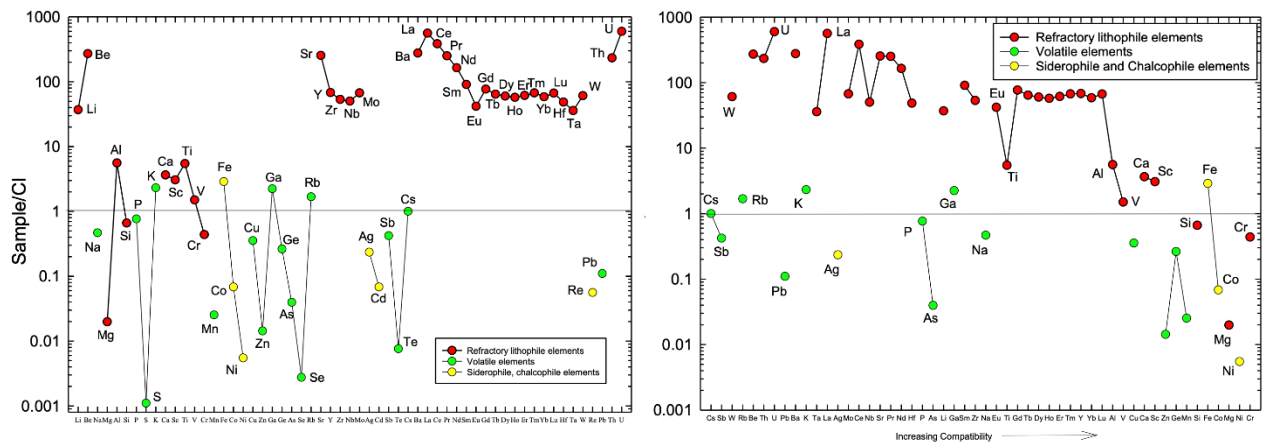
Figure 17: a) The "BeLaU" elemental abundances of the spherule S21 (normalized to CI chondrites) versus atomic number for 56 elements. The solar system standard of CI chondrites is represented by a value of unity on the plot. b) Abundances versus compatibility (see text) for S21. Elements ordered with increasing compatibility towards the right.
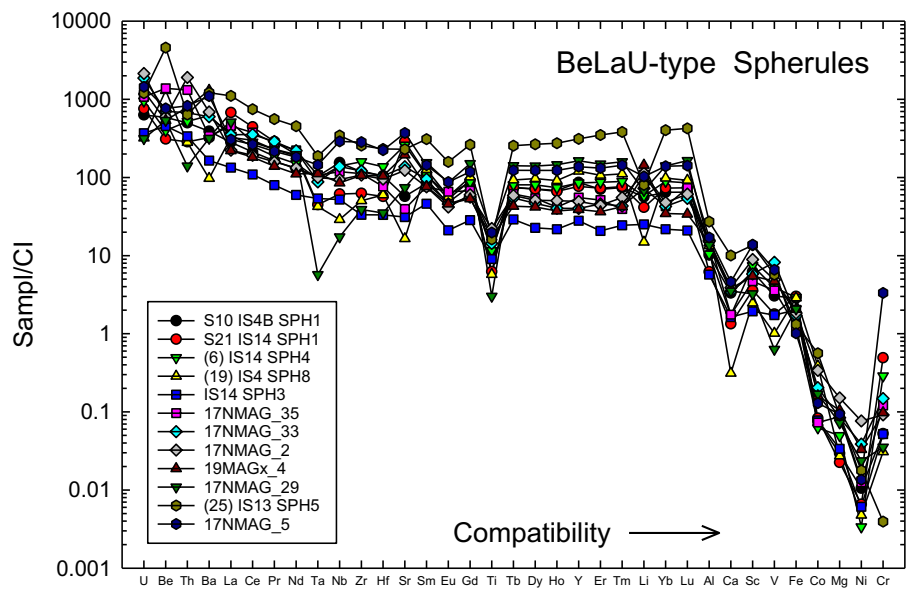
Figure 18. Abundances of refractory lithophile elements as function of their compatibility for all 12 "BeLaU"-type spherules.
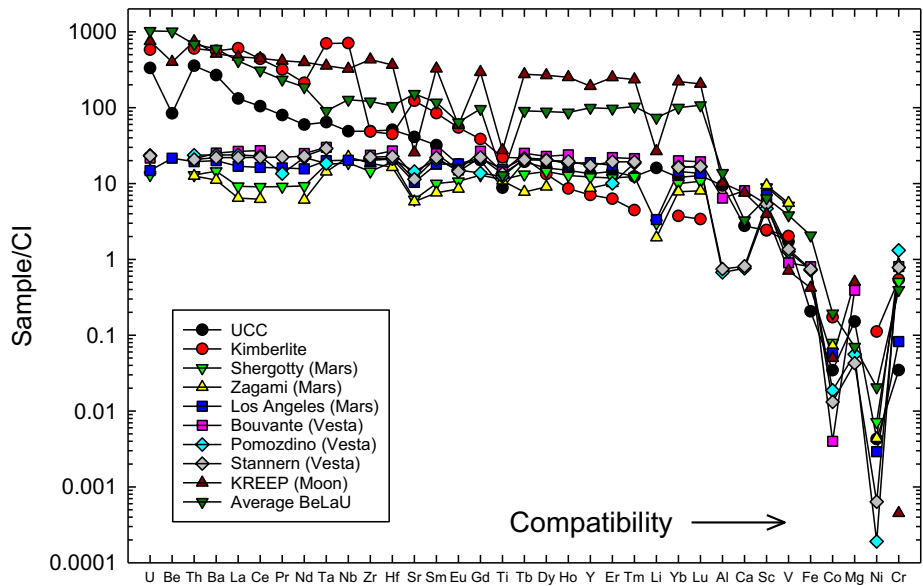
Figure 19. The "BeLaU" element abundance and pattern distinguish from the enriched sources from the solar system bodies. Elements are ordered with increasing compatibility. Data source: Earth's upper continental crust (Rudnick and Gao, 2014); kimberlites (Giuliani et al., 2020); lunar KREEP (Warren, 1989); shergottites (Shergotty, Zagami, and Los Angeles) (Lodders, 1998; Jambon et al, 2002); eucrites (Bouvante, Pomozdino, and Stannern) (Kitts and Lodders, 1998).
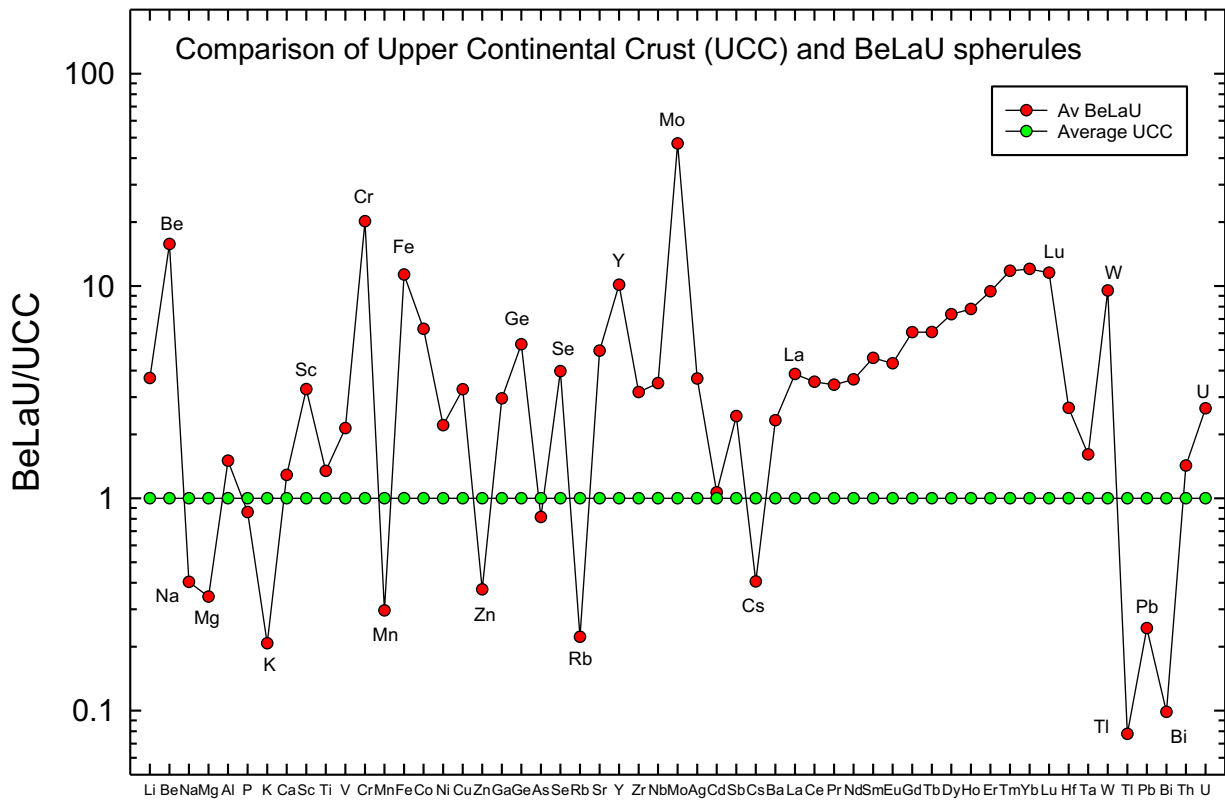
Figure 20. Comparison of average BeLaU-type spherules with average upper continental crust.

Conclusions

The magnetic sled survey around IM1's path during 14–28 June 2023 resulted in 850 magnet particles (consisting mostly of spherules) of diameters within the range of 0.1-1.3 millimeters through 26 runs surveying 0.06 km^2. It is not yet clear as to whether any of these specimens are associated with the IM1 bolide. We identified four distinct groups of primitive spherules (S-type, G-type, I-type high Ni, I-type low-Ni). We also identified a substantial fraction (22%) of the spherules as being derived from igneous precursors. As these are clearly not related to typical achondrite meteorites as for previously discussed differentiated spherules we denote these new types of differentiated spherules as D-type spherules. The D-type spherules were classified into four distinct groups. The chemical compositions of 10 % of the spherules show extremely strong enrichment of refractory lithophile elements such as Be, La and U (BeLaU-type spherule), but very low refractory siderophile elements such as Re. Volatile elements, such as K, Mn, Zn and Pb are very low in the BeLaU-type spherules and were most likely lost by evaporation during passage through the Earth's lower atmosphere. While the BeLaU-type spherules clearly appear to be derived from material formed by igneous fractionation, their chemical composition is novel in that there it is different from known existing solar system materials that have been analyzed thus far, with the KREEP component of the lunar crust being closest. The "BeLaU" samples reflect a highly differentiated, extremely evolved composition, of an unknown origin.

These interpretations will be considered critically along with additional results from spherule analysis in future publications. Recovering larger pieces of similar composition from the search area and comparing the findings to distant control regions would certainly help in the interpretation.

References

Alexander C. M. O'D. (2019a) Quantitative models for the elemental and isotopic fractionations in chondrites: The carbonaceous chondrites, Geochimica et Cosmochimica Acta 254, 277–309. https://doi.org/10.1016/j.gca.2019.02.008

Alexander C. M. O'D. O'D. (2019b) Quantitative models for the elemental and isotopic fractionations in the chondrites: The non-carbonaceous chondrites, Geochimica et Cosmochimica Acta 254, 246–276. https://doi.org/10.1016/j.gca.2019.01.026

Anders E. and Grevesse N. (1989) Abundances of the elements: Meteoritic and solar, Geochimica et Cosmochimica Acta 53, 197-214. https://doi.org/10.1016/0016-7037(89)90286-X

Beckhoff, B.; Kanngießer, B.; Langhoff, N.; Wedell, R.; Wolff, H. (Eds.) 2006, Handbook of Practical X-Ray Fluorescence Analysis. XXIV, ISBN: 3-540-28603-9ASTM E2926 – 13

Blanchard M.B., Brownlee D.E., Bunch T.E., Hodge P.W. and Kyte F.T (1980) Meteoroid ablation spheres from deep-sea sediments, Earth and Planetary Science Letters 46, 178-190. https://doi.org/10.1016/0012-821X(80)90004-7

Brown, P.G. and Borovicka, J. (2023) On the proposed interstellar origin of the USG 20140108 fireball. The Astrophyiscal Journal 953, 167-179

Brownlee, D., Bates, B., Schramm, L., (1997) The Leonard award address presented 1996 july 25, Berlin, Germany: The elemental composition of stony cosmic spherules. Meteoritics & Planetary Science 32, 157–175. https://doi.org/10.1111/j.1945-5100.1997.tb01257.x

Charlier, B., Grove, T. L., Namur, O., Holtz, F. (2018) Crystallization of the lunar magma ocean and the primordial mantle-crust differentiation of the Moon. Geochim. Cosmochim. Acta 234, 50–69.

Dreibus G. and Wänke H. (1980) The bulk composition of the Eucrite arent asteroid and its bearing on planetary evolution, Z. Naturforsch. 35a, 204-216.

Engrand, C., McKeegan, K.D., Leshin, L.A., Herzog, G.F., Schnabel, C., Nyquist, L.E., Brownlee, D.E., (2005) Isotopic compositions of oxygen, iron, chromium, and nickel in cosmic spherules: Toward a better comprehension of atmospheric entry heating effects. Geochimica et Cosmochimica Acta 69, 5365–5385.

Folco L, Cordier C (2015) Micrometeorites. In European Mineralogical Union Notes in Planetary Mineralogy, 15:253-297. https://doi.org/10.1180/EMU-notes.15.9

Gale A., Dalton C. A., Langmuir C. H., Su Y., and Schilling J.-G. (2013) The mean composition of ocean ridge basalts, Geochem. Geophys. Geosyst., 14, 489–518, https://doi.org/10.1029/2012GC004334.

Gallardo, P. A. 2023, *Research Notes of the American Astronomical Society* **7**, 10. https://doi.org/10.3847/2515-5172/ad03f9

Giuliani, A., Pearson, D.G., Soltys, A., Dalton, H., Phillips, D., Foley, S.F., Lim, E., Goemann, K., Griffin, W.L., Mitchell, R.H. (2020) Kimberlite genesis from a common carbonate-rich primary melt modified by lithospheric mantle assimilation. Science Advances 6, eaaz0424. https://doi.org/10.1126/sciadv.aaz0424

Halliday A.N., Porcelli D. (2001) In search of lost planets - the paleocosmochemistry of the inner solar system, Earth and Planetary Science Letters 192, 545-559.

Hauri E.H., Saal A.E., Rutherford M.J., Van Orman J.A. (2015) Water in the Moon's interior: Truth and consequences, Earth and Planetary Science Letters 409, 252–264.

Herzog G.F.H., Xue S., Hall G.S., Nyquist L.E., Shih C.Y., Wiesmann H., Brownlee D.E. (1999) Isotopic and elemental composition of iron, nickel, and chromium in type I deep-sea spherules: Implications for origin and composition of the parent micrometeoroids. Geochimica et Cosmochimica Acta 63, 1443–1457. https://doi.org/10.1016/S0016-7037(99)00011-3.

Jambon et al, 2002 Jambon, A., Barrat, J., Sautter, V., Gillet, P., 403 Gopel, C., Javoy, M., Joron, J., Lesourd, M. (2002) The basaltic shergottite northwest Africa: Petrology and chemistry. Meteoritics & Planetary Science 37, 1147–1164. https://doi.org/10.1111/j.1945-5100.2002.tb00885.x

Jochum K.P, Nohl U., Herwig K., Lammel E., Stoll B. and Hofmann A.W. (2007) GeoReM: A New Geochemical Database for Reference Materials and Isotopic Standards Geostandards and Geoanalytical Research 29 (3) [2005] 333-338. https://doi.org/10.1111/j.1751-908X.2005.tb00904.x

Kitts, K., Lodders, K., (1998) Survey and evaluation of eucrite bulk compositions. Meteoritics and Planetary Science Supplement 33, 197–213. https://doi.org/10.1111/j.1945-5100.1998.tb01334.x

Loeb, A., Adamson, S., Bergstrom, S., Cloete, R., Cohen, S. et al. (2024a) Recovery and Classification of Spherules from the Pacific Ocean Site of the CNEOS 2014 January 8 (IM1) Bolide, RNAAS **8**, 39 https://doi.org/10.3847/2515-5172/ad2370

Loeb, A., Jacobsen, S., Adamson, S., Bergstrom, S., Cloete, R., et al. (2024b) Spherules Recovered from the Pacific Ocean Site of the CNEOS 2014 January 8 (IM1) Bolide, 55th LPSC, https://www.hou.usra.edu/meetings/lpsc2024/pdf/2130.pdf

Loeb A., MacLeod, M. (2024) Interstellar Meteors from Tidal Disruption of Rocky Planets on Eccentric Orbits Around M-Dwarfs. Astronomy & Astrophysics, in press

Lodders, K. (1998) A survey of shergottite, nakhlite and chassigny meteorites whole-rock compositions. Meteoritics & Planetary Science 33, A183–A190. https://doi.org/10.1111/j.1945-5100.1998.tb01331.x

Marvin U.B. and Einaudi M.T. (1967) Black, magnetic spherules from Pleisocene and recent beach sands, Geochimica et Cosmochimica Acta 81, 1871-1884. https://doi.org/10.1016/0016-7037(67)90128-7

McDonough W.F. and Sun S.-s. (1995) The composition of the Earth, Chemical Geology 120, 223-253. https://doi.org/10.1016/0009-2541(94)00140-4

Mutschler, F.E.; Rougon, D.J.; Lavin, O.P. and Hughes R.D. (1977) PETROS - Worldwide Databank of Major Element Chemical Analyses of Igneous Rocks. version 6.1. NOAA National Centers for Environmental Information. https://doi.org/10.7289/V5QN64NM.

Papike J.J., Burger P.V., Bell A.S., and Shearer C.K. (2017) Mn-Fe systematics in major planetary body reservoirs in the solar system and the positioning of the Angrite Parent Body: A crystal-chemical perspective American Mineralogist, 102, 1759–1762. http://dx.doi.org/10.2138/am-2017-6112

Petaev M.I. and Jacobsen S.B. (2009) Petrologic study of SJ101, a new forsterite-bearing CAI from the Allende CV3 chondrite. *Geochim. Cosmochim. Acta* 73, 5100–5114.

Rapp, J.F., & Draper, D.S. (2018). Fractional crystallization of the lunar magma ocean: Updating the dominant paradigm. *Meteoritics & Planetary Science, 53*.

Ray E. and Paul D. (2021) Major and Trace Element Characteristics of the Average Indian Post-Archean Shale: Implications for Provenance, Weathering, and Depositional Environment, ACS Earth Space Chem. 5, 1114−1129. https://doi.org/10.1021/acsearthspacechem.1c00030

Rickwood P. C. (1989) Boundary lines within petrologic diagrams which use oxides of major and minor elements Lithos, 22 (1989) 247-263.

Rudnick and Gao, 2014 Rudnick, R., Gao, S. (2014) The composition of the continental crust, the crust. Treatise on Geochemistry 3. https://doi.org/10.1016/B0-08-043751-6/03016-4

Rudraswami N. G., Shyam Prasad M., Babu E. V. S. S. K., Vijaya Kumar T. (2016) *Meteoritics & Planetary Science* 51, 718-742. https://doi.org/10.1111/maps.12618

Sherman J. (1955) The theoretical derivation of fluorescent X-ray intensities from mixtures. Spectrochimica Acta 7, 283-306.

Siraj, A., Loeb, A., (2022a) A meteor of apparent interstellar origin in the cneos fireball catalog. The Astrophysical Journal 939, 53. https://

Siraj, A., Loeb, A. (2022b) Interstellar meteors are outliers in material strength. The Astrophysical Journal Letters 941, L28. URL: https://dx.doi.org/10.3847/2041-8213/aca8a0

Siraj, A., Loeb, A. (2023) Localizing The First Interstellar Meteor With Seismometer Data. arXiv e-prints, arXiv:2303.07357doi:10.48550/arXiv.2303.07357, arXiv:2303.07357. *Signals 4*, 644–650.

Snyder, G. A., Taylor, A., Neal, C. R. (1992) A chemical model for generating the sources of mare basalts: Combined equilibrium and fractional crystallization of the lunar magmasphere. Geochim. Cosmochim. Acta 56, 3809–3823.

Tankersley K.B., Meyers S.D. and Meyers S.A. (2024) The Hopewell Cosmic Airburst Event: A review of the empirical evidence, Airbursts and Cratering Impacts 2, 1–33. https://doi:10.14293/ACI.2024.0001

Taylor S., Lever J.H and Harvey R.P. (2000) Numbers, types, and compositions of an unbiased collection of cosmic spherules, Meteoritics & Planetary Science 35, 651-666. https://doi.org/10.1111/j.1945-5100.2000.tb01450.x

van Ginneken, M., Goderis, S., Artemieva, N., Debaille, V., Decree, S., Harvey, R.P., Huwig, K.A., Hecht, L., Yang, S., Kaufmann, F.E.D., Soens, B., Humayun, M., Van Maldeghem, F., Genge, M.J., Claeys, P., (2021) A large meteoritic event over Antarctica ca. 430 ka ago inferred from chondritic spherules from the Sør Rondane Mountains. Sci. Adv. 7, eabc1008. https://doi.org/10.1126/sciadv.abc1008

van Ginneken M., Harvey R.P, Goderis S., Artemieva N., Boslough M., Maeda R., Gattacceca J., Folco L., Yamaguchi A., Sonzogni C., Wozniakiewicz P. (2024) The identification of airbursts in the past: Insights from the BIT-58 layer, Earth Planet. Sci. Lett. 627, 118562. https://doi.org/10.1016/j.epsl.2023.118562

Warren, P.H. (1989) KREEP: major-element diversity, trace-element uniformity (almost)., in: Moon in transition: Apollo 14, KREEP, and evolved lunar rocks, pp. 149–153. https://ui.adsabs.harvard.edu/abs/1989mtak.conf..149W

Yoshizaki, T., McDonough, W.F. (2020). The composition of Mars. Geochim. Cosmochim. Acta 273, 137162. https://doi.org/10.1016/j.gca.2020.01.011

Supplementary Material.

Data tables in Excel spreadsheets:
Table S1. Major and trace elements concentrations (ppm) measured by micro-XRF for 745 samples (data plotted in Figures 5, 6, 7, 8, 9a, 10a).
Table S2. Major elements, Be, Cr, Co, Ni, Sr, La and U concentrations (ppm) measured by ICP-MS for 68 samples (data plotted in Figures 9b, 10b, 11, 12, 13, 14, 15).
Table S3. Elemental data (ppm) measured by ICP-MS for 12 BeLaU-type spherules and the CI normalizing values of Anders and Grevesse (1989).

Table S4. Electron microprobe data on the chemical composition in the different region on the surface of the spherule S21, as labeled in **Figure S1.**

Element	Pt#1 (weight %)	Pt#2 (weight %)	Pt#3 (weight %)	Pt#4 (weight %)	Pt#5 (weight %)	Pt#6 (weight %)	Pt#7 (weight %)
C	0.64		0.7	1.5	2.1	5.48	2.66
O	13.95	28.9		32.35	29.18	18.66	34.19
Na	0.63	0.73			0.7	0.72	
Mg	0.28				0.42	0.15	
Al	2.93	3.48		1.15	2.45	1.44	1.18
Si	6.4	10.85			2.92	4.2	0.97
P		0.31					
Cl	0.26	0.4			0.51	1.28	
K	0.39						
Ca	3.88	4.55			1.73	1.85	0.23
Cr					0.31		
Fe	70.65	50.78	99.3	65.01	59.69	66.22	60.77
Total	100	100	100	100	100	100	100
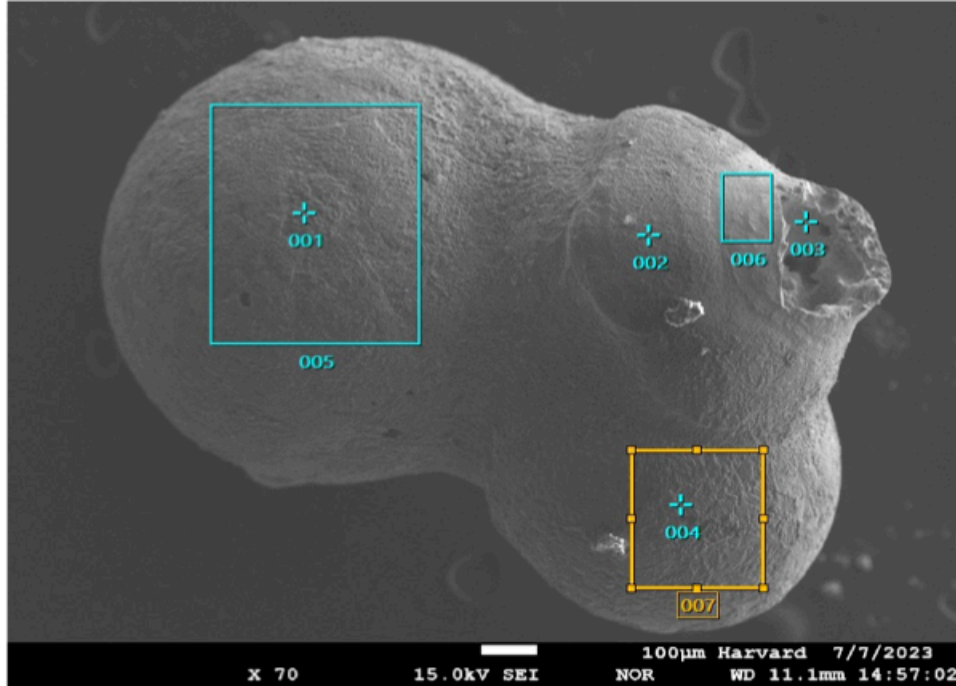
Figure S1. An example of a large (1.3 mm in maximum diameter, 0.9 mm average) spherule in the region along IM1's path is S21 (IS14-SPH1) from run 14.

An example of a large (1.3 mm in maximum diameter, 0.9 mm average) spherule in the region along IM1's likely path is S21 (IS14-SPH1) from run 14. This lopsided spherule, shown in **Fig. S1**, is a composite of three spherules that solidified shortly after merger but too late for the merger product to become spherical. The mass of S21 (1.7 mg) is about twice that of IS16A SPH1 (0.84 mg). The existence of a triple-merger like S21 can potentially be explained as a product of a meteoric airburst. The total mass collected by S21-like spherules in all our runs is of order ~0.1g. Given the sled's width of 1m, the total surveyed area, ~0.06 km^2, constitutes a fraction of $\sim10^{-3}$ of IM1's strewn field. This implies a total mass in S21-like spherules in our estimated strewn field of order ~100g, as expected given that most of IM1's mass evaporated to undetectable particles (well below tens of μm in size) or gas (Tillinghast-Raby et al., 2022). Assigning a mass of $\sim10^{-3}$ g per spherule implies a total number of $\sim10^5$ such spherules. Based on IM1's speed and fireball energy, the total mass ablated by IM1's fireball is $\sim5\times10^5$ g corresponding to an object radius of R ~50 cm (Siraj and Loeb, 2022b). The total number of spherules divided by the initial volume associated with R yields an initial spherule number density of n ~0.2 cm^{-3} which gets diluted as the material expands. For the characteristic diameter of a spherule, ~1mm, the geometric cross-section for spherule-spherule collisions is $\sigma \sim 4\times10^{-2}$ cm^2. The resulting collision probability is $\tau \sim n\sigma(2R) \sim$ (0.2 cm^{-3}) x (4x10^{-2} cm^2) x (100 cm) ~0.8, implying a likelihood of $\tau^2 \sim0.6$ for triple-spherule mergers such as S21. Mergers that occur inside a liquid envelope would result in a spherical shell with embedded sub-spherules inside of it.

Additional images of spherules are shown in Figure S2.
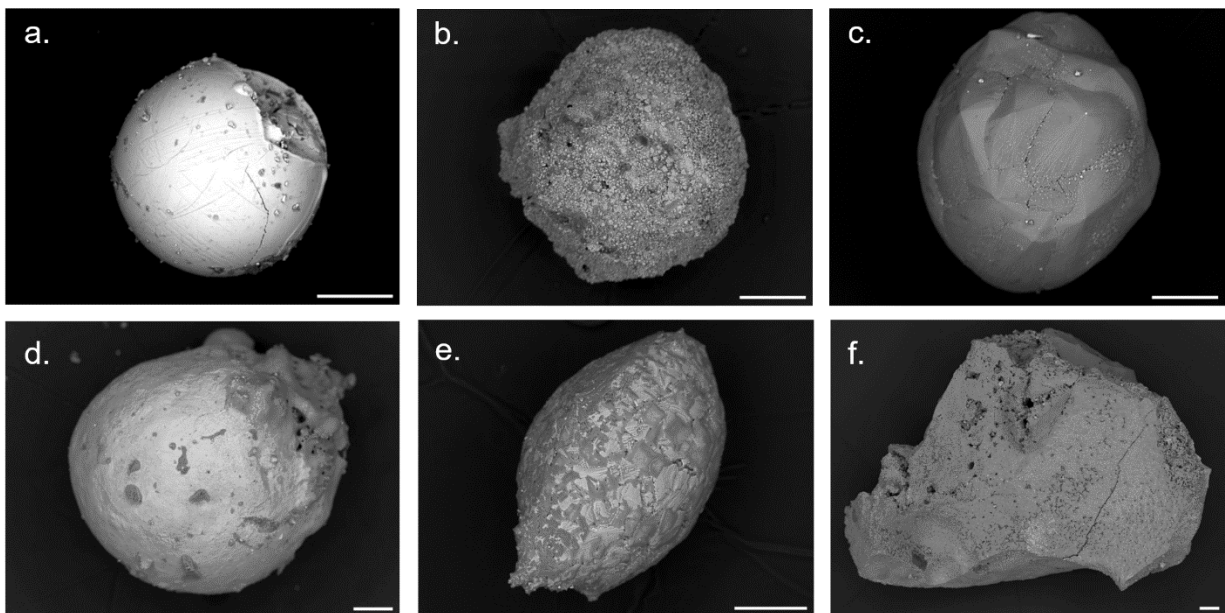
Figure S2. BSE images displaying varied morphologies of the samples in this study: a) IS8M2-1 (I-type, low Ni), b) IS13M1-19 (D-type, low Sr, low Si), c) IS20M-18 (S-type spherule displaying a polyhedral or "turtle-back" morphology), d) IS22M-16 (D-type, high Sr, low Si), e) IS14M(A)-7 (S-type spherule), and f) IS22M1-18 (identified as "shard," no compositional classification). The scale bars indicate 100 microns.

Comparison to Coal Fly Ash and Spherule Data Reported by Rudraswami et al. (2016)
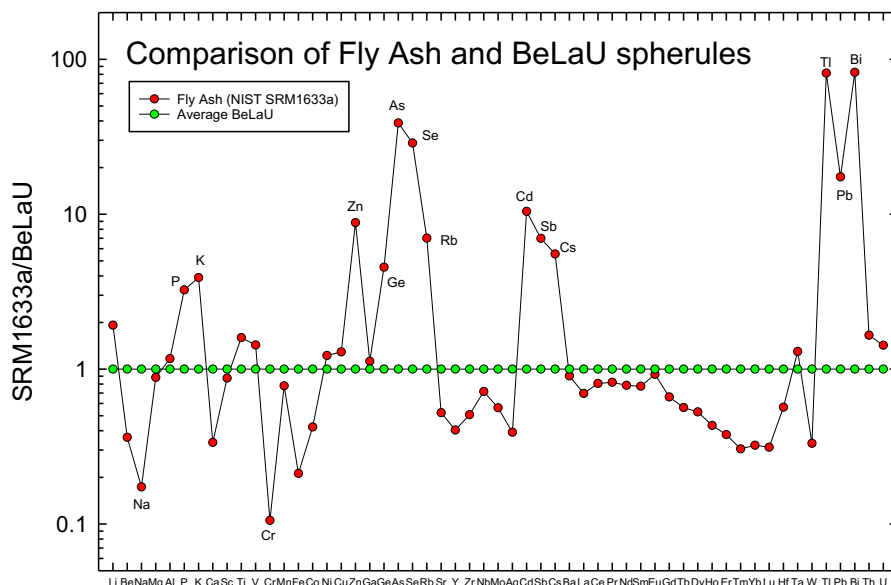
Figure S3. Comparison BeLaU with the NIST coal fly ash standard SRM1633a for 55 elements**.**

It has been claimed that the compositions of BelaU spherules are consistent with coal ash (Gallardo 2023). The National Institute of Standards and Technology (NIST) has provided standards of coal fly ash. The best documented standard for many elements is SRM 1633a (Jochum et al. 2005). We compare the

average composition of BeLaU spherules for 55 elements with the SRM1633a coal fly ash standard in **Figure S3**. Many volatile elements (Zn, As, Se, Cd, Tl, Pb and Bi) are enriched in the coal fly ash by factors of about 10 to 100 compared to the BeLaU spherules. Some refractory elements (Be, Ca, Cr, Fe, Y, Tm, Yb, Lu W) are depleted by factors of 3 to 10 in coal fly ash when compared to BeLaU spherules. Thus, BeLaU spherules do not have the composition of coal fly ash, making the claim of Gallardo (2023) invalid (Loeb et al. 2024a). The BeLaU composition shows an excess of Be, La and U, and other elements by up to three orders of magnitude relative to the solar system standard of CI chondrites.

Many of these elements are 1–2 orders of magnitude more abundant than for the spherules reported by Rudraswami et al. (2016) (their Figure 2). All spherules, except for one, reported by Rudraswami et al. (2016) are S-type spherules (**Figure S4**), and the one exception does not have trace element enrichments like our BeLaU spherules.
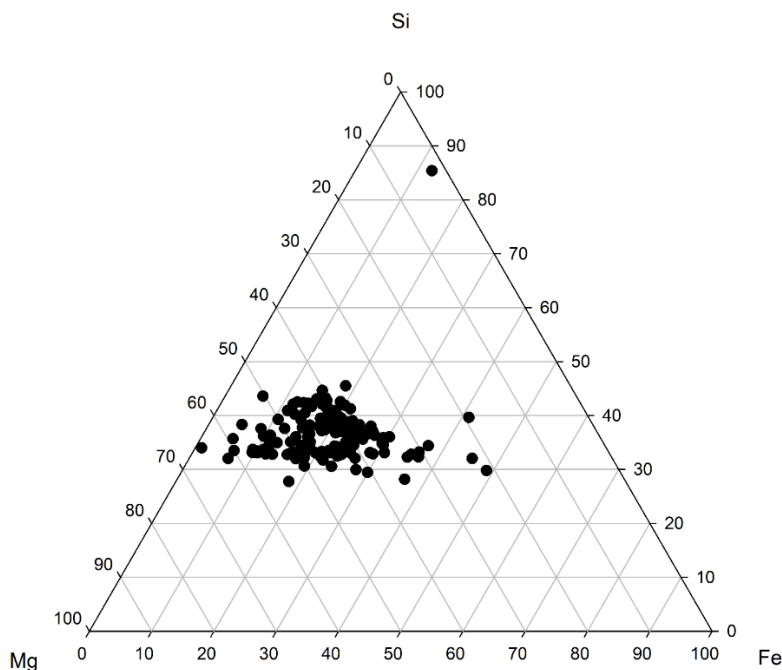
Figure S4 Ternary Mg-Si-Fe plot (atom %) of spherules from Rudraswami et al. (2016) normalized to (Mg + Fe + Si) and plotted in elemental proportions. The spherules in this study have been characterized to be S-type spherules.

Table S1. Major and trace elements concentrations (ppm) measured by micro-XRF for 745 samples (data plot

Type	Sub-type	Track	Sample name	O	Na	Mg
I-type	High Ni	15	IS 15 MAG-1__5_2	274729	15459	340
I-type	High Ni	6	IS 6_1	304404	0	1663
I-type	High Ni	19	19MAGx_25	291485	0	576
I-type	High Ni	8	IS 8-MAG-2__20_1	297798	1999	2288
I-type	High Ni	12	IS 12-MAG-2__24_2	303632	15843	6400
I-type	High Ni	12	IS 12-MAG-2__25_1	303632	15843	6400
I-type	High Ni	12	IS 12 -MAG 1__32_1	297950	0	43
I-type	High Ni	13	IS 13M UNSIFTED 1 s__14_1	301568	0	0
I-type	High Ni	13	IS 13M UNSIFTED 60 s__14_1	302748	3873	1165
I-type	High Ni	12	IS 12 -MAG 1__15_1	298838	0	374
I-type	High Ni	14	IS 14M Unsifted__22_1	301799	0	7305
I-type	High Ni	22	IS 22-MAG -1__12_1	302124	3920	900
I-type	High Ni	12	IS 12-MAG-2__8_1	305536	9908	1127
I-type	High Ni	14	IS 14M Unsifted__42_1	302032	2072	195
I-type	High Ni	22	IS 22-MAG-3__8_1	300689	15033	4190
I-type	High Ni	24	IS 24 -MAG__4_1	300929	4216	0
I-type	High Ni	12	IS 12 -MAG 1__10_1	302259	0	201
I-type	High Ni	12	IS 12-MAG-2__10_1	334652	23474	475
I-type	Low Ni	17	17MAG_37	300569	1247	1270
I-type	Low Ni	15	IS 15 MAG-1__3_1	304121	23761	0
I-type	Low Ni	10	IS 10 -MAG__3_1	307534	8489	8556
I-type	Low Ni	13	IS 13-M-1__11_1	303294	689	38
I-type	Low Ni	16	IS 16 MAG_2__13_2	306420	3088	3762
I-type	Low Ni	11	IS 11-MAG__13_1	303069	0	0
I-type	Low Ni	12	IS 12 -MAG 1__33_1	306796	1290	1315
I-type	Low Ni	20	IS 20 MAG__22_1	303053	721	508
I-type	Low Ni	12	IS 12-MAG-2__26_1	307734	9472	0
I-type	Low Ni	14	IS 14M Unsifted__38_1	304500	2098	608
I-type	Low Ni	20	IS 20 MAG__33_2	317672	8769	107
I-type	Low Ni	16	IS 16 MAG_2__2_2	305332	11039	589
I-type	Low Ni	17	17MAG_42	306544	2546	3681
I-type	Low Ni	19	19NMAG_3	304372	753	1487
I-type	Low Ni	24	IS 24 -MAG__14_1	303837	1307	1283
I-type	Low Ni	19	IS 19 M__23_1	305791	7426	359
I-type	Low Ni	19	IS 19 M__24_1	301555	17591	3086
I-type	Low Ni	12	IS 12-MAG-2__23_1	316414	13455	1868
I-type	Low Ni	12	IS 12 -MAG 1__9_2	303406	0	551
I-type	Low Ni	24	IS 24 -MAG__1_1	304920	660	1258
I-type	Low Ni	16	IS 16 MAG_2__17_1	313828	2688	5057
I-type	Low Ni	14	IS 14M UNSIFTED B 60 s_5_1	309689	7552	7565
I-type	Low Ni	13	IS 13M UNSIFTED 60 s__27_1	306750	1912	2991
I-type	Low Ni	19	19NMAG_46	305305	0	1566
I-type	Low Ni	15	IS 15 MAG-1__4_1	317903	8047	3985
I-type	Low Ni	13	IS 13M UNSIFTED 60 s__40_1	305544	709	319
I-type	Low Ni	20	IS 20 MAG__32_1	310137	3592	3198

I-type	Low Ni	13	IS 13M UNSIFTED 1 s__37_1	316618	629	6424
I-type	Low Ni	8	IS 8-MAG-2__6_2	301860	4121	109
I-type	Low Ni	24	IS 24 -MAG__7_1	306571	3804	0
I-type	Low Ni	12	IS 12-MAG-2__2_2	303385	6386	44
I-type	Low Ni	17	IS 17-MAG__4_1	308712	522	1698
I-type	Low Ni	17	17NMAG_30	300436	25	1427
I-type	Low Ni	22	IS 22-MAG-3__9_2	308601	1625	649
I-type	Low Ni	19	IS 19 M__8_1	301286	598	0
I-type	Low Ni	19	IS 19 M 24 Small	302242	22600	3702
I-type	Low Ni	12	IS 12 -MAG 1__5_1	306791	2481	1814
I-type	Low Ni	13	IS 13M UNSIFTED 60 s__37_1	317105	5035	11639
I-type	Low Ni	13	IS 13-M-1__1_1	302524	12630	203
I-type	Low Ni	13	IS 13M UNSIFTED 60 s__12_1	311555	3571	6895
I-type	Low Ni	13	IS 13M UNSIFTED 60 s__24_1	304994	2598	600
I-type	Low Ni	13	IS 13M UNSIFTED 1 s__27_1	306739	12459	3969
I-type	Low Ni	14	IS 14M Unsifted__15_1	304205	10353	734
I-type	Low Ni	13	IS 13M UNSIFTED 1 s__12_1	312012	0	6130
I-type	Low Ni	9	IS 9C S18	303107	413	343
I-type	Low Ni	20	IS 20 MAG__31_1	302571	71764	1066
I-type	Low Ni	19	IS 19 M__15_1	316972	44498	12078
I-type	Low Ni	13	IS 13M UNSIFTED 60 s__25_1	325212	83	6902
I-type	Low Ni	8	IS 8-MAG-2__29_2	317850	83137	4147
I-type	Low Ni	8	IS 8-MAG-2__14_1	304988	1289	1685
I-type	Low Ni	19	IS 19 M__11_1	308426	1331	1121
I-type	Low Ni	12	IS 12 -MAG 1__1_1	305523	0	953
I-type	Low Ni	12	IS 12-MAG-3__8_1	302331	3397	0
I-type	Low Ni	13	IS 13M UNSIFTED 60 s__61_1	308334	5484	2485
I-type	Low Ni	13	IS 13M UNSIFTED 60 s__54_1	306127	16085	3746
I-type	Low Ni	19	19MAG_3	305049	0	2051
I-type	Low Ni	17	17MAG_44	304852	1048	1630
I-type	Low Ni	13	IS 13M UNSIFTED 1 s__40_1	305830	0	0
I-type	Low Ni	15	IS 15 M 2__1_1	307071	26682	192
I-type	Low Ni	20	IS 20 MAG__19_2	308853	3007	4221
I-type	Low Ni	12	IS 12 -MAG 1__39_2	303983	0	2389
I-type	Low Ni	15	IS 15 MAG-1__7_2	300615	68362	0
I-type	Low Ni	10	IS 10 -MAG__1_1	310690	25911	2354
I-type	Low Ni	13	IS 13M UNSIFTED 60 s__56_1	304021	3135	488
I-type	Low Ni	22	IS 22 MAG-2__2_1	311239	6443	1115
I-type	Low Ni	19	IS 19 M__10_1	313124	26606	3863
I-type	Low Ni	12	IS 12-MAG-3__3_1	311601	30776	1513
I-type	Low Ni	24	IS 24 -MAG__6_1	304628	3489	109
I-type	Low Ni	13	IS 13M UNSIFTED 60 s__41_1	304452	786	627
I-type	Low Ni	12	IS 12 -MAG 1__36_1	310819	2860	0
I-type	Low Ni	12	IS 12 -MAG 1__41_1	303105	2134	505
I-type	Low Ni	9	IS 9-MAG__2_1	321539	0	10430
I-type	Low Ni	19	IS 19 M__5_1	304980	7650	415
I-type	Low Ni	15	IS 15 C_1	303211	0	0

I-type	Low Ni	22	IS 22 MAG-2__4_1	311591	25815	833
I-type	Low Ni	9	IS 9-MAG__13_1	322906	1351	8302
I-type	Low Ni	11	IS 11-MAG__6_1	307017	22785	1929
I-type	Low Ni	12	IS 12 -MAG 1__11_2	304108	0	386
I-type	Low Ni	17	17NMAG_10	303211	0	359
I-type	Low Ni	11	IS 11-MAG__16_1	306152	4015	1130
I-type	Low Ni	13	IS 13-MAG B__1_1	318856	9258	1787
I-type	Low Ni	9	IS 9-MAG__12_1	305239	11302	259
I-type	Low Ni	19	IS 19 M__20_1	307664	14294	1205
I-type	Low Ni	14	IS 14M Unsifted__26_1	304683	1675	141
I-type	Low Ni	8	IS 8-MAG-2__15_2	312871	11036	2424
I-type	Low Ni	12	IS 12 -MAG 1__22_1	304282	943	0
I-type	Low Ni	12	IS 12 -MAG 1__23_1	304282	943	0
I-type	Low Ni	17	IS 17-MAG__2_1	305218	13267	1465
I-type	Low Ni	24	IS 24 -MAG__3_1	303392	1129	0
I-type	Low Ni	16	IS 16 MAG_2__16_1	301584	62995	0
I-type	Low Ni	13	IS 13M UNSIFTED 60 s__15_1	307017	3900	1068
I-type	Low Ni	8	IS 8-MAG-2__32_2	299878	6331	241
I-type	Low Ni	8	IS 8-MAG-2__24_1	321588	5077	1095
I-type	Low Ni	13	IS 13M UNSIFTED 60 s__58_1	304529	0	898
I-type	Low Ni	20	IS 20 MAG__24_2	307420	4875	614
I-type	Low Ni	8	IS 8-MAG-2__10_2	306838	16907	1744
I-type	Low Ni	20	IS 20 MAG__23_1	303529	578	0
I-type	Low Ni	8	IS 8-MAG-2__13_2	304694	6798	271
I-type	Low Ni	19	IS 19__2_1	306343	2948	1441
I-type	Low Ni	9	IS 9-MAG__8_1	309129	8807	520
I-type	Low Ni	17	IS 17-MAG__13_1	319034	28867	4116
I-type	Low Ni	19	IS 19 M__9_1	302780	4699	62
I-type	Low Ni	7	IS 7 MAG__1_1	309721	14287	799
I-type	Low Ni	20	IS 20 MAG__17_2	302407	0	327
I-type	Low Ni	16	IS 16 MAG_2__6_2	302723	0	0
I-type	Low Ni	12	IS 12-MAG-2__22_1	302679	311	0
I-type	Low Ni	19	19NMAG_66	303100	1518	628
I-type	Low Ni	8	IS 8-MAG-2__12_2	303698	545	398
I-type	Low Ni	13	IS 13M UNSIFTED 1 s__24_1	305375	0	0
I-type	Low Ni	20	IS 20 MAG__26_2	307435	2168	2340
I-type	Low Ni	19	IS 19 M__26_1	303824	547	0
I-type	Low Ni	13	IS 13M UNSIFTED 60 s__21_1	314461	4386	3424
I-type	Low Ni	16	IS 16 MAG_2__19_1	302695	26223	0
I-type	Low Ni	11	IS 11-MAG__3_1	302476	5357	0
I-type	Low Ni	13	IS 13M UNSIFTED 60 s__45_1	304274	3406	292
I-type	Low Ni	8	IS 8-MAG-2__16_1	303874	0	0
I-type	Low Ni	12	IS 12 -MAG 1__30_1	304146	484	551
I-type	Low Ni	13	IS 13-M-1__20_1	309800	2260	709
I-type	Low Ni	12	IS 12 -MAG 1__27_1	315155	6798	9696
I-type	Low Ni	21	IS 21__2_1	305416	532	0
I-type	Low Ni	13	IS 13M UNSIFTED 1 s__25_1	321377	0	6183

I-type	Low Ni	12	IS 12-MAG-2__21_2	303142	4282	0
I-type	Low Ni	13	IS 13M UNSIFTED 60 s__63_1	309629	0	849
I-type	Low Ni	22	IS 22-MAG -1_right__3_1	302585	0	0
I-type	Low Ni	12	IS 12-MAG-2__17_2	304442	3901	502
I-type	Low Ni	13	IS 13-M-1__17_1	307994	1208	2065
I-type	Low Ni	8	IS 8-MAG-2__27_1	301094	0	635
I-type	Low Ni	22	IS 22-MAG-3__7_1	305239	143	3790
I-type	Low Ni	11	IS 11-MAG__9_1	303248	3760	0
I-type	Low Ni	14	IS 14M Unsifted__9_1	306804	1849	894
I-type	Low Ni	12	IS 12-MAG-2__14_2	308090	9670	757
I-type	Low Ni	14	IS 14M Unsifted__19_1	303889	3449	117
I-type	Low Ni	12	IS 12 -MAG 1__21_2	323199	0	0
I-type	Low Ni	8	IS 8-MAG-2__1_1	302148	2528	0
I-type	Low Ni	4	IS 4-MAG-A__6_2	299707	4128	0
I-type	Low Ni	19	19MAGx_13	301177	0	0
I-type	Low Ni	19	19NMAG_62	301190	0	0
I-type	Low Ni	8	IS 8-MAG-2__26_1	302948	2292	0
I-type	Low Ni	15	IS 15 B_1	302555	0	0
I-type	Low Ni	19	19NMAG_64	300566	2187	454
I-type	Low Ni	4	IS 4-MAG-A__2_2	301636	4612	276
I-type	Low Ni	16	IS 16 MAG_2__5_2	301914	0	0
I-type	Low Ni	19	19NMAG_59	300764	0	59
I-type	Low Ni	19	19MAGx_17	301508	0	0
I-type	Low Ni	19	19NMAG_72	291486	0	0
I-type	Low Ni	19	19MAGx_16	299706	0	0
I-type	Low Ni	8	IS 8-MAG-2__4_2	303195	1078	26
I-type	Low Ni	19	19NMAG_63	301288	558	181
I-type	Low Ni	24	IS 24 -MAG__2_1	302160	8166	0
I-type	Low Ni	12	IS 12 -MAG 1__26_1	301734	0	0
I-type	Low Ni	19	19MAGN_61	301094	0	0
I-type	Low Ni	19	19NMAG_56	301816	0	232
I-type	Low Ni	17	IS 17-MAG__16_1	299372	1412	566
I-type	Low Ni	12	IS 12 -MAG 1__29_1	302833	0	0
I-type	Low Ni	21	IS 21__3_1	302564	0	351
I-type	Low Ni	19	IS 19 M__22_1	303896	7406	0
I-type	Low Ni	19	19MAG_4 part2	301434	0	859
I-type	Low Ni	17	17NMAG_13	302636	0	277
I-type	Low Ni	12	IS 12-MAG-2__15_1	303075	3030	0
I-type	Low Ni	13	IS 13M UNSIFTED 1 s__45_1	304219	0	0
I-type	Low Ni	13	IS 13M UNSIFTED 1 s__58_1	303600	0	0
I-type	Low Ni	13	IS 13-M-1__4_1	302291	28908	22
I-type	Low Ni	19	19MAG_2	302995	0	1010
I-type	Low Ni	13	IS 13M UNSIFTED 1 s__41_1	302236	11252	2706
I-type	Low Ni	19	19NMAG_55	300711	0	784
I-type	Low Ni	17	17NMAG_33	303534	0	0
I-type	Low Ni	12	IS 12 S3_1	308739	109	0
I-type	Low Ni	13	IS 13M UNSIFTED 1 s__50_1	306017	0	0

I-type	Low Ni	13	IS 13M UNSIFTED 1 s__56_1	304250	0	0
I-type	Low Ni	17	17MAG_22	302679	0	148
I-type	Low Ni	13	IS 13M UNSIFTED 60 s__50_1	306219	2032	593
I-type	Low Ni	13	IS 13M UNSIFTED 60 s__19_1	304622	13	0
I-type	Low Ni	13	IS 13M UNSIFTED 1 s__19_1	305194	0	0
I-type	Low Ni	13	IS 13M UNSIFTED 1 s__15_1	304430	8872	0
I-type	Low Ni	19	19NMAG_1	302643	0	1387
I-type	Low Ni	13	IS 13M UNSIFTED 1 s__63_1	307685	3607	0
I-type	Low Ni	13	IS 13M UNSIFTED 1 s__17_1	302515	6464	0
I-type	Low Ni	19	19NMAG_45	304570	1049	1697
I-type	Low Ni	13	IS 13M UNSIFTED 60 s__17_1	302010	7842	389
I-type	Low Ni	17	17NMAG_1	304293	831	1338
I-type	Low Ni	15	IS 15 M 2__6_2	303118	45031	0
I-type	Low Ni	19	IS 19 M__25_1	302451	57807	422
I-type	Low Ni	17	17MAG_31	304884	0	808
I-type	Low Ni	17	17MAG_21	307583	0	554
I-type	Low Ni	24	IS 24 -MAG__13_1	307228	664	1791
I-type	Low Ni	17	17MAG_17	314489	332	3192
I-type	Low Ni	17	17MAG_7	314790	431	3272
I-type	Low Ni	9	IS 9-MAG__14_1	306549	6991	915
I-type	Low Ni	15	IS 15 M 2__7_1	307075	18239	721
I-type	Low Ni	13	IS 13M UNSIFTED 1 s__54_1	306314	3743	289
I-type	Low Ni	13	IS 13M UNSIFTED 1 s__61_1	307945	0	0
I-type	Low Ni	17	17MAG_13	306549	842	1335
I-type	Low Ni	17	17MAG_3	306743	1051	1360
I-type	Low Ni	19	19NMAG_60	306014	7436	1930
I-type	Low Ni	17	17NMAG_16	306426	1572	2501
I-type	Low Ni	8	IS 8-MAG-2__7_1	313229	12079	3769
I-type	Low Ni	17	17MAG_4	307099	6483	2845
I-type	Low Ni	17	17MAG_14	307282	6613	2814
I-type	Low Ni	19	19MAG_1	308981	383	2004
I-type	Low Ni	17	17NMAG_3	309058	0	740
I-type	Low Ni	8	IS 8-MAG-2__23_1	314708	4997	1727
I-type	Low Ni	15	IS 15 MAG-1__8_2	305036	23560	799
I-type	Low Ni	19	19MAG_4 part1	308221	0	1102
I-type	Low Ni	17	17NMAG_33 TI	313464	0	0
I-type	Low Ni	16	IS 16 MAG_2__15_1	320752	8234	0
I-type	Low Ni	17	17MAG_45	319207	1275	3687
I-type	Low Ni	14	IS 14M Unsifted__37_1	307241	15108	516
I-type	Low Ni	4	IS 4-MAG-A__14_2	306685	37256	1523
I-type	Low Ni	17	17NMAG_14	315012	0	6850
I-type	Low Ni	13	IS 13M UNSIFTED 1 s__21_1	311553	762	1386
I-type	Low Ni	17	IS 17-MAG__5_2	302101	41437	10841
I-type	Low Ni	8	IS 8-MAG-2__5_1	318119	4581	1624
S-type		13	IS 13M UNSIFTED 60 s__39_1	424509	6207	300999
S-type		13	IS 13M UNSIFTED 1 s__39_1	426929	0	297282
S-type		19	IS 19 M__4_1	423368	7216	284811

S-type	13	IS 13-M-1__15_1	423460	11655	207412
S-type	14	IS 14M Unsifted__16_1	429669	1838	189171
S-type	13	IS 13 NM-1_1	409190	19531	238724
S-type	24	IS 24 -MAG__10_1	414197	5606	231467
S-type	12	IS 12 -MAG 1__4_2	426257	1196	174517
S-type	12	IS 12 -MAG 1__17_1	416818	1655	208220
S-type	13	IS 13M UNSIFTED 1 s__18_1	419059	0	210453
S-type	14	IS 14M Unsifted__17_1	420644	8407	172138
S-type	17	17MAG_25	430676	1001	123697
S-type	13	IS 13M UNSIFTED 1 s__22_1	413807	0	209210
S-type	13	IS 13M UNSIFTED 60 s__18_1	415868	5982	195664
S-type	13	IS 13M UNSIFTED 60 s__22_1	412143	3971	206779
S-type	22	IS 22-MAG -1__6_1	410058	6150	212022
S-type	13	IS 13M UNSIFTED 60 s__60_1	414126	30071	155147
S-type	12	IS 12-MAG-3__1_1	405851	5743	219176
S-type	17	IS 17-MAG__6_1	409178	1878	200909
S-type	19	19NMAG_6	429362	0	119911
S-type	13	IS 13M UNSIFTED 1 s__60_1	415101	18949	153922
S-type	19	19MAGx_9	403826	3268	215969
S-type	13	IS 13M UNSIFTED 1 s__30_1	411375	3511	158050
S-type	13	IS 13M UNSIFTED 60 s__30_1	411003	4453	155165
S-type	13	IS 13-M-1__10_1	409782	8888	162241
S-type	11	IS 11-MAG__2_1	400244	8028	213773
S-type	4	IS 4-MAG-A__13_2	404890	2454	198300
S-type	13	IS 13M UNSIFTED 1 s__2_1	404979	3124	165528
S-type	15	IS 15 MAG-1__9_1	403869	2570	188538
S-type	20	IS 20 MAG__16_1	401715	14025	176990
S-type	19	IS 19 M__2_1	405519	1672	184568
S-type	13	IS 13M UNSIFTED 1 s__33_1	397646	0	221201
S-type	17	17NMAG_7	404935	576	179978
S-type	13	IS 13M UNSIFTED 60 s__33_1	396531	4933	215750
S-type	22	IS 22-MAG -1_right__1_1	402847	1438	170453
S-type	17	17MAG_12	403453	732	173962
S-type	19	IS 19 M__6_1	397711	17093	180988
S-type	12	IS 12 -MAG 1__8_1	396431	2567	196626
S-type	20	IS 20 MAG__14_1	403281	4473	163112
S-type	12	IS 12 -MAG 1__28_1	391487	3917	198416
S-type	24	IS 24 -MAG__8_1	399426	9243	182589
S-type	11	IS 11-MAG-3__3_1	400735	13804	144242
S-type	11	IS 11-MAG__8_1	395308	837	188612
S-type	17	17MAG_2	402816	807	171423
S-type	8	IS 8-MAG-2__2_2	398296	11618	164366
S-type	13	IS 13M UNSIFTED 60 s__64_1	395157	2719	168690
S-type	13	IS 13M UNSIFTED 1 s__64_1	395504	0	171417
S-type	19	IS 19 M__7_1	409863	21459	116216
S-type	22	IS 22-MAG -1__15_1	410799	4097	130001
S-type	12	IS 12-MAG-2__12_2	398339	27823	147629

S-type	13	IS 13M UNSIFTED 60 s__20_1	403221	7352	147499
S-type	13	IS 13M UNSIFTED 1 s__20_1	402884	7077	148604
S-type	13	IS 13-M-1__7_1	393705	5416	194176
S-type	13	IS 13-M-1__13_1	392377	23543	176165
S-type	17	17MAG_1	387780	1159	200283
S-type	17	17MAG_11	387676	787	200340
S-type	16	IS 16 M 1__1_1	397982	23047	147977
S-type	19	19MAGx_10	390505	524	189744
S-type	17	IS 17-MAG__10_1	401322	5121	135113
S-type	19	19NMAG_68 NI	379679	0	162195
S-type	13	IS 13-M-1__2_1	392930	11271	160558
S-type	16	IS 16 MAG_2__11_1	392585	10715	152189
S-type	22	IS 22-MAG -1__4_2	384194	3258	186056
S-type	13	IS 13M UNSIFTED 60 s__10_1	410549	2802	117792
S-type	12	IS 12 -MAG 1__43_1	386998	2951	178097
S-type	12	IS 12 -MAG 1__13_1	391942	1973	181966
S-type	16	IS 16 MAG_2__1_1	390265	6364	186370
S-type	17	IS 17-MAG__14_1	393716	5683	172129
S-type	19	19NMAG_71	390771	0	172736
S-type	18	IS 18-MAG__2_1	387182	709	180884
S-type	13	IS 13M UNSIFTED 60 s__55_1	389798	5660	164231
S-type	14	IS 14M Unsifted__23_1	393024	2170	156739
S-type	19	19MAGx_5	393166	857	164627
S-type	13	IS 13M UNSIFTED 60 s__43_1	402816	12228	127159
S-type	17	17MAG_39	393964	758	157239
S-type	13	IS 13M UNSIFTED 1 s__65_1	393835	0	168839
S-type	12	IS 12 -MAG 1__2_1	390055	3486	185381
S-type	19	19MAGx_18	392870	0	157287
S-type	13	IS 13M UNSIFTED 60 s__34_1	386499	1873	174983
S-type	13	IS 13M UNSIFTED 60 s__65_1	394167	1888	162827
S-type	12	IS 12 -MAG 1__12_2	390458	397	165424
S-type	12	IS 12-MAG-2__1_1	391764	34887	135656
S-type	13	IS 13M UNSIFTED 1 s__34_1	386189	0	174984
S-type	4	IS 4-MAG-A__10_2	387464	18196	153478
S-type	13	IS 13M UNSIFTED 60 s__36_1	386733	4422	170722
S-type	13	IS 13M UNSIFTED 60 s__8_1	396434	129	139751
S-type	13	IS 13M UNSIFTED 1 s__43_1	401711	1298	131719
S-type	13	IS 13M UNSIFTED 60 s__2_1	393091	5716	149331
S-type	17	17NMAG_11 NI	373299	0	164624
S-type	13	IS 13M UNSIFTED 60 s__62_1	392909	8642	154631
S-type	20	IS 20 MAG__18_1	390754	3698	165615
S-type	4	IS 4-MAG-A__1_1	391862	3167	155502
S-type	13	IS 13M UNSIFTED 1 s__55_1	387716	248	156768
S-type	13	IS 13M UNSIFTED 1 s__10_1	408362	3768	101879
S-type	13	IS 13M UNSIFTED 1 s__36_1	386336	9433	162852
S-type	14	IS 14M Unsifted__18_1	378760	15774	176632
S-type	13	IS 13M UNSIFTED 1 s__62_1	394483	0	152458

S-type	13	IS 13M UNSIFTED 60 s__59_1	382106	2619	171259
S-type	22	IS 22-MAG -1__5_1	387769	2100	162890
S-type	13	IS 13M UNSIFTED 1 s__59_1	382423	152	172103
S-type	20	IS 20 MAG__10_2	385922	5603	175092
S-type	13	IS 13M UNSIFTED 1 s__8_1	394525	0	134670
S-type	17	17MAG_5	384722	4435	142980
S-type	17	17NMAG_9	387752	590	159571
S-type	12	IS 12 -MAG 1__16_2	392582	1569	141980
S-type	13	IS 13M UNSIFTED 1 s__57_1	387559	0	161666
S-type	24	IS 24_1	382774	832	166896
S-type	12	IS 12 -MAG 1__18_2	383750	1747	165346
S-type	16	IS 16 MAG_2__18_1	382297	35250	154487
S-type	8	IS 8-MAG-2__8_1	383587	444	163208
S-type	18	IS 18-MAG__4_1	378493	61459	144134
S-type	19	IS 19 M__21_1	380702	8096	165854
S-type	17	17NMAG_23	385013	854	161215
S-type	19	19NMAG_48	382990	1928	173897
S-type	8	IS 8-MAG-2__18_2	380087	20667	159243
S-type	13	IS 13M UNSIFTED 60 s__29_1	387367	0	148170
S-type	22	IS 22-MAG -1__22_2	377266	40443	151334
S-type	13	IS 13-M-1__6_1	378577	6524	171987
S-type	13	IS 13M UNSIFTED 60 s__57_1	384275	8322	154590
S-type	17	17MAG_15	383527	4391	137149
S-type	20	IS 20 MAG__11_1	382461	2744	170687
S-type	11	IS 11-MAG-3__2_2	387805	6333	153330
S-type	17	17NMAG_26	379501	1417	157207
S-type	19	19MAGx_1	380843	2513	163734
S-type	4	IS 4-MAG-A__12_1	381232	3839	157362
S-type	17	17MAG_10	385272	629	161503
S-type	13	IS 13M UNSIFTED 1 s__29_1	386587	0	141851
S-type	16	IS 16 MAG_2__3_1	381647	6672	153113
S-type	17	IS 17-MAG__1_1	387221	3741	148440
S-type	19	19MAGx_2	386114	0	142145
S-type	11	IS 11-MAG__7_1	379822	21810	160793
S-type	17	17MAG_20	384258	551	160477
S-type	13	IS 13M UNSIFTED 60 s__49_1	377028	4001	159079
S-type	24	IS 24 -MAG__9_1	379892	9425	164621
S-type	22	IS 22-MAG-3__5_1	377493	13803	158316
S-type	9	IS 9-MAG__9_1	385431	6131	149577
S-type	16	IS 16 M 1__3_1	379262	18258	146619
S-type	14	IS 14M Unsifted__3_1	374306	13713	157095
S-type	14	IS 14M Unsifted__43_1	374425	15367	159829
S-type	13	IS 13M UNSIFTED 1 s__49_1	377159	677	156463
S-type	17	17NMAG_11	375072	203	159579
S-type	14	IS 14M Unsifted__7_1	385942	3437	140193
S-type	15	IS 15 M 2__5_1	375263	34029	154842
S-type	13	IS 13M UNSIFTED 1 s__13_1	382128	0	158458

S-type	13	IS 13M UNSIFTED 60 s__13_1	381418	4902	153600
S-type	13	IS 13M UNSIFTED 60 s__47_1	377747	1790	151576
S-type	19	19NMAG_47	383577	1718	130369
S-type	17	17MAG_19	378881	141	142437
S-type	19	19MAGx_3	378285	0	146778
S-type	14	IS 14M Unsifted__21_1	378985	775	152943
S-type	22	IS 22-MAG-3__1_1	379542	8372	154466
S-type	13	IS 13M UNSIFTED 60 s__66_1	376510	5122	132240
S-type	22	IS 22-MAG -1__10_1	375415	4217	153202
S-type	12	IS 12-MAG-3__9_2	377946	13580	149391
S-type	22	IS 22-MAG -1__9_1	375055	2969	153340
S-type	19	19NMAG_53	376505	261	152475
S-type	13	IS 13M UNSIFTED 60 s__32_1	379317	11345	131291
S-type	13	IS 13M UNSIFTED 1 s__47_1	376041	0	150669
S-type	4	IS 4-MAG-A__16_1	378887	23471	127728
S-type	12	IS 12-MAG-2__19_2	377050	21534	134525
S-type	17	17NMAG_21	371953	145	148820
S-type	21	IS 21__1_1	373203	1147	150366
S-type	17	17MAG_18	371257	356	149113
S-type	17	17MAG_6 Ni	377094	0	145479
S-type	17	17MAG_9	377741	393	136845
S-type	9	IS 9-MAG__11_1	369549	22070	132957
S-type	13	IS 13M UNSIFTED 60 s__48_1	375086	2004	147777
S-type	24	IS 24 -MAG__12_1	374476	3459	140133
S-type	12	IS 12-MAG-3__2_2	371375	34685	117133
S-type	13	IS 13M UNSIFTED 1 s__48_1	375017	0	148109
S-type	13	IS 13M UNSIFTED 1 s__32_1	379746	1035	130212
S-type	17	17MAG_16	375990	519	142592
S-type	12	IS 12 -MAG 1__35_1	373818	7830	146280
S-type	9	IS 9-MAG__7_1	379971	8114	132614
S-type	17	17MAG_9 Ni	374902	0	138677
S-type	13	IS 13-M-1__3_1	378001	3156	151612
S-type	17	17MAG_6	375637	70	141349
S-type	17	17MAG_43	375030	2547	146452
S-type	4	IS 4-MAG-A__7_2	371096	5212	145881
S-type	14	IS 14M Unsifted__10_1	375986	0	128374
S-type	12	IS 12 -MAG 1__42_1	371517	2773	141660
S-type	13	IS 13-M-1__14_2	377496	23144	122658
S-type	12	IS 12-MAG-2__9_2	368173	20237	141666
S-type	13	IS 13M UNSIFTED 60 s__51_1	373830	8156	136496
S-type	20	IS 20 MAG__1_1	372851	5716	144065
S-type	17	17MAG_8	368718	617	146044
S-type	8	IS 8-MAG-2__30_1	371528	9795	137218
S-type	17	17MAG_19 Ni	373679	0	135439
S-type	19	19MAG_6	378722	0	131988
S-type	13	IS 13M UNSIFTED 1 s__66_1	374396	0	121926
S-type	12	IS 12 -MAG 1__31_1	379710	4441	125749

S-type	12	IS 12-MAG-2__5_2	376986	29016	111321
S-type	11	IS 11-MAG__1_1	373217	11194	131566
S-type	20	IS 20 MAG__4_1	369318	1780	144201
S-type	15	IS 15 MAG-1__2_1	370937	20285	123835
S-type	10	IS 10 -MAG__2_1	372166	39812	102606
S-type	9	IS 9-MAG__5_1	374237	9655	141036
S-type	11	IS 11-MAG__14_1	371673	4709	134151
S-type	8	IS 8-MAG-2__3_2	359089	107679	118941
S-type	8	IS 8-MAG-2__19_2	365953	22196	127730
S-type	12	IS 12 -MAG 1__38_1	366392	7667	128870
S-type	19	19MAGx_14	368669	1372	141865
S-type	17	17MAG_5 Fe	383950	2433	90895
S-type	12	IS 12 -MAG 1__40_1	370727	1653	142155
S-type	14	IS 14M Unsifted__13_1	367134	8334	146020
S-type	19	19NMAG_74	365689	0	128389
S-type	19	19MAGx_6	372389	813	119533
S-type	17	17NMAG_20	370520	286	138816
S-type	17	17MAG_40	403234	3473	54414
S-type	13	IS 13M UNSIFTED 60 s__16_1	381318	3144	104806
S-type	19	19NMAG_49	370319	0	128549
S-type	17	17MAG_26	371036	1648	131322
S-type	12	IS 12-MAG-3__11_1	356946	134119	98393
S-type	13	IS 13M UNSIFTED 1 s__51_1	371212	0	128067
S-type	17	17NMAG_25	367762	882	138793
S-type	15	IS 15 M 2__2_1	365517	27091	123832
S-type	13	IS 13M UNSIFTED 60 s__53_1	371443	9469	114131
S-type	13	IS 13M UNSIFTED 1 s__44_1	368900	0	126508
S-type	13	IS 13M UNSIFTED 1 s__23_1	371047	0	131794
S-type	4	IS 4-MAG-A__9_1	372479	7930	125426
S-type	13	IS 13-M-1__18_1	365438	35118	128515
S-type	13	IS 13M UNSIFTED 60 s__44_1	366644	3114	128126
S-type	12	IS 12-MAG-3__4_1	365468	11868	128423
S-type	19	19NMAG_54	363051	0	132898
S-type	13	IS 13M UNSIFTED 1 s__16_1	378318	0	103359
S-type	13	IS 13M UNSIFTED 60 s__53_1 1	370494	7575	111679
S-type	13	IS 13M UNSIFTED 60 s__53_1 B	370494	7575	111679
S-type	17	17NMAG_19	367483	0	119257
S-type	4	IS 4-MAG-A__11_2	367087	4979	129976
S-type	12	IS 12-MAG-3__7_2	370150	13965	115803
S-type	17	17MAG_5 Cr	350790	0	116990
S-type	4	IS 4-MAG-A__5_2	364901	6516	127519
S-type	13	IS 13M UNSIFTED 60 s__23_1	369828	1289	124191
S-type	15	IS 15 M 2__3_2	377178	0	104067
S-type	4	IS 4-MAG-A__8_2	363858	19925	122336
S-type	15	IS 15 MAG-1__12_2	365983	33703	99723
S-type	19	19NMAG_68	367180	0	104984
S-type	19	IS 19 M__1_1	360764	18503	118894

S-type	19	19NMAG_47-Ni	347055	0	82940
S-type	14	IS 14M Unsifted__45_1	365768	8030	126943
S-type	12	IS 12-MAG-2__7_2	362026	12355	127929
S-type	14	IS 14M Unsifted__34_1	361564	18690	124140
S-type	13	IS 13M UNSIFTED 1 s__53_1	372980	2239	96437
S-type	17	IS 17-MAG__7_2	363980	8002	121013
S-type	12	IS 12 -MAG 1__19_1	365921	0	121278
S-type	17	17NMAG_22	360451	0	116136
S-type	14	IS 14M Unsifted__8_1	366701	812	116550
S-type	4	IS 4-MAG-A__3_2	365103	6435	107461
S-type	17	17NMAG_12	361089	0	117706
S-type	19	IS 19 M 24 Large	364540	49495	99600
S-type	11	IS 11-MAG__12_1	368234	8172	118065
S-type	14	IS 14M Unsifted__5_1	366293	2782	115064
S-type	19	19MAGx_15	370226	520	102140
S-type	14	IS 14M Unsifted__44_1	361730	6849	117624
S-type	17	17NMAG_18 NI	357564	0	113415
S-type	19	19MAGx_12	361581	0	120731
S-type	14	IS 14M Unsifted__39_1	367746	1259	91307
S-type	13	IS 13-M-1__12_1	366626	3604	114981
S-type	17	17NMAG_26 NI	286392	0	89431
S-type	13	IS 13M UNSIFTED 1 s__5_1	360880	11082	112295
S-type	13	IS 13M UNSIFTED 60 s__5_1	362338	1554	113247
S-type	9	IS 9-MAG__10_1	370136	17673	58171
S-type	19	IS 19 M__17_1	360662	28557	90148
S-type	11	IS 11-MAG__5_1	366136	7504	103076
S-type	15	IS 15 MAG-1__6_1	363257	26980	91305
S-type	13	IS 13M UNSIFTED 1 s__31_1	357287	0	100716
S-type	12	IS 12 -MAG 1__6_2	363394	0	97661
S-type	17	IS 17-MAG__11_1	355538	38881	102306
S-type	12	IS 12 -MAG 1__37_1	363015	10870	99312
S-type	14	IS 14M Unsifted__12_1	356571	3799	113531
S-type	14	IS 14M Unsifted__41_1	357084	14762	113940
S-type	12	IS 12 -MAG 1__24_1	378208	3	57538
S-type	9	IS 9B S15	354458	805	113525
S-type	12	IS 12-MAG-2__13_1	349418	44344	102832
S-type	22	IS 22 MAG-2__1_1	357572	21747	92802
G-type	13	IS 13M UNSIFTED 60 s__31_1	355351	554	90465
G-type	8	IS 8-MAG-2__11_1	357208	8474	93016
G-type	19	IS 19 M__3_1	360493	30864	77353
G-type	19	19MAGx_22	344059	0	109472
G-type	15	IS 15 M 2__4_1	353694	55476	78226
G-type	12	IS 12 B_1	368411	823	63222
G-type	16	IS 16 MAG_2__12_1	357962	28965	81501
G-type	11	IS 11-MAG__11_1	364730	8567	73700
G-type	12	IS 12-MAG-2__20_1	350310	21238	99386
G-type	17	17NMAG_22 NI	336269	0	89668

G-type	23	IS 23 M__1_1	352447	9314	74961
G-type	17	17NMAG_18	354958	0	96309
G-type	14	IS 14M Unsifted__31_1	357474	11227	87198
G-type	16	IS 16 M 1__4_2	353641	4336	95788
G-type	13	IS 13M UNSIFTED 1 s__52_1	343901	0	96053
G-type	12	IS 12-MAG-2__16_1	348245	8453	92979
G-type	22	IS 22-MAG -1__21_2	358786	5275	72340
G-type	15	IS 15 MAG-1__1_1	355498	20718	89431
G-type	13	IS 13M UNSIFTED 60 s__11_1	350645	558	79357
G-type	17	IS 17-MAG__8_2	361608	47022	42746
G-type	13	IS 13M UNSIFTED 1 s__11_1	353094	0	72131
G-type	22	IS 22-MAG -1_right__2_1	353619	0	82844
G-type	20	IS 20 MAG__20_1	350246	5790	85655
G-type	13	IS 13M UNSIFTED 60 s__52_1	341358	0	88820
G-type	12	IS 12-MAG-2__11_1	346400	19129	86667
G-type	17	17NMAG_27	348925	0	76819
G-type	19	IS 19 M__19_1	362724	4658	47359
G-type	14	IS 14M Unsifted__28_1	349334	3676	78842
G-type	12	IS 12 -MAG 1__34_1	352140	15203	71386
G-type	20	IS 20 MAG__21_1	354097	967	67521
G-type	14	IS 14M Unsifted__20_1	358630	0	63086
G-type	19	19MAGx_11	359099	0	49463
G-type	9	IS 9-MAG__4_1	339786	4022	78928
G-type	16	IS 16 M 1__2_1	354153	21570	59244
G-type	14	IS 14M Unsifted__14_1	352159	88	83659
G-type	13	IS 13-MAG B__4_1	345516	18886	63884
G-type	11	IS 11-MAG__15_1	336416	6496	95302
G-type	12	IS 12-MAG-2__18_2	342171	24157	88719
G-type	19	19MAGx_8	345873	0	58888
G-type	14	IS 14M UNSIFTED B 60 s_8_1	336664	28680	74511
G-type	17	IS 17-MAG__3_1	351304	0	52913
G-type	12	IS 12-MAG-3__10_1	343264	15493	54634
G-type	19	19NMAG_51	345182	0	49683
G-type	24	IS 24_2	351608	762	56158
G-type	12	IS 12-MAG-2__4_2	355387	23962	38717
G-type	19	19MAGx_19	344882	0	46529
G-type	17	17MAG_40 Cu	357525	0	31244
G-type	13	IS 13M UNSIFTED 1 s__42_1	327446	0	67877
G-type	13	IS 13M UNSIFTED 60 s__42_1	326083	145	68734
G-type	14	IS 14M Unsifted__35_1	335228	1216	51206
G-type	17	17MAG_29	342864	249	48349
G-type	24	IS 24 -MAG__5_1	340260	10581	35862
G-type	13	IS 13-M-1__5_1	337168	4734	57868
G-type	14	IS 14M Unsifted__46_1	338658	0	41353
G-type	17	17MAG_38 Ni 2	323440	0	42638
G-type	17	17MAG_38 Ni 1	323342	0	36850
G-type	19	19MAGx_23	322806	0	43618

G-type		12	IS 12-MAG-2__3_1	328044	28748	34990
G-type		8	IS 8-MAG-2__17_2	335003	6231	27975
G-type		9	IS 9-MAG__6_1	322387	12044	25626
G-type		8	IS 8-MAG-2__31_2	338208	11794	14422
G-type		13	IS 13-MAG B__6_2	320600	9724	31562
G-type		17	IS 17-MAG__12_2	326308	4669	23151
G-type		14	IS 14M Unsifted__40_1	316210	0	29934
G-type		17	17MAG_38	318704	0	24428
G-type		23	IS 23 M__2_1	315572	0	27717
G-type		19	19MAGx_26	313495	0	25064
G-type		8	IS 8-MAG-2__25_1	314169	2042	26197
G-type		12	IS 12 -MAG 1__25_2	316372	0	18807
G-type		17	17MAG_30	332538	2223	15316
G-type		8	IS 8-MAG-2__28_1	313121	4155	19557
G-type		15	IS 15 MAG-1__11_1	326571	12153	12512
G-type		13	IS 13-MAG B__7_1	313702	1119	22777
G-type		22	IS 22-MAG -1__17_1	321809	3568	14547
G-type		19	IS 19__1_1	316606	6058	9016
G-type		20	IS 20 MAG__3_1	302106	0	19229
G-type		12	IS 12 -MAG 1__20_1	310861	1587	16986
G-type		13	IS 13M UNSIFTED 1 s__9_1	320215	0	7847
D-type	High Sr, high Si	17	IS 17-MAG__17_2	433886	9357	8953
D-type	High Sr, high Si	13	IS 13M UNSIFTED 1 s__3_1	465744	14498	5220
D-type	High Sr, high Si	15	IS 15 MAG-1__10_1	438607	33752	3585
D-type	High Sr, high Si	22	IS 22-MAG -1__3_2	452383	19390	4328
D-type	High Sr, high Si	22	IS 22 MAG-2__8_1	426804	25964	6328
D-type	High Sr, high Si	13	IS 13M UNSIFTED 60 s__3_1	463100	18292	10580
D-type	High Sr, high Si	13	IS 13M UNSIFTED 1 s__1_1	433442	12348	7057
D-type	High Sr, high Si	13	IS 13M UNSIFTED 60 s__1_1	432651	22002	12455
D-type	High Sr, high Si	11	IS 11-MAG 2__1_1	437156	24059	10306
D-type	High Sr, high Si	17	17MAG_33 Ni	457285	14467	8073
D-type	High Sr, high Si	19	IS 19 M__14_1	451431	35573	3000
D-type	High Sr, high Si	17	17MAG_36	424408	22240	12236
D-type	High Sr, high Si	20	IS 20 MAG__7_2	412896	33192	10642
D-type	High Sr, high Si	22	IS 22-MAG -1__7_1	419925	27766	11242
D-type	High Sr, high Si	22	IS 22-MAG -1__8_1	419925	27766	11242
D-type	High Sr, high Si	11	IS 11-MAG 2__3_1	443060	21195	10888
D-type	High Sr, high Si	17	17NMAG_29	428520	22656	14645
D-type	High Sr, high Si	17	17NMAG_5	449883	17085	5571
D-type	High Sr, high Si	16	IS 16 MAG_2__4_1	438108	15952	67785
D-type	High Sr, high Si	22	IS 22 MAG-2__6_1	436079	11419	27254
D-type	High Sr, low Si	8	IS 8-MAG-2__9_2	421225	3465	2355
D-type	High Sr, low Si	19	IS 19 M__16_1	408695	1778	8536
D-type	High Sr, low Si	22	IS 22-MAG -1__20_1	397243	7029	9384
D-type	High Sr, low Si	17	17MAG_35 Ni 1	403346	0	714
D-type	High Sr, low Si	17	IS 17-MAG__15_1	391021	39726	5580
D-type	High Sr, low Si	24	IS 24 -MAG__11_1	392147	15882	12288

D-type	High Sr, low Si	17	17MAG_35 Ni 2	391872	0	838
D-type	High Sr, low Si	19	19NMAG_50	378417	2222	12512
D-type	High Sr, low Si	17	17MAG_35	372911	2299	4300
D-type	High Sr, low Si	19	IS 19 M__18_1	369510	2982	8808
D-type	High Sr, low Si	22	IS 22-MAG-3__4_2	362544	97144	14232
D-type	High Sr, low Si	17	17MAG_33	350941	0	9317
D-type	High Sr, low Si	17	17NMAG_6	353270	2353	7556
D-type	High Sr, low Si	9	IS 9-MAG__3_1	345775	21453	16793
D-type	High Sr, low Si	19	19MAGx_4	347850	9926	4935
D-type	High Sr, low Si	14	IS 14M UNSIFTED B 60 s_2_1	333734	60742	5309
D-type	High Sr, low Si	14	IS 14M Unsifted__48_1	344885	7822	11025
D-type	High Sr, low Si	17	17NMAG_2	342753	1226	10054
D-type	High Sr, low Si	15	IS 15 M 2__8_1	328989	73345	2554
D-type	High Sr, low Si	13	IS 13-MAG B__3_2	314504	139827	1078
D-type	High Sr, low Si	17	17NMAG_28	329648	0	628
D-type	High Sr, low Si	22	IS 22-MAG -1__16_1	326467	4293	0
D-type	High Sr, low Si	14	IS 14M Unsifted__47_1	329013	5190	2721
D-type	Low Sr, high Si	13	IS 13 NM-2_1	452594	32227	4936
D-type	Low Sr, high Si	14	IS 14 NM__1_1	470732	32625	1735
D-type	Low Sr, high Si	17	IS 17-MAG__19_1	463670	32183	2658
D-type	Low Sr, high Si	9	IS 9-NM_1	466003	31583	8480
D-type	Low Sr, high Si	16	IS 16 MAG_2__14_1	447115	60422	1522
D-type	Low Sr, high Si	17	17NMAG_4	460671	26930	9084
D-type	Low Sr, high Si	20	IS 20 MAG__8_2	467580	28765	806
D-type	Low Sr, high Si	12	IS 12 M4_1	461701	40861	16899
D-type	Low Sr, high Si	13	IS 13 NM-1_2	447871	50816	9366
D-type	Low Sr, high Si	22	IS 22 MAG-2__7_1	444757	65937	8190
D-type	Low Sr, high Si	14	IS 14M Unsifted__4_1	464441	27797	10371
D-type	Low Sr, high Si	12	IS 12-MAG-3__6_1	446815	59013	5124
D-type	Low Sr, high Si	19	19MAG_10Fe	449248	27457	19308
D-type	Low Sr, high Si	17	17MAG_28 Particle 2	449969	27637	9556
D-type	Low Sr, high Si	17	17MAG_23	453317	29122	1411
D-type	Low Sr, high Si	14	IS 14M UNSIFTED B 60 s_3_1	446133	30597	11779
D-type	Low Sr, high Si	11	IS 11-MAG 2__2_2	445398	30319	12256
D-type	Low Sr, high Si	12	IS 12-MAG-3__12_1	435658	48719	8952
D-type	Low Sr, high Si	19	19NMAG_7	445505	26015	1709
D-type	Low Sr, high Si	19	19NMAG_8	443276	14831	40910
D-type	Low Sr, high Si	22	IS 22-MAG -1__2_2	440110	34934	923
D-type	Low Sr, high Si	17	IS 17-MAG__18_2	447091	7253	2861
D-type	Low Sr, high Si	20	IS 20 MAG__9_1	438556	28914	15167
D-type	Low Sr, high Si	17	17MAG_27	439219	24942	4035
D-type	Low Sr, high Si	19	IS 19__3_1	438905	34504	3011
D-type	Low Sr, high Si	15	IS 15 M_1	435337	20077	39668
D-type	Low Sr, high Si	14	IS 14M UNSIFTED B 60 s_4_1	432868	42545	10262
D-type	Low Sr, high Si	19	19MAG_5	447848	26489	33684
D-type	Low Sr, high Si	14	IS 14 NM__4_1	425715	33699	23071
D-type	Low Sr, high Si	22	IS 22-MAG -1__19_1	427420	25527	1653

D-type	Low Sr, high Si	14	IS 14M UNSIFTED B 60 s_6_1	424739	27994	2604
D-type	Low Sr, high Si	19	19NMAG_5	437566	9007	3059
D-type	Low Sr, high Si	19	19NMAG_8 Ti	430215	4446	0
D-type	Low Sr, high Si	17	17NMAG_32	439629	3206	1869
D-type	Low Sr, high Si	19	19NMAG_57	424905	20028	2145
D-type	Low Sr, high Si	19	19NMAG_4	422780	17768	0
D-type	Low Sr, high Si	19	19NMAG_7 Ti	418183	26951	0
D-type	Low Sr, high Si	22	IS 22-MAG-3__10_1	411095	50410	2493
D-type	Low Sr, high Si	13	IS 13M UNSIFTED 60 s__38_1	414005	21392	1305
D-type	Low Sr, high Si	20	IS 20 MAG__5_1	419252	22982	39
D-type	Low Sr, high Si	18	IS 18-MAG__1_1	402636	69149	485
D-type	Low Sr, high Si	20	IS 20 MAG__28_2	415320	35576	852
D-type	Low Sr, high Si	13	IS 13M UNSIFTED 60 s__28_1	417000	24028	1690
D-type	Low Sr, high Si	16	IS 16 MAG_2__10_2	415191	36571	8497
D-type	Low Sr, low Si	13	IS 13M UNSIFTED 1 s__28_1	416861	14098	0
D-type	Low Sr, low Si	17	17MAG_28 Particle 1	412894	24553	1444
D-type	Low Sr, low Si	17	17NMAG_31	414250	19824	3142
D-type	Low Sr, low Si	19	19MAGx_7	412082	20789	2813
D-type	Low Sr, low Si	22	IS 22-MAG -1__13_1	411523	23792	886
D-type	Low Sr, low Si	17	17NMAG_8	406689	18030	1417
D-type	Low Sr, low Si	13	IS 13M UNSIFTED 1 s__7_1	419069	2084	14009
D-type	Low Sr, low Si	19	19MAGx_21	408206	26557	5491
D-type	Low Sr, low Si	22	IS 22 MAG-2__3_1	399739	57659	3157
D-type	Low Sr, low Si	13	IS 13M UNSIFTED 60 s__7_1	419916	5911	21699
D-type	Low Sr, low Si	14	IS 14M UNSIFTED B 60 s_7_1	403493	41715	1954
D-type	Low Sr, low Si	12	IS 12 -MAG 1__7_1	406772	20366	1614
D-type	Low Sr, low Si	20	IS 20 MAG__25_2	404791	20375	2106
D-type	Low Sr, low Si	11	IS 11-MAG__10_1	406264	25269	2098
D-type	Low Sr, low Si	11	IS 11-MAG__4_1	405621	21909	1313
D-type	Low Sr, low Si	19	IS 19 M__12_1	405510	40967	1214
D-type	Low Sr, low Si	19	19NMAG_58	399114	20565	2051
D-type	Low Sr, low Si	19	19NMAG_73	400576	18561	0
D-type	Low Sr, low Si	13	IS 13M UNSIFTED 1 s__6_1	398404	22678	0
D-type	Low Sr, low Si	4	IS 4-MAG-A__4_2	394778	56956	3457
D-type	Low Sr, low Si	19	19NMAG_70	399980	14959	0
D-type	Low Sr, low Si	17	17MAG_32	397453	23316	3580
D-type	Low Sr, low Si	13	IS 13-M-1__16_2	398270	22080	521
D-type	Low Sr, low Si	22	IS 22-MAG -1__8_2	401027	21054	3138
D-type	Low Sr, low Si	17	17MAG_25 Ti	400172	14789	9836
D-type	Low Sr, low Si	14	IS 14M Unsifted__36_1	400206	22343	2486
D-type	Low Sr, low Si	20	IS 20 MAG__27_1	392043	39113	1648
D-type	Low Sr, low Si	14	IS 14 NM__2_1	395909	8327	12663
D-type	Low Sr, low Si	9	IS 9-MAG__1_1	404750	18563	13320
D-type	Low Sr, low Si	13	IS 13M UNSIFTED 60 s__6_1	396008	22957	3744
D-type	Low Sr, low Si	17	17MAG_24	393962	15312	2811
D-type	Low Sr, low Si	18	IS 18-MAG__3_1	382774	78154	1176
D-type	Low Sr, low Si	8	IS 8-MAG-2__21_2	392537	29683	1718

D-type	Low Sr, low Si	19	19MAGx_20	393339	18436	2908
D-type	Low Sr, low Si	12	IS 12-MAG-2__6_1	383553	61479	1001
D-type	Low Sr, low Si	14	IS 14M Unsifted__24_1	393662	15875	8515
D-type	Low Sr, low Si	19	19MAGx_29	388524	27767	5394
D-type	Low Sr, low Si	19	19MAGx_27	386662	10765	7706
D-type	Low Sr, low Si	17	IS 17-MAG__9_2	386894	4312	338
D-type	Low Sr, low Si	19	19MAGx_24	383297	11477	3843
D-type	Low Sr, low Si	18	IS 18-MAG__6_1	389336	13246	14783
D-type	Low Sr, low Si	21	IS 21__4_1	385227	10297	5105
D-type	Low Sr, low Si	12	IS 12-MAG-3__5_1	388345	14847	21257
D-type	Low Sr, low Si	14	IS 14M UNSIFTED B 60 s_1_1	376127	2570	11873
D-type	Low Sr, low Si	14	IS 14M Unsifted__30_1	380882	7679	4580
D-type	Low Sr, low Si	19	IS 19 M__12_map	372836	27122	355
D-type	Low Sr, low Si	17	17MAG_34	366157	13289	2511
D-type	Low Sr, low Si	19	19MAG_10Ti	366554	7538	15633
D-type	Low Sr, low Si	19	19MAG_67	370964	10404	1620
D-type	Low Sr, low Si	16	IS 16 MAG_2__21_2	360940	6541	121
D-type	Low Sr, low Si	19	19NMAG_67	364132	6792	1173
D-type	Low Sr, low Si	14	IS 14M Unsifted__2_1	349902	38779	9163
D-type	Low Sr, low Si	13	IS 13-M-1__19_1	355786	14855	1615
D-type	Low Sr, low Si	11	IS 11-MAG-3__4_1	348510	860	1573
D-type	Low Sr, low Si	22	IS 22-MAG-3__3_1	344368	59112	19033
D-type	Low Sr, low Si	7	IS 7 MAG__3_1	340175	23496	612
D-type	Low Sr, low Si	19	19MAG_9	339764	8018	7261
D-type	Low Sr, low Si	13	IS 13M UNSIFTED 60 s__46_1	348450	19765	11880
D-type	Low Sr, low Si	19	19NMAG_52	338553	3423	3769
D-type	Low Sr, low Si	19	19MAG_7	336641	4860	1610
D-type	Low Sr, low Si	19	19NMAG_9	338218	5487	4981
D-type	Low Sr, low Si	16	IS 16 MAG_2__20_1	334096	2340	1069
D-type	Low Sr, low Si	7	IS 7 MAG__2_1	333451	7381	1075
D-type	Low Sr, low Si	19	19MAGx_28	328460	2624	1811
D-type	Low Sr, low Si	19	19NMAG_11 FeTi	331773	0	9939
D-type	Low Sr, low Si	13	IS 13M UNSIFTED 60 s__9_1	328940	3775	5641
D-type	Low Sr, low Si	22	IS 22-MAG-3__2_2	331799	16683	4961
D-type	Low Sr, low Si	20	IS 20 MAG__15_2	326975	5818	4681
D-type	Low Sr, low Si	13	IS 13-M-1__8_1	318026	29002	2396
D-type	Low Sr, low Si	8	IS 8-MAG-2__22_1	327176	10512	6195
D-type	Low Sr, low Si	19	19MAG_8	329135	2548	4839
D-type	Low Sr, low Si	13	IS 13M UNSIFTED 60 s__4_1	318945	25125	1849
D-type	Low Sr, low Si	13	IS 13M UNSIFTED 1 s__4_1	319143	14591	545
D-type	Low Sr, low Si	17	17MAG_41	321451	0	4572
D-type	Low Sr, low Si	19	19NMAG_69	310790	5541	4129

Al	Si	K	Ca	Ti	Cr	Mn	Fe	Ni
1792	9531	292	393	2550	99	0	590334	102811
2877	16985	87	999	652	3726	561	601403	51004
1926	6383	0	496	137	36	0	655832	33693
1185	6420	804	374	265	598	0	666758	20804
2637	15437	673	1003	445	718	240	634589	17641
2637	15437	673	1003	445	718	240	634589	17641
624	5442	0	213	0	563	0	677360	16948
1847	10361	186	856	1666	759	0	666997	15516
3719	11186	221	1102	1670	837	0	658125	14888
410	5186	0	177	68	273	0	679923	13882
951	7967	160	2503	184	1431	0	665329	11949
1473	9777	0	365	222	231	122	668334	11938
2839	16898	992	3239	623	2567	1494	642196	10364
2155	8349	128	158	616	1133	0	672229	10233
2555	10085	526	620	884	12623	0	646029	6125
508	5420	0	65	92	708	77	681217	6106
1024	6685	27	188	209	1546	5	682446	4887
7120	30379	1805	11687	1838	205	1489	554693	4058
978	7511	0	1732	139	4068	4394	662231	2418
2079	10805	2401	919	142	331	0	653294	1796
1606	13656	246	411	138	2252	0	654595	1687
1706	6549	38	325	226	1638	0	683447	1589
1791	14091	57	2569	192	90	6366	658832	1320
1120	5503	0	328	104	158	0	687880	1316
1843	11967	129	803	173	317	0	673627	1137
1415	6493	138	190	76	233	2426	682891	1081
794	17454	306	545	227	891	1192	659518	915
2498	8245	145	1542	351	1298	0	676592	816
6329	32498	632	2945	975	483	140	627455	816
3262	11958	226	12819	2885	761	5688	643343	732
2341	16223	2	1302	112	558	1122	649351	605
3793	10237	50	1058	220	210	2901	665113	568
847	7377	11	234	4441	112	2292	674951	547
1395	12584	55	428	93	969	1547	667970	540
915	7942	98	60	128	95	4568	659311	537
7707	19996	938	1208	31811	282	2844	600114	534
518	5748	267	347	39	323	0	687970	510
1539	8808	27	335	289	264	593	679787	505
9970	14269	263	504	25087	1372	3230	621845	494
1808	15759	354	672	279	631	66	654249	472
1890	12763	217	1033	629	816	3017	665313	468
1383	12377	72	1087	3733	276	4022	660153	465
9817	24537	517	2608	22454	966	4609	602164	446
3793	7391	93	1481	1191	156	0	678054	427
726	20042	608	5017	2508	47	608	647100	424

18058	11114	0	874	25932	578	802	618061	420
447	6905	0	34	238	1328	4497	678371	410
3489	10338	342	1457	13804	501	5019	652710	376
1073	7715	281	182	41	436	846	676957	350
871	14497	46	3685	238	172	119	666231	323
1604	18664	174	972	2280	21705	20006	624080	307
3382	16071	71	2268	3737	220	2332	658105	305
426	6361	136	63	13	4111	1533	682733	296
1206	9732	240	213	249	85	4593	649902	296
3659	12586	162	1006	1110	543	3848	665451	288
17933	11456	121	1263	25461	673	943	607251	270
1144	11636	90	214	59	395	9468	659813	262
10306	9058	128	564	24292	2376	2137	627596	256
1451	10614	158	503	305	354	2671	673899	253
1156	13236	0	820	676	624	2692	655970	251
939	11547	399	393	455	1298	3994	663502	248
11203	8818	63	473	24846	2133	1966	631000	231
579	8202	0	96	87	393	3800	681061	230
2853	13103	441	992	182	1511	2762	598971	203
17236	13920	440	746	31216	664	1168	559293	201
35563	19244	421	1397	25826	1540	2538	579229	185
14759	20634	521	281	47202	470	2188	506477	183
2082	10715	37	681	486	750	2245	671971	182
4573	14728	242	5982	375	525	1391	660158	182
1547	8584	41	926	6541	287	3759	670251	174
448	6019	625	65	59	292	2588	683452	172
2955	15408	117	1320	216	262	2767	658666	170
2246	13974	665	2511	735	277	3281	647184	169
1633	12669	864	732	579	763	5958	663118	167
2171	10735	0	1611	167	647	1701	664564	166
3744	8017	0	1384	992	169	0	679519	164
3358	11046	160	5980	43397	492	17063	581721	163
389	15658	559	853	1909	233	1225	661739	152
1928	7710	26	695	125	839	2507	678439	151
1061	7989	429	462	666	319	1666	617017	150
1356	23619	2505	541	1526	197	2658	627321	150
893	9185	43	525	239	535	2702	676979	147
5863	18387	274	4105	1473	468	995	648559	146
2836	19999	372	967	21748	107	1124	607403	144
7472	21961	360	1179	134	146	1791	622053	136
1126	8652	105	431	1401	209	1661	677453	123
1864	8732	0	548	99	800	1695	679202	116
1058	29584	98	195	126	3057	10556	639157	110
695	6873	0	248	155	666	1911	682707	110
16760	15850	215	2421	43758	974	3276	583099	102
2012	12355	150	1126	68	461	5715	663986	99
637	9080	39	121	16	345	5841	680038	90

6181	20114	427	4154	2893	322	1618	623870	86
24939	17941	485	581	36155	1794	3198	580670	83
2072	12991	324	773	1502	371	2133	644995	82
576	8148	35	80	172	390	1258	683475	77
1593	8148	0	538	509	398	32	678019	76
2846	10729	67	953	1008	196	2909	668977	75
16337	26660	1760	3601	2757	124	114	616282	74
819	10364	67	353	4502	225	2173	663014	73
2653	12145	120	4332	21034	315	6731	627591	70
994	9718	133	486	1332	225	2781	676215	69
1678	21771	514	4753	10236	159	1775	630604	63
455	6684	0	100	3446	371	1366	679378	62
455	6684	0	100	3446	371	1366	679378	62
3934	13544	67	1685	249	273	8964	649995	61
546	6242	167	102	1199	143	297	685373	60
1292	9195	243	336	908	208	1606	620845	60
2225	13887	0	634	402	175	3346	665241	60
505	6401	35	451	379	1511	8767	673062	58
8355	29941	304	23094	25926	1537	42	581005	49
1172	8915	115	688	395	138	2759	679760	49
5991	14131	745	1302	1213	587	4733	656121	49
1463	14313	7	1211	112	332	2014	653961	49
621	6059	28	132	1466	336	756	686090	46
1312	9126	93	151	4	178	305	676015	42
1018	10910	51	591	994	264	367	674720	41
2549	19337	166	351	0	308	3508	654479	41
30186	23736	1118	7614	2295	221	5716	573767	39
815	7618	35	170	1810	4210	2125	673832	38
4927	17390	597	769	189	292	2638	646248	37
634	5789	0	80	48	371	3279	686243	37
632	6816	42	62	536	471	3465	684160	36
498	5804	85	190	16	1274	1431	686869	35
1248	8458	0	418	310	602	1041	675676	35
1587	7934	0	438	89	129	1979	680803	34
648	10683	110	417	351	272	2207	678637	34
6822	7171	111	55	15218	1564	3232	652721	32
1241	6737	223	423	630	327	1288	684020	30
6140	24995	620	1271	273	500	359	641647	27
1029	8508	39	431	215	190	1767	657558	24
530	6283	43	42	179	494	2473	681446	24
1137	8254	95	598	461	410	557	679250	24
1321	6932	0	175	39	264	477	685561	23
1124	7520	0	243	444	694	1327	682752	23
1947	17302	70	288	12939	83	5804	647669	22
10101	8014	689	475	47023	513	3908	596155	20
1707	7160	0	3427	5962	262	2302	671776	19
28534	15298	253	1442	26974	1454	2083	595358	19

803	7693	172	68	563	603	3371	678238	17
12048	12007	650	8808	1245	56	0	651924	16
332	5130	0	48	48	332	1032	689548	15
1166	8056	151	539	39	275	1239	678651	12
3827	19150	479	1803	1543	195	11289	649227	11
1164	7610	148	157	876	6318	4929	675285	10
3735	10313	66	1876	20534	1512	9055	634789	8
456	7091	93	59	277	192	2009	681908	7
1792	12801	379	1466	848	204	3333	668142	6
3046	12585	695	2030	11660	263	2560	646063	5
510	6981	0	259	333	74	575	683382	4
17736	34372	407	1020	968	93	0	621008	4
587	5881	32	417	58	578	3604	683766	2
832	2154	44	68	94	274	5670	686426	0
303	5222	0	100	163	149	4794	682784	0
412	5287	0	85	86	232	1655	684679	0
302	5374	0	23	65	107	487	688122	0
360	5577	17	151	311	640	562	687897	0
756	5037	0	31	54	367	7242	677025	0
1778	5288	113	1084	116	117	5321	677961	0
511	5715	0	259	122	260	466	685789	0
822	5736	0	133	62	326	4026	679943	0
544	5839	0	111	97	277	1171	683736	0
410	5825	55	2356	515	452	1687	657286	0
667	6147	0	200	852	317	3802	675663	0
1088	6398	481	102	55	207	1732	685013	0
1139	6254	30	241	191	294	4621	677750	0
603	6559	85	161	1079	1075	3412	675492	0
1094	6641	89	203	820	758	7593	680774	0
1046	6797	2	365	377	263	4233	676586	0
1421	6674	121	1308	836	203	3330	676061	0
1609	6262	0	392	645	665	14924	672826	0
1019	7173	127	224	81	497	5377	681084	0
864	6991	106	670	1073	449	5729	680877	0
689	7403	101	188	1148	205	449	677951	0
724	6490	99	875	785	225	2594	677459	0
1842	7446	139	810	3638	877	3032	671341	0
579	7897	175	95	76	1234	2519	680391	0
0	8012	24	478	705	245	394	685138	0
0	8213	0	751	552	111	2777	683160	0
899	8001	464	241	0	129	1489	656484	0
1191	7023	0	745	6150	328	4109	669292	0
0	5409	0	293	71	690	1511	675338	0
1533	7573	0	436	146	324	6117	663075	0
3663	8772	0	329	600	223	186	674133	0
12488	9050	102	330	257	197	71	667749	0
3351	9438	0	1660	61	33	0	678520	0

0	9546	0	400	235	356	2622	681957	0
1351	9607	84	563	280	380	9066	668314	0
3687	9708	110	1698	119	62	63	674635	0
1406	10459	425	2652	464	850	3110	673150	0
1729	10693	572	3262	469	843	2723	673585	0
301	10667	0	569	382	141	2812	671212	0
2170	9382	0	1127	475	215	2861	669035	0
9258	10809	387	8483	1088	0	0	655500	0
747	11194	3022	221	428	459	9997	663497	0
618	9420	0	537	1786	304	1766	669164	0
1090	10814	3436	281	270	581	10258	661586	0
2682	10031	42	1117	179	315	3372	668390	0
610	11441	285	261	941	428	1961	635470	0
914	11254	1505	599	210	229	1595	621800	0
2461	11689	154	5872	306	137	3961	661804	0
9351	12610	243	1145	637	140	175	659314	0
2794	11602	119	1578	804	246	611	671880	0
29755	9147	0	2042	7344	153	1879	624304	0
30307	9236	0	2069	7403	156	1881	623301	0
3218	12905	507	3187	940	160	3359	660162	0
2550	13602	554	1113	669	107	0	653659	0
590	14375	459	2384	666	234	2932	665263	0
1476	15418	0	1172	230	204	2561	669494	0
3719	14620	181	1894	1294	831	4859	655755	0
3780	14721	185	1919	1277	818	4833	655583	0
3173	14109	36	1048	196	343	1075	653524	0
1522	13976	0	846	3223	452	7013	657058	0
7545	11760	275	694	36447	455	3042	609091	0
1909	13819	137	2322	530	621	2638	642485	0
1901	13915	136	2381	534	617	2643	641916	0
1063	15708	139	2185	1560	413	4011	650237	0
5598	17558	346	2224	715	126	475	654396	0
7375	15096	9292	274	42248	775	1768	599976	0
3225	17895	460	3959	392	95	13979	629864	0
4494	18156	832	5638	4311	605	3842	642990	0
12557	19043	270	345	14377	174	235	629710	0
4608	19217	2712	3189	217	103	9	621166	0
4420	15325	341	4539	928	147	3497	621137	0
1021	20290	77	403	29	287	8800	645085	0
3475	18506	981	501	195	250	7842	620212	0
16658	11661	73	1745	35620	404	2543	597220	0
3334	21221	240	902	426	532	0	657480	0
1880	13553	88	1272	4151	454	3332	604717	0
10272	31428	499	9988	5455	305	6648	610067	0
1443	157117	159	1830	379	2120	1399	99546	3469
0	163338	186	1806	363	2205	1300	102707	3445
909	159443	35	5289	171	1585	3636	112675	24

4853	182840	615	8055	701	1120	3372	154170	1349
4257	202034	93	2078	732	5193	2891	160262	1145
3332	144705	230	7798	604	2798	1319	170679	384
5696	156555	104	1936	995	3006	3213	173722	2354
5311	199942	201	7800	655	7923	2324	173056	60
7038	168159	368	10828	819	4406	2311	177471	1406
2247	172515	700	5259	1860	1513	3532	180966	808
6296	187520	78	14743	590	755	3573	182846	1765
8526	224897	1549	13902	1265	457	9743	174142	0
2649	163176	37	11284	666	2266	3776	192826	0
5880	169623	801	6937	2258	1690	3548	189594	944
6204	158633	20	11494	777	2263	3718	193296	7
4949	154447	966	5269	464	734	4777	198009	712
10106	181262	472	10906	1037	3611	5531	186566	174
2727	143724	29	4869	415	1773	3532	210399	671
3804	157824	0	9421	351	745	3147	207109	5280
13347	210921	0	19571	1375	0	10042	188123	0
6533	185438	262	11135	932	3663	5975	197221	52
2806	139194	0	7563	2093	103	1840	219441	0
5066	181675	0	10994	663	1947	3691	208934	13842
6494	181123	0	11204	671	2102	3774	209775	13556
11055	166094	1813	18734	6113	3441	3172	206413	1474
2037	134045	140	6593	777	874	3075	228858	628
2800	147229	28	1317	135	133	3889	238443	0
5617	155518	2495	26497	789	1929	2512	221428	4531
3982	150098	57	6292	792	3713	1655	235635	1766
7858	148543	554	12051	1068	4269	1346	227086	3297
6916	151291	0	7604	577	1226	1967	236149	2040
0	125905	502	2469	394	205	1441	249543	489
9815	149256	0	13363	918	188	2034	234326	592
829	125668	678	2591	355	307	1595	249524	483
10185	151410	0	15979	906	367	1967	236002	7834
6089	152505	0	6022	304	277	3778	245832	3693
1680	142330	489	7813	723	3036	2760	244522	393
1801	134398	67	1899	1481	4349	3944	253991	1101
7010	157212	124	9788	747	397	5302	243120	4823
3420	127853	121	5719	442	3840	2112	251358	10354
821	146315	0	1083	54	3148	4789	251509	565
17226	156044	2521	17399	1849	1204	3125	228494	11978
8956	131091	130	16005	1043	3934	2369	247133	3878
6068	151908	0	5941	314	270	3791	249870	3634
6517	149723	71	8357	689	1475	1888	246226	10262
5745	146564	163	8492	931	3874	1542	248745	16540
2176	147565	177	9341	757	3914	1284	252094	15364
13198	181008	187	14821	799	1491	3599	235421	1345
8549	180246	0	7513	482	1546	3869	248814	2991
4461	155579	784	3754	515	5529	4412	249091	309

10278	158420	0	13452	775	2686	4140	251190	246
10076	156961	0	13549	848	2538	3700	253156	145
1582	127148	264	1999	0	656	1444	271545	612
4078	130347	16	9602	859	320	2424	259800	0
3099	116871	0	4528	573	831	1488	272180	7700
3125	116644	0	4486	574	831	1494	272675	7711
7473	151513	0	8271	447	3444	4116	253142	765
4941	122591	0	10457	631	1326	1671	270500	3675
12407	161027	513	15710	1184	5356	7899	252443	771
3885	129119	0	26749	206	3843	5928	255513	29830
6505	139789	0	11486	599	2857	1853	263183	8083
6444	145130	44	12707	582	3180	2373	260288	12792
2224	122015	42	1682	831	13931	2857	274722	7443
13003	179857	0	9572	148	1078	3090	259418	1066
3783	124980	123	9317	834	2965	1939	275370	11885
4401	124698	0	11937	762	465	1641	279479	57
1695	123092	70	3115	474	1389	1549	283124	1708
4158	132378	0	9553	669	837	2382	277526	316
8114	128387	0	10139	466	811	1537	276321	7153
3013	123061	5	9973	690	2325	1902	280284	9335
6118	134853	171	5760	769	4937	1950	274096	10988
4475	143355	0	7071	720	3270	1525	275265	11439
5481	136391	0	9787	565	1267	2783	277226	3052
21835	156630	1502	10245	612	1141	1907	260699	2563
3841	142924	0	5255	723	7534	3948	279430	81
5643	133906	11	7068	586	1544	1931	283651	2868
1590	122364	0	1228	297	188	2009	291274	1603
7311	138798	0	9238	590	2316	3974	277892	5478
2739	124622	413	8686	662	2899	2059	284245	9714
7312	136207	59	7016	712	1637	2181	282107	3138
3759	135078	0	3498	738	2303	2503	284558	10711
9082	143272	504	13159	748	344	3282	261912	4219
1467	124170	0	8303	729	2928	1836	289539	9606
3484	135307	488	4084	615	2975	1052	279615	12245
3552	124429	225	8590	607	3431	3952	288566	3895
9723	148993	127	13246	696	3148	3728	279537	3708
16962	154446	841	10268	567	999	1740	276566	2581
5394	142060	75	9273	289	2101	2807	284454	4374
3973	119400	0	3905	625	2949	7168	282264	38672
2707	139777	213	2117	430	4680	1372	291080	419
4262	128017	0	10651	823	749	2181	292430	164
7471	131665	136	19062	690	487	2276	286786	51
2636	134935	0	5686	822	5308	1699	292120	11856
10646	181848	0	10180	218	1021	3136	277202	1010
3061	126114	126	8710	587	3240	3834	291563	3707
9126	106598	436	5715	1209	11089	2629	288836	2190
1262	143263	0	1947	577	4675	1189	298987	414

2964	119127	330	3009	476	3513	2067	298878	12874
2503	126787	0	12157	663	1623	1734	297139	3904
711	120145	46	2871	443	3391	1985	302769	12751
2572	116341	31	7185	772	802	2148	302856	258
5996	149127	1	13432	732	3232	3495	290381	3922
6392	136479	166	5747	957	3727	3335	287906	16719
6619	125184	0	14379	676	1318	2049	295748	1156
3263	144096	0	8977	657	5652	3984	296294	266
4425	127231	0	4790	611	2150	1896	302338	7136
2194	121217	19	5269	449	2276	2083	302664	12605
4859	119502	2	10722	821	3236	1864	300176	7372
4531	118448	304	8498	593	1222	2842	290240	207
3380	121332	0	10346	581	2532	1856	303016	9244
3903	116842	1065	10110	777	807	2069	278231	652
4079	116228	344	4829	532	3836	2308	302365	9605
6202	121598	21	4583	1709	2899	2026	304564	5010
3522	113472	0	2339	419	1706	1361	311282	3122
4189	115551	207	10211	679	2179	2120	297343	6814
6601	131456	16	10681	657	3752	2156	301132	7050
4754	114359	0	8747	739	2722	2203	288740	7075
3251	110019	150	2422	580	3426	1400	310343	10629
5368	123991	110	5090	541	2289	2061	304543	7707
6457	135716	174	5739	900	3978	3407	296103	16212
2485	115042	0	874	588	2177	2021	314439	5746
6085	124734	345	7458	693	990	2333	308054	405
4226	118412	4	10124	709	4053	2084	306441	10807
4343	114115	173	6852	645	1851	1698	312855	5056
6444	117171	42	7710	1026	2739	2478	309907	8963
6107	118138	0	3292	1047	1279	2228	316305	549
4069	133351	36	11009	603	3836	2028	309158	7019
5678	119132	149	11018	706	2466	2147	308503	7954
4444	128568	107	4893	715	3440	1509	314891	1777
10263	129671	71	3659	994	4065	1549	309381	6794
2425	111050	745	2315	174	1733	2190	314470	894
5954	116548	0	3212	1039	1276	2241	320205	539
3172	113557	93	5944	675	3328	2072	316185	13857
3137	110480	200	3129	690	1931	1500	320200	4278
2210	112712	268	5031	589	1870	1918	314819	10457
5146	123870	15	889	3114	2368	4410	316163	1628
4153	117785	453	7663	485	1505	2035	309418	10570
3412	109322	222	5542	859	2644	1597	314385	16053
2545	107093	350	4461	671	2872	2151	318393	10999
1255	115268	0	4687	611	3504	1952	323929	14037
2953	110914	0	2275	512	4220	2034	323732	14760
1235	132125	0	1149	169	1213	5813	326199	1726
899	106757	435	1707	342	1507	1618	317873	3206
1571	115922	0	1743	698	1556	2556	333199	1903

3887	115609	0	1710	655	1582	2722	330942	2014
2712	115934	0	1832	329	4386	1760	330171	10440
9946	127829	0	12530	855	6466	3935	316322	2446
5037	120275	99	4220	589	3362	3555	326496	7824
6206	113766	0	12855	720	1749	2428	326044	7482
4611	112072	51	6822	780	1876	2256	332752	5414
3044	110921	493	2356	460	1289	1846	335170	1400
3320	125831	228	2873	496	4013	2232	324824	20616
2898	109632	100	3753	507	3225	2276	334526	9572
4651	111194	318	1186	537	1925	1772	332114	4756
2708	109299	0	1783	572	4145	2595	336831	9208
3766	109082	0	6640	578	2313	2258	336173	5979
6200	121799	0	12191	701	2478	2266	323846	7547
0	113557	0	1628	431	4421	1522	341009	10524
10706	118804	2617	1846	803	3935	894	316018	11007
2673	119508	547	1303	307	4852	4477	326202	4729
4962	107992	0	4747	849	3960	2569	333342	16678
4283	105026	0	9587	1327	2749	2002	338057	11546
3791	106177	0	5560	706	3371	2170	338090	13579
7265	109574	0	9398	706	2028	1599	337744	4996
4930	118609	165	4101	587	3312	3652	337048	7781
12465	102850	1418	23811	1751	3198	2209	312621	14040
4313	108613	464	5532	624	3072	1942	340762	9072
4458	112216	3	11564	694	2967	1959	335042	12468
7923	120388	1027	4349	236	2315	2948	313690	22014
2025	109414	185	5454	469	2973	1666	344923	9188
5543	122127	0	12111	623	2520	1944	335896	7821
6694	110098	0	8667	620	1890	1769	339344	4365
3465	106305	53	8178	438	2566	2051	340410	7598
4014	119941	25	8022	484	3692	2088	338318	1835
2796	114933	0	3952	1290	3313	3449	341461	10971
3584	106468	66	1950	802	550	1517	351654	35
6299	110094	0	8519	621	1871	1787	341560	4207
3374	107092	0	6055	543	2112	3697	346211	3084
3945	105631	115	2178	444	3772	2512	343816	14528
6869	119794	54	9793	491	1631	1682	336577	17169
4105	108673	355	3516	1356	4237	2314	342477	16108
6280	121438	1709	3585	754	2282	4246	331537	4145
2973	102970	279	3575	668	1750	1790	337667	16466
5149	108019	0	20129	616	2373	2346	336626	5222
2701	107454	580	2510	573	4707	2499	348348	7442
3603	102908	0	5274	653	3339	2268	346060	13399
3766	109962	0	1207	498	3538	1986	344420	15174
3117	113387	0	4029	1367	3347	3406	346848	11238
5230	116286	11	10272	1166	1638	2975	345694	1220
1385	126174	165	2672	465	3988	2075	343791	21712
3220	123829	81	4147	450	3621	4400	346726	2597

6262	124942	0	6492	1519	4135	1874	328523	6266
5005	110499	0	12173	664	2315	1951	341034	9290
3555	103218	0	4438	671	4133	2258	350788	15051
6369	112649	201	11204	534	3138	2156	333398	14646
6143	126562	2511	3365	540	4129	2276	321797	17146
3447	105649	356	3903	565	2061	1983	353477	2435
4704	109040	0	6933	653	3306	2022	347771	14044
1627	94373	82	3594	257	1105	2518	308510	1722
4755	104961	460	11004	1216	3299	2259	336950	18315
10903	103322	871	10819	979	4339	2085	338016	24327
4297	99352	34	12845	450	1813	1792	353056	4674
8903	145530	0	7696	959	3581	3791	336716	9843
2706	103168	0	3279	559	2808	2147	360005	9921
5502	95639	200	451	562	9177	1338	356325	8076
3825	109244	292	6918	407	3447	2136	348039	25421
9526	115534	515	7736	1050	4300	2065	345986	16008
11594	98002	638	8182	2332	3121	2100	352559	6698
64144	149862	1315	15242	7224	151	1636	293058	158
13568	129023	90	5405	1322	3278	3181	346773	7218
8497	106785	226	7264	720	3133	2036	354465	10222
10216	103084	366	6515	654	3919	1789	357528	7658
4871	95023	600	11220	1364	385	2393	293266	103
2628	106295	0	21510	824	2380	2296	359127	5142
4642	97823	54	3714	556	2148	2152	367400	9314
5026	102188	671	2433	792	4293	2223	351581	13166
7966	114756	463	3145	639	3521	2424	356092	14540
3233	107966	136	3021	597	4790	1804	367611	14755
1727	104020	0	9889	613	2093	2151	371514	4611
5533	107069	890	4448	504	5047	2164	366866	525
3667	95319	49	7304	509	1835	4062	356165	1153
7177	101084	326	3500	602	5021	2183	366585	14435
3033	99320	0	5950	496	2568	1821	366928	13103
4036	96183	0	5880	495	3920	1995	369998	15143
11487	124143	0	5637	1533	3286	3055	361498	7239
7766	113530	473	3196	679	3492	2469	362412	14747
7766	113530	473	3196	679	3492	2469	362412	14747
6643	105434	0	9274	1529	3517	2410	366122	13729
3735	99556	248	1391	746	3398	1984	376151	10056
8622	104442	65	14841	1234	1676	2301	360837	5185
3387	99369	0	3704	2295	36453	4640	356474	17966
4804	98439	130	2316	582	4652	1974	373583	13242
4722	103044	80	9739	773	2202	2686	375616	4937
5283	123628	0	4552	461	4195	2559	374642	2601
6826	96675	1244	2408	592	3513	1473	366877	12707
10359	108496	249	13969	872	3560	2679	344870	13919
9651	108803	29	24984	489	3974	6913	356511	12535
5346	98248	496	4156	423	4722	1917	366104	19740

8984	117891	164	13884	722	5068	3731	332777	76694
2976	96360	53	4494	651	2291	2213	382247	6943
3464	92667	556	1956	530	2783	2063	379252	13052
3574	92584	257	6165	2087	3535	2646	372682	10701
7875	123285	688	3392	630	3418	2312	370780	15470
5258	98523	0	2707	578	3329	4378	378434	12872
4555	99497	0	8621	940	3268	2354	381983	10146
3517	102025	0	1999	423	5078	3073	378402	23304
7407	101381	89	9416	1633	3335	2000	378426	11590
8339	105659	67	10400	634	3925	2117	370659	18515
2794	100659	0	2377	603	3161	2270	382216	22154
6299	103102	590	9614	2075	2425	1597	356058	3837
3303	101054	276	2654	723	980	3781	389984	1874
5444	100480	27	10926	545	2322	2534	384663	8198
2242	116283	0	1039	285	7937	3783	387735	3329
3633	97146	270	2723	819	3774	2389	386344	15530
4933	98660	0	2834	666	4432	2093	381463	29132
4690	94838	170	2836	676	3593	1896	390090	14470
9330	114708	149	23756	1093	5838	1678	367444	14972
5966	99575	259	3810	799	1987	2174	392569	6876
2340	77770	0	6475	417	2897	1886	310477	213973
3471	95484	306	10104	1054	3069	2257	386268	12814
5452	96290	178	10112	1131	3102	2478	389855	12791
12350	128290	241	48287	2146	15288	696	341559	3746
9387	107091	508	4410	396	4560	1833	369305	22559
6470	102276	739	7634	626	2159	1702	393127	7327
9115	104000	264	7289	676	9545	3360	381056	2657
6868	97473	92	11067	814	6665	948	392461	24713
8370	101342	151	12660	632	4536	2890	396765	10522
4443	88899	392	6703	642	3863	2473	385262	9770
10147	96684	1060	8250	1339	2699	1779	396230	7422
4393	87304	187	1264	593	4667	2513	409745	14912
2264	85449	252	3083	408	2246	2198	408898	8248
5840	141537	178	4841	587	2889	6479	398837	2333
1975	84641	482	1909	825	3886	2227	416388	16826
2039	81343	0	7768	445	2782	2081	389240	16073
7071	95354	218	3892	635	5087	2745	394052	16382
10786	94606	191	11340	1023	5946	1395	401876	25087
6152	93623	121	2189	728	5090	1796	416586	13901
7113	103053	507	2833	1024	6013	2359	402024	5463
3614	73098	0	1904	432	6627	1998	427548	23997
19832	85306	840	5392	1688	4759	1828	376921	13499
8701	118936	81	11909	1005	3826	4278	413188	4846
5796	95278	494	8783	743	5559	2574	409794	1820
12652	103825	202	14935	1217	5345	3433	409068	983
3061	79031	1199	4637	676	2764	2396	421673	12098
1587	85092	0	1149	552	7156	2471	412620	58687

6079	100383	189	3904	693	4418	2681	410172	32690
4505	85286	0	2051	668	4652	2574	438342	5392
2920	91440	331	5104	759	1101	2314	433983	4544
4096	82326	248	4412	1338	2080	919	439089	10823
2750	78539	173	4884	843	5280	1329	433284	32593
6287	79799	602	4204	466	4034	1729	429726	21392
10812	100048	69	9543	631	4617	2781	421688	12501
5092	82615	446	6296	554	1482	1456	434373	496
7666	89353	123	3492	708	6307	2543	436218	21242
12762	112592	132	14665	3844	5898	4106	393331	735
6189	96837	0	3357	442	5364	2486	437813	21374
7512	86365	0	5000	843	5267	8763	444866	4070
3925	83636	0	903	516	1661	1168	447003	18328
4864	74408	361	4936	904	5194	1470	444663	31913
4389	74833	1148	2294	502	3464	1945	444635	13237
9049	84821	131	4055	487	5105	2185	444567	17199
13177	112225	0	11479	1440	6508	2751	429360	7209
5624	81350	118	6726	810	4228	2516	453376	11513
6996	86217	88	8177	839	4230	2579	444027	6907
7882	90969	0	8356	1100	5921	2346	452812	7462
8711	96238	0	9471	626	3480	2412	454482	1800
15059	105329	0	9511	776	4585	2744	436714	10622
8084	74085	368	2928	814	16934	2086	447416	23256
9370	93032	742	6844	638	5943	6034	437335	2873
2382	76284	0	1881	736	521	708	481137	18
8409	81493	946	2006	672	4687	2411	452166	17248
13834	46941	429	16687	1157	4318	6741	459029	11000
699	59022	767	1264	485	179	1259	477531	0
4111	87054	0	5253	584	4952	2637	466592	14558
3479	62130	1293	970	213	4959	2519	462359	15844
13786	85567	30	11681	923	6804	2683	468747	5031
7602	79813	510	1773	870	6047	2436	469806	16117
9624	85533	70	7204	873	5890	2366	469816	17570
7309	82607	0	2321	469	2157	1219	493710	805
29280	77226	14906	1321	32609	379	1554	422397	39
7397	85362	0	3692	637	3497	2522	483435	14919
37453	87913	737	15290	4607	83	3676	449302	33
7092	47368	0	11875	1320	12658	2532	503161	17730
10417	44442	109	11649	1472	14983	2655	500055	18010
6367	61958	1597	7834	666	3524	2358	513297	13661
34103	54258	2844	15083	1020	171	8244	484169	0
2636	74931	164	1121	155	3548	3782	522817	3445
8623	51166	978	3310	449	372	0	533637	716
4461	62141	0	6686	1952	1587	838	541466	633
5325	53077	20	12851	2386	2788	2285	518395	31384
5975	56082	0	8473	859	3384	3408	522844	32780
8047	46699	0	2298	720	3529	1342	538903	20597

4725	52017	0	4743	740	3755	2052	531443	7462
5585	58495	774	5637	2831	699	3195	549148	416
5378	45898	1344	59388	875	5010	3825	509721	3989
42010	47536	2124	14314	20208	485	2700	477712	233
6525	39351	325	2144	659	3573	2574	567398	14481
9571	45909	2793	14998	2110	98	9752	558288	44
2949	39840	156	1110	761	9311	482	575962	22793
4554	39437	0	7146	582	3752	2592	580927	10362
6999	32461	154	1084	1092	10947	29	588566	14877
6763	32628	20	7271	658	4245	2546	579347	18321
3610	32487	627	2019	877	7433	0	591620	18418
6855	37628	331	4055	2627	2176	1029	584768	24765
26959	36072	672	418	37644	419	3428	535415	0
4288	30794	319	2932	892	1130	160	600383	21189
13374	31900	297	4743	34337	741	2360	559739	108
2914	20189	436	2467	232	509	3192	626690	2516
29111	25904	269	8989	2044	56	7896	582853	75
7658	29614	686	9019	306	260	362	611354	60
1831	17975	126	1201	222	275	109	620588	35928
2588	17814	250	1891	652	4135	0	640047	2709
8623	22232	0	40373	43280	507	4205	551529	0
149943	177905	1203	172603	8523	2	526	29486	1
152824	238246	13029	35901	12847	1251	484	56562	26
60480	251475	13110	124798	3094	6	1528	65608	107
123396	233822	10291	83717	2314	21	1109	67009	1
58379	228742	14610	169808	4186	58	1267	61072	49
145036	237760	12591	36921	11701	1036	669	57576	126
60396	239060	14787	154853	4485	205	1337	70484	0
68239	233176	20212	137202	4291	31	1502	65347	107
63677	243936	18216	114614	4272	42	1769	79455	10
173560	199909	7926	37004	26185	211	1448	66313	2308
66289	267873	4831	36772	11449	93	930	115243	46
63585	218664	16371	140344	4966	76	1913	90912	0
61624	199010	13999	173537	4549	11	1682	85345	0
57141	214965	13112	150293	3952	46	1866	95238	0
57141	214965	13112	150293	3952	46	1866	95238	0
76030	245017	16789	56921	4152	44	2131	119211	34
70492	220584	16360	117479	4630	58	2221	97760	5
161191	203062	7690	20668	9415	1768	153	114602	130
19408	252410	2434	110183	3667	32	4958	83527	7
94087	207717	623	50012	1623	6	1426	167645	0
126437	164469	12516	10243	7370	236	133	248960	34
53259	185976	13316	19789	7540	598	271	296772	788
97061	139053	4419	89750	6991	353	4943	238416	536
75803	161637	4172	17205	5391	54	6119	310934	6985
60169	156035	7808	17219	10216	194	3792	292930	382
60309	151978	16159	29376	7548	220	587	305656	319

69876	142787	4472	17288	5106	201	6534	348694	4800
68526	116870	19102	6230	7634	208	1008	380415	33
67034	104520	3149	14408	4857	214	7345	408739	41
56641	102416	3148	21521	5417	123	1235	425273	122
139577	55764	5158	78123	7259	92	3335	218157	26
28778	84335	1927	19221	4013	116	11804	478569	143
52375	74513	1376	13980	4070	124	666	479676	12
32544	74904	1695	11393	1287	31	10129	481197	0
59280	62385	2440	13792	1375	81	0	488847	76
22578	61307	8922	8202	6343	170	422	484770	264
65258	53388	4910	22666	7372	211	4792	467368	475
49844	54944	2749	13927	5600	248	6174	497204	500
30772	48888	9318	6526	2911	182	150	491281	0
7297	37564	2901	8593	1616	191	160	478980	319
29268	43887	832	4730	2940	131	0	579845	338
28658	40383	5420	5793	5267	455	846	573568	400
29911	39570	1939	11106	2973	17	10	574260	0
132603	229210	5825	107953	1352	72	389	32222	0
83421	299181	17600	33860	2941	5	745	55873	12
65756	295348	13687	59871	4390	74	1534	59709	7
92865	280302	16790	45779	4260	14	1023	52076	13
54687	274900	15394	57731	3741	0	4415	78398	99
83946	275689	17263	51353	3116	44	1187	65602	244
60088	304399	10112	24652	3846	17	1107	98325	0
79088	278768	16145	41692	4742	17	1143	58249	23
85679	251779	20096	55339	3727	19	1438	72432	1
62176	259695	18789	47539	4023	9	1870	82573	23
78664	280642	7987	34169	3265	148	1203	88997	52
73235	258481	17540	39584	3527	10	1471	92989	170
48630	272094	5385	99831	2369	38	4612	67690	0
74125	261870	21690	43611	5010	22	2201	99644	0
60148	276347	8355	32577	5421	23	1789	127931	0
73151	253655	24587	54616	5361	21	2480	95217	0
83715	244427	16647	54258	5893	36	1833	101505	1715
65594	238947	18526	50672	4865	19	2004	123347	289
54840	265851	9015	24812	2937	0	8114	157262	0
40233	256087	5403	117922	3433	27	3946	70095	0
49572	232029	7256	9672	73849	44	1599	148589	0
70766	259698	23349	11318	5281	300	4568	164851	70
71780	239061	21097	47554	5357	28	2812	127774	33
65221	243219	5882	43623	5802	149	1792	161597	0
67761	242776	17650	21691	4876	70	1761	165222	32
51538	235751	8148	117011	3096	33	1633	86915	133
55043	232979	10621	35080	10200	115	1544	166764	10
65347	243549	1109	26182	20512	70	2575	128784	0
56357	214333	8097	94183	10579	102	1960	129336	32
49621	226455	8588	34512	15420	104	1969	207834	24

51759	220408	9569	44385	10600	221	2331	203152	144
90562	221495	12276	10493	6850	129	87	205255	0
45431	231396	6173	28215	19667	0	1927	228958	0
153199	181860	814	2960	12069	81	330	194570	61
50165	222103	5596	9264	11544	16	1157	246475	0
45518	217524	5771	12986	19537	22	2072	249747	0
47701	209457	7542	13078	19911	19	2260	249007	0
39528	201559	10003	23752	12558	109	2353	243112	579
41652	187653	6105	25455	61923	80	2097	236798	9
43143	211936	4258	6298	16447	296	2333	272163	0
39014	186418	5526	35294	17818	122	2052	240378	0
43411	203840	5014	8569	18696	144	2022	265653	0
45659	205689	5562	11266	18336	136	1997	266475	0
63526	191512	10264	23683	14750	272	1420	233523	80
44221	204674	5285	11569	19816	136	1857	280377	0
44482	198379	5154	12590	19467	273	2495	272117	0
45383	198062	4459	12611	23348	41	2261	270744	0
45216	195019	4827	20496	20549	0	1855	269794	0
42933	194985	4580	18916	21313	152	2119	278143	0
40429	190852	6902	28424	13603	9	3230	283257	0
88132	183506	4086	27495	2857	29	6733	250995	0
58241	179728	7763	13474	22245	0	2824	270025	0
48754	172164	12715	19128	18787	316	1576	264350	36
90949	181720	4172	27066	2709	108	6607	237687	18
40373	181791	4991	12933	17386	445	2744	289289	84
41967	184723	4195	13932	22610	189	2315	300236	0
41170	182391	5437	24295	20233	129	2087	295874	124
51778	178859	9053	5789	21245	226	1884	296926	0
41484	182386	3657	8944	23705	365	2282	307089	346
101080	153201	6246	19706	3963	56	0	265154	72
41642	164699	4336	40260	22803	0	2553	289160	0
39994	174556	3680	15354	22770	0	2233	316353	0
31743	176482	4050	20305	20085	257	3511	320129	95
42918	165292	4376	16790	13596	211	1343	299194	0
39874	175652	3336	9322	16657	0	1980	332878	0
41330	166996	11078	7313	29484	0	4179	309557	0
34485	174726	5294	9838	19334	161	2876	331387	0
41718	174138	2937	8968	17921	772	1592	325160	0
33408	175998	4834	7601	23796	127	3292	318580	0
39800	174594	3438	6602	13752	882	844	334319	3
38632	162222	10478	9351	24602	167	5812	314350	145
11854	189830	23647	7920	1755	113	1380	345231	35
57906	167028	1457	18939	16389	352	1119	299179	208
31560	169386	3418	18028	22259	265	3022	326049	322
37749	158095	5126	31627	31419	0	2960	312412	0
31274	148816	5320	4396	24456	186	2485	318735	536
37250	157924	2149	5815	25790	95	3033	342598	0

37260	160047	2572	4532	26132	22	2879	346159	0
31965	151623	4688	7803	10945	321	1210	344272	0
75475	143183	20686	4583	12706	374	2439	320136	1665
61521	122283	1920	20564	70626	0	2045	289992	0
43740	144475	1657	11018	17624	247	1782	365691	40
58987	142854	2256	14001	926	40	8202	379708	0
37838	142784	2454	3919	18717	143	1389	384339	632
48686	140699	1004	16485	15055	904	953	357031	557
70453	128276	8398	32305	4575	96	227	352016	0
54387	137222	2712	18796	5083	805	1022	354438	166
21149	140159	18724	3648	1785	175	14	421431	361
86866	104082	502	43067	11828	354	1413	357177	15
75985	101800	4663	16356	3650	58	0	393682	619
29095	105930	1937	7938	31575	0	3522	429155	0
24401	106790	3111	24402	33534	8	4059	405538	0
39558	91492	741	43278	23184	19	2459	390142	0
16694	113122	2873	1703	627	90	499	495276	95
35569	85038	611	30604	23546	16	2590	428432	0
8457	96270	12888	1656	712	152	276	476116	1265
56223	77290	3891	10624	1720	135	0	477030	21
24357	81785	647	20319	2569	128	0	517191	279
16552	74087	616	9119	22114	296	3932	448719	159
11922	75767	3074	8433	2385	63	338	532246	13
30285	63886	1341	4605	38970	414	2640	470627	232
25954	63658	1247	5984	50794	533	1276	467243	2049
25506	64229	5254	4846	3461	164	572	543262	0
18972	64633	507	10262	378	151	0	555198	0
16729	57160	485	1624	34034	97	4152	531319	0
18228	56791	2129	3506	2989	202	263	576705	3
19079	55067	829	16873	4211	212	460	559553	0
7433	51561	1568	3824	13473	1088	3106	570256	271
12304	44545	434	8862	38000	14	3717	542751	0
12791	39672	583	51116	40899	506	3917	510734	0
22306	36520	1777	1242	55677	425	3298	519419	0
12584	34937	477	9260	39561	282	3852	559530	100
8589	33478	1594	41569	11815	750	3514	547862	78
13696	34282	852	9727	36107	702	1428	558088	179
12672	33441	461	9969	38613	7	4294	549224	0
6184	35243	561	7655	7140	280	101	593104	224
5717	35292	357	7546	7032	255	0	606427	0
21634	32544	121	13118	372	157	4317	593931	0
7771	29430	370	6763	1158	318	3738	594769	4424

Sr
9
17
179
2
0
0
9
79
2
24
0
0
115
0
17
0
48
45
196
0
21
0
73
0
5
5
0
53
52
9
151
21
30
9
1702
0
0
27
89
5
66
114
0
46
351

4
0
0
50
48
74
123
93
2067
33
13
32
30
74
0
0
66
0
30
34
86
0
72
16
20
44
4
25
89
261
0
9
4
30
33
6
38
0
0
0
93
92
49
38
31
27
0

41

48

0

50

72

0

155

14

18

65

24

39

39

26

0

6

44

39

55

18

68

23

7

19

18

27

307

55

26

0

109

108

127

54

76

0

0

16

67

10

54

5

10

1

70

66

0

4
442
44
4
12
66
336
20
45
63
0
34
91
0
134
105
0
6
129
52
0
155
114
173
143
28
81
0
0
65
63
35
4
0
44
30
106
52
0
32
72
103
0
124
233
43
160

21
111
92
115
0
32
57
373
66
113
46
99
28
4
94
290
26
76
77
120
418
0
0
192
186
156
107
24
145
151
98
357
7
0
215
329
0
189
29
0
123
48
25
57
48
21
32

26

0

7

44

27

56

46

69

139

0

42

51

12

37

5

31

62

46

93

37

38

63

27

9

0

54

13

9

15

156

25

23

215

21

21

51

23

5

68

52

122

14

32

0

25

54

109

27
0
4
23
124
115
13
86
55
149
23
45
37
26
41
20
5
26
139
28
47
62
167
26
119
0
0
185
35
32
31
52
36
51
66
42
0
57
185
48
30
100
0
12
0
81
27

52

27

0

0

0

168

157

16

0

7

79

32

6

25

33

108

63

32

36

14

18

49

130

47

8

121

89

34

132

12

63

0

79

6

137

48

14

6

43

24

25

35

0

88

37

37

0

65

55

156

83

96

34

20

66

38

0

47

143

57

0

0

151

93

17

99

60

75

30

29

6

33

0

0

146

23

27

102

32

152

97

17

11

26

28

32

71

0

142

50

94

132

102

26

150
21
18
47
43
9
0
0
13
26
207
133
25
77
103
66
278
186
27
97
107
1
0
129
51
86
0
0
37
40
68
38
134
15
87
87
101
36
42
500
21
37
55
78
32
123
39

145
90
27
66
0
0
2
85
31
29
121
62
67
20
90
29
378
118
38
49
296
129
103
36
18
19
28
118
85
33
31
41
35
69
61
31
77
81
25
50
166
42
82
38
54
69
253

47

191

72

11

0

139

44

3

247

29

235

49

69

84

16

100

53

6

57

68

16

106

79

54

0

152

121

179

207

34

32

42

135

5

95

135

384

163

64

71

820

0

17

2

296

447

98

71

0

552

57

55

384

13

325

0

308

0

7

37

19

55

84

822

76

49

5

77

2340

1006

1345

578

787

1142

552

906

777

1063

2091

988

1293

1841

1841

1455

687

2804

473

859

634

927

1131

504

2920

1325

687
549
1336
845
8759
696
1299
537
839
1971
3250
2116
1620
1120
490
3204
842
211
289
203
155
145
352
41
134
167
391
45
191
79
425
229
107
276
275
65
86
23
319
428
179
154
153
24
137
146
55

108
372
106
126
51
89
89
62
53
60
51
26
87
46
25
99
72
59
52
118
158
54
29
177
75
75
22
47
30
397
119
43
116
62
52
39
42
75
61
23
41
128
44
165
122
33
22

55
31
86
114
37
88
122
25
232
28
120
195
437
104
124
138
81
92
36
58
274
85
177
34
56
382
261
33
404
409
325
111
155
57
160
75
21
183
172
66
330
166

Table S2. Major elements, Be, Cr, Co, Ni, Sr, La and U concentrations (ppm) measured by ICP-MS for 68 sam

Type	Sub-type	Track	Sample name	Be	Na	Mg	Al
S-type	Chondritic	4	IS4 SPH4		9542	177567	4157
S-type	Chondritic	4	IS4 SPH5		4832	172742	16224
S-type	Chondritic	13	IS13 SPH4	0.156	6421	166184	9791
S-type	Chondritic	17	IS17 SPH2		178	133511	15097
S-type	Chondritic	19	S25 IS19 SPH2		1919	140779	7730
S-type	Chondritic	4	S12 IS4D SPH3		184	146583	15371
S-type	Chondritic	4	S9 IS4A SPHS		155	161306	15441
S-type	Chondritic	22	IS22 SPH2		642	155559	11244
S-type	Chondritic	22	IS22 SPH3	3.318	763	164573	9706
S-type	Chondritic	13	(4) IS13 SPH11	0.008	759	177936	5736
S-type	Chondritic	14	(8) IS14 SPH8	0.019	656	155222	14846
S-type	Chondritic	22	(16) IS22 SPH5	0.0004	1163	152596	13280
S-type	Chondritic	4	(20) IS4 SPH9		2195	145125	15516
S-type	Chondritic	8	(23) IS8 SPH5		640	157212	11706
S-type	Chondritic	13	(27) IS13 SPH7		181	139668	17950
S-type	Chondritic	13	(29) IS13 SPH10		348	183043	4311
S-type	non-Chondritic	14	(7) IS14 SPH7		44	216146	412
S-type	Chondritic	14	(9) IS14 SPH9	0.004	376	137838	8850
S-type	Chondritic	22	(1) IS22 SPH1	0.426	8168	104355	22530
I-type	Ni-rich	13	IS13 SPH3		749	235	1748
I-type	Ni-rich	4	S11 IS4C SPH2		176	19263	2512
I-type	Ni-rich	14	(12) IS14 SPH14		664	628	2047
I-type	Ni-rich	8	(24) IS8 SPH6		183	85	927
I-type	Ni-rich	17	17NMAG_37		2680	3197	521
I-type	Ni-poor	8	IS8 SPH1	0.019	1578	964	875
I-type	Ni-poor	8	IS8 SPH2		330	798	1531
I-type	Ni-poor	16	S7 IS16A SPH1		850	166	348
I-type	Ni-poor	12	S16 IS12C SPH1	0.629	623	345	7764
I-type	Ni-poor	19	S23 IS19 SPH1		536	573	404
I-type	Ni-poor	19	S29 IS19 SPH7		822	725	1603
I-type	Ni-poor	8	S5 IS8 SPHR	0.199	384	401	856
I-type	Ni-poor	13	S19 IS13B SPH2		203	295	188
I-type	Ni-poor	22	(2) IS22 SPH4	0.012	387	100	109
I-type	Ni-poor	13	(5) IS13 SPH9	0.008	154	339	151
I-type	Ni-poor	14	(10) IS14 SPH10		514	327	570
I-type	Ni-poor	8	(22) IS8 SPH4		1765	10533	17786
I-type	Ni-poor	13	(26) IS13 SPH6		320	87	367
I-type	Ni-poor	17	17NMAG_15	0.465	5316	6178	10622
I-type	Ni-poor	4	(18) IS4 SPH7	0.010	3943	7496	15125
I-type	Ni-poor	13	(30) IS13 SPH12	0.030	2069	11399	14476
I-type	Ni-poor	14	(31) IS14 SPH5	0.006	2101	8362	13894
I-type	Ni-poor	4	(17) IS4 SPH6	2.62	979	9470	10844

D-type	High Sr, high Si	17	IS17 SPH1	1.46	61972	32998	210325
D-type	High Sr, high Si	17	(14) IS17 SPH4	1.42	61916	28451	209998
D-type	High Sr, high Si	13	(28) IS13 SPH8b	2.03	49383	33244	195530
D-type	High Sr, high Si	17	(13) IS17 SPH3	1.53	49431	27214	122313
D-type	High Sr, high Si	17	(15) IS17 SPH5	1.22	41987	24935	124433
D-type	High Sr, high Si	17	17NMAG_36	0.83	18354	12657	59920
D-type	High Sr, low Si	17	17NMAG_6	2.87	11147	37615	124736
D-type	High Sr, low Si	14	(32) IS14 SPH6	5.05	1712	6220	94992
D-type	High Sr, low Si	14	IS14 SPH2	1.51	13933	7114	57204
D-type	High Sr, low Si	19	19NMAG_50	2.37	910	6387	53827
D-type	High Sr, low Si	19	19NMAG_52	3.13	7914	10729	46119
D-type	Low Sr, low Si	14	(11) IS14 SPH11	6.31	6653	10818	43731
D-type	Low Sr, low Si	8	(21) IS8 SPH3	2.01	1539	20310	35301
D-type	Low Sr, low Si	19	S31 IS19 SPH8		211	3912	84288
D-type	BeLaU low Si	4	S10 IS4B SPH1	14.7	13864	2907	88610
D-type	BeLaU low Si	14	S21 IS14 SPH1	7.8	2618	2231	53878
D-type	BeLaU low Si	14	(6) IS14 SPH4	10.0	7902	4911	90915
D-type	BeLaU low Si	4	(19) IS4 SPH8	32.4	3977	2704	115941
D-type	BeLaU low Si	14	IS14 SPH3	11.4	9001	3336	49658
D-type	BeLaU low Si	17	17NMAG_35	34.6	13854	8615	137992
D-type	BeLaU low Si	17	17NMAG_33	17.6	4740	8348	136612
D-type	BeLaU low Si	17	17NMAG_2	15.0	11780	14941	132262
D-type	BeLaU low Si	19	19MAGx_4	13.5	6623	10360	126494
D-type	BeLaU low Si	17	17NMAG_29	13.4	13895	7152	118488
D-type	BeLaU high Si	13	(25) IS13 SPH5	114.7	13169	8884	236886
D-type	BeLaU high Si	17	17NMAG_5	19.1	17227	9240	148150

P	K	Ca	Ti	Cr	Mn	Fe	Co	Ni
546	702	14512	486	2755	1651	201084	326	1484
578	1667	42093	689	762	1838	174601	124	421
569	1310	10107	321	8850	2858	222319	159	6262
1782	581	62464	1139	6359	1359	254052	699	12225
2234	3786	32720	509	6493	1911	271410	578	10610
473	1146	14659	703	4430	2098	269312	699	10253
220	808	19190	678	2109	1946	231199	368	3727
443	3925	21412	934	2742	1953	245727	401	5558
1007	3428	18623	214	3817	1983	221658	630	10550
635	412	3871	479	4363	2098	207312	465	10511
535	343	14309	759	2640	2275	246444	887	12302
1469	75	15121	803	5394	2203	257609	881	4653
126	304	7850	612	4171	2009	280680	462	9650
316			829	3515	1938	265567	534	7504
742		24680	682	4647	2272	278641	652	5677
312	187		343	5819	1459	207997	567	6954
18	53	936	54	49	3043	124011	1.22	
370	220	17121	377	3291	1898	304464	477	6812
7908	3340	174568	14586	6	6351	197902	63	12
88	632	8396	405	5174	4	696801	2486	12023
126	567	3019	92	500	212	618980	4145	56989
	981		189	6455	10	695233	3114	24436
68	43		12	237	14	711965	2828	16474
447	872	10010	38	6278	5361	640609	63	5032
410	318	6818	610	184	2838	708703	7.28	37.3
468	615	14555	269	203	4398	699909	7.56	55.1
117	211	1154	28	209	6381	716287	2.91	6.5
41	370	2509	133	4	11	708875	6.78	32.3
324	607	16015	8	226	4673	700901	17.0	85.6
250	409	15526	2696	382	4324	697265	11.1	90.6
211	261	1797	660	255	2642	715797	61.4	287.2
70	179	590	320	252	4366	714310	7.8	18.0
179	31	2578	493	443	4164	716564	27.0	142.5
43	38		1191	454	3912	715407	57.4	242.4
238	394	6080		77	3636	712442	12.2	50.0
464	229		30503	30	3195	645119	145.5	11.0
52				69	3133	721557	15.3	37
285	7763	35475	64502	1421	77906	336797	21.5	140
5157	1652	7023	37988	37	5396	634286	117.9	31
3282	613	7300	47461	100	5250	620426	113.1	11
1243	727	1170	39657	6	7442	642043	83.2	47
352	221	18309	457	87	14757	651822	19.0	15

3898	27420	140984	5521	87	2492	126468	34.8	133
3892	26583	121006	7407	63	2377	159124	43.2	178
3517	25784	133210	7319	28	3300	162544	49.7	99
2038	22566	304747	5688	19	2582	111080	39.3	25
1878	22661	316450	5765	29	2382	107793	36.5	27
1512	10441	146340	2888	47	1613	53625	21.1	39
2402	6474	33724	1781	102	5551	392982	10.4	138
1552	1220	21112	4442	109	515	534548	36.9	190
34	1716	9908	1673	56	621	601274	25.0	86
293	2275	20653	3303	64	342	605322	12.6	35.37
495	3123	24108	4468	470	291	593238	23.1	33.68
1005	9972	26224	829	40	16407	582408	13.4	33
1899	913	6588	2063	39	12966	598647	14.8	69
390	537	8430	740	223	863	587174	18.3	48.4
449	4759	30786	5005	140	267	543731	38.1	116
982	1350	12378	2729	1307	57	571591	41.7	72
161	2276	15958	5050	765	202	554415	31.3	37
593	2772	2901	2507	82	84	546719	194.3	52
453	7259	15157	3940	138	550	384635	39.1	67
919	25489	16249	7843	321	847	235061	36.7	138
8241	5146	32043	6249	394	6694	322928	102.5	425
3492	6217	36015	9701	243	7383	349500	170.1	842
8185	7479	35109	7580	260	6131	391681	80.7	363
1106	4159	32561	1312	94	112	395260	84.7	259
548	12044	93260	7045	11	550	250278	281.9	196
647	5724	42783	8606	8838	217	192194	64.9	149

Sr	La	U
5.066	0.331	
11.700	0.461	0.055
18.076	0.489	0.076
13.969	0.596	0.002
20.091	0.536	0.022
13.172	0.306	
42.101	0.407	
12.414	0.191	
24.518	0.397	
27.48	0.371	0.016
11.67	0.303	
15.89	0.571	0.033
22.51	0.664	0.003
6.04	0.386	
19.19	0.848	0.027
10.23	0.270	0.054
0.31	0.008	
9.95	0.404	
110	16.520	0.310
2.296	0.182	0.022
3.114	0.008	

103.30	0.24	0.81
57.099	0.339	0.293
6.909	0.326	0.062
1.322	0.026	0.007
11.184	2.001	0.115
4.070	0.122	0.001
13.463	0.188	0.048
8.264	0.588	0.104
1.017	0.026	0.006
5.303	0.090	0.015
1.077	0.024	0.062
2.389		
20.973	0.418	0.101
1.913	0.024	0.002
50.9	4.54	3.14
30.0	13.233	0.135
27.4	3.847	0.091
25.8	2.734	0.119
117.4	5.735	0.696

1349	20.056	1.562
1377.9	19.994	1.373
1435.2	23.869	1.853
2128.1	19.699	1.389
2230.3	19.724	1.584
995.1	9.42	14.58
930.4	20.81	5.39
1172.3	25.67	3.42
859.9	11.160	1.180
508.3	34.976	4.304
651.2	19.294	2.820
119.1	5.890	0.998
132.8	15.998	2.147
3.730	0.214	0.109
447.1	66.3	5.114
2242.8	159.4	6.148
2021.6	81.2	7.685
128.6	76.4	2.595
243.2	31.45	2.98
307.7	107.25	8.69
1071.0	82.99	15.17
962.6	52.55	17.31
1517.1	51.86	10.30
577.9	120.34	2.54
1792.7	260.4	9.715
2892	71.97	11.7

Table S3. Elemental data (ppm) measured by ICP-MS for 12 BeLaU-type spherules and the CI normalizing val

Type	Sub-type	Track	Sample name	Li	Be	Na	Mg
D-type	BeLaU low Si	4	S10 IS4B SPH1	84.7	14.7	13864	2907
D-type	BeLaU low Si	14	S21 IS14 SPH1	62.2	7.8	2618	2231
D-type	BeLaU low Si	14	(6) IS14 SPH4	87.0	10.0	7902	4911
D-type	BeLaU low Si	4	(19) IS4 SPH8	22.4	32.4	3977	2704
D-type	BeLaU low Si	14	IS14 SPH3	37.7	11.4	9001	3336
D-type	BeLaU low Si	17	17NMAG_35	162.7	34.6	13854	8615
D-type	BeLaU low Si	17	17NMAG_33	108.9	17.6	4740	8348
D-type	BeLaU low Si	17	17NMAG_2	170.0	15.0	11780	14941
D-type	BeLaU low Si	19	19MAGx_4	216.0	13.5	6623	10360
D-type	BeLaU low Si	17	17NMAG_29	102.2	13.4	13895	7152
D-type	BeLaU high Si	13	(25) IS13 SPH5	120.4	114.7	13169	8884
D-type	BeLaU high Si	17	17NMAG_5	154.4	19.1	17227	9240
			CI(ppm) Anders and Grevesse (1989)	1.5	0.025	5000	98990

ues of Anders and Grevesse (1989).

Al	Si	P	K	Ca	Sc	Ti	V	Cr
88610		449	4759	30786	36.3	5005	171	140
53878		982	1350	12378	20.9	2729	101	1307
90915		161	2276	15958	43.2	5050	220	765
115941		593	2772	2901	14.4	2507	57	82
49658		453	7259	15157	11.2	3940	98	138
137992		919	25489	16249	27.2	7843	202	321
136612		8241	5146	32043	34.0	6249	465	394
132262		3492	6217	36015	51.9	9701	277	243
126494		8185	7479	35109	31.9	7580	266	260
118488		1106	4159	32561	18.8	1312	36	94
236886		548	12044	93260	79.3	7045	323	11
148150		647	5724	42783	80.3	8606	372	8838
8680	106400	1220	558	9280	5.82	436	56.5	2660

Mn	Fe	Co	Ni	Cu	Zn	Ga	Ge	As
267	543731	38	116	117	44	42.3	8.44	2.06
57	571591	42	72	54	9	27.7	9.50	1.04
202	554415	31	37	47		20.2	9.21	1.41
84	546719	194	52	125		61.2	9.11	13.06
550	384635	39	67		1414	14.6	6.53	1.00
847	235061	37	138		478	28.8	3.91	2.96
6694	322928	103	425	24	542	51.6	5.57	2.59
7383	349500	170	842		1314	73.0	6.50	4.47
6131	391681	81	363	346	83	103.6	6.79	3.77
112	395260	85	259		1503	24.5	6.96	1.82
550	250278	282	196	108		68.8	4.90	4.24
217	192194	65	149	98	97	89.5	3.51	1.70
1990	190400	502	11000	126	312	10	32.7	1.86

Se	Rb	Sr	Y	Zr	Nb	Mo	Ag	Cd
0.25	17.6	447	135	465	38.2	4.9	0.24	0.09
0.25	4.5	2243	120	247	15.1	77.5	0.07	0.05
0.24	6.8	2022	133	626	34.5	19.8	0.21	0.06
0.24	13.9	129	188	199	7.1	22.7	0.11	
0.13	40.9	243	44	131	12.8	6.7	0.05	0.29
0.28	173.9	308	86	441	29.2	10.3		0.03
0.11	27.8	1071	63	477	34.0	18.2	0.16	0.08
0.19	31.7	963	77	423	23.2	13.4	0.15	1.59
0.16	33.7	1517	61	420	21.0	14.2	0.08	0.12
0.37	11.6	578	255	153	4.3	27.4	0.03	0.02
0.71	46.7	1793	487	1008	84.8	179.2	0.23	0.24
0.44	22.6	2892	214	1117	71.2	5.4	0.304	0.132
18.6	2.3	7.8	1.56	3.94	0.246	0.928	0.199	0.686

Sb	Cs	Ba	La	Ce	Pr	Nd	Sm	Eu
1.28	1.09	914	66.3	128	14.5	58.2	12.4	2.68
0.05	0.18	759	159.4	267	25.6	89.4	16.0	2.96
0.55	0.37	1452	81.2	152	16.7	68.0	15.6	3.35
0.68	1.92	228	76.4	181	20.3	85.5	18.6	3.20
2.83	2.89	385	31.5	66	7.1	27.1	6.8	1.18
12.41	17.80	792	107.2	227	24.6	100.5	11.2	3.69
9.70	4.94	1404	83.0	214	25.7	99.4	14.0	2.57
11.61	4.62	1613	52.6	116	14.1	60.2	11.1	2.35
1.96	3.17	3052	51.9	110	12.4	50.3	11.3	2.57
10.35	2.27	740	120.3	170	20.5	88.7	22.8	4.83
2.35	5.67	2848	260.4	451	49.8	204.6	45.5	8.87
0.94	2.68	2573	72.0	159	19.2	82.5	21.2	4.90
0.142	0.187	2.34	0.235	0.603	0.089	0.452	0.147	0.056

Gd	Tb	Dy	Ho	Er	Tm	Yb	Lu	Hf
15.30	2.68	17.36	3.79	11.26	1.80	10.57	1.58	10.92
17.87	2.72	17.26	3.70	11.59	1.85	11.92	1.79	5.95
17.23	2.93	19.56	4.12	13.81	2.16	14.57	2.08	14.27
19.96	3.37	23.51	5.08	17.00	2.70	16.00	2.24	6.22
5.61	1.06	5.53	1.21	3.30	0.59	3.55	0.51	3.45
13.33	2.23	13.23	2.32	8.18	0.96	6.98	1.78	7.97
11.07	1.98	11.37	2.25	7.30	1.05	6.96	1.31	10.88
11.83	2.14	12.42	2.81	7.02	1.34	7.81	1.49	9.93
10.53	1.56	10.20	2.08	5.80	1.03	5.64	0.83	10.90
29.60	5.14	34.05	8.09	23.62	3.85	22.88	4.00	3.65
51.72	9.28	64.72	15.28	55.64	9.26	65.66	10.34	24.11
23.30	4.49	29.94	6.85	20.94	3.47	22.72	3.45	23.20
0.197	0.0363	0.243	0.0556	0.159	0.0242	0.163	0.0243	0.104

Ta	W	Re	Tl	Pb	Bi	Th	U
1.45	17.96	0.001	0.322	3.76	0.032	14.70	5.11
0.63	7.53	0.002		0.34	0.002	8.41	6.15
1.34	4.39	0.002	0.001	1.01		15.32	7.68
0.60	8.62	0.002		1.55		8.26	2.60
0.76	7.12	0.131	0.338	2.20	0.461	9.90	2.98
1.50	12.64	0.015	1.221	4.35	0.999	38.73	8.69
1.23	20.12	0.022	0.611	17.85	0.119	19.80	15.17
1.40	9.28	0.010	0.153	10.05	0.656	56.05	17.31
1.57	12.13	0.002	0.010	2.46	0.079	23.33	10.30
0.08	669.18	0.015	0.210	3.90	0.557	4.13	2.54
2.64	63.34	0.008	0.044	10.49	0.021	18.76	9.72
2.03	6.71	0.005	0.053	7.78	0.040	24.28	11.69
0.014	0.093	0.0365	0.142	2.47	0.114	0.0294	0.0081